Adeno-associated viral gene transfer to prevent the cellular phenotype of cortical organotypic brain-slice cultures derived from Gaucher's disease type II mice.

Dissertation zur Erlangung des akademischen Grades des

Doktors der Naturwissenschaften (Dr. rer. nat.)

eingereicht im Fachbereich Biologie, Chemie, Pharmazie

der Freien Universität Berlin

vorgelegt von

Karen Henning

aus Berlin

2013

II

Die experimentellen Arbeiten der vorliegenden Dissertation wurden in der Zeit vom Oktober 2009 bis März 2013 in der Arbeitsgemeinschaft Klinische Zell- und Neurobiologie am Institut für Integrative Neuroanatomie der Charité-Universitätsmedizin Berlin unter der Leitung von Prof. Dr. Thomas Georg Ohm durchgeführt.

1. Gutachter: Prof. Dr. Thomas Georg Ohm

2. Gutachter: Prof. Dr. Burghardt Wittig

Tag der Disputation: 27.03.2014

Hiermit erkläre ich, die vorliegende Arbeit selbstständig und unter Verwendung der angegebenen Literatur und Hilfsmittel angefertigt zu haben. Stellen, die anderen Werken im Wortlaut oder Sinn entnommen sind, wurden mittels Quellenangabe kenntlich gemacht. Die dem Verfahren zugrunde liegende Promotionsordnung ist mir bekannt.

Berlin, den 26.09.2013

Karen Henning

IV

Acknowledgements

First, I want to thank Prof. Dr. Thomas Georg Ohm, group leader in the Institute for Integrative Neuroanatomy Charité, Berlin, who has given me the chance to work on my PhD project in his laboratory, for his support and for overlooking my manuscript.

Further, I am grateful to Prof. Dr. Burghardt Wittig, chairman of the Foundation Institute Molecular Biology and Bioinformatics, Foundation by Mologen AG and FU Berlin, for his willingness to appraise and to represent this thesis in front of the faculty of biology, chemistry and pharmaceutics of the FU Berlin.

This PhD project was part of the BMBF funded project "Gene and cell therapy of Morbus Gaucher type II". I want to thank all members of this consortium for the successful collaboration, in particular Nico Jäschke for providing me with the vectors and Marta Swierczek for providing me with the fibroblasts used in the present study. Especially I want to thank Brita Vorwerk, for teaching me how to prepare organotypic slice cultures, for great teamwork during our PhD projects, for sticking together the whole time and for always being open for discussions.

I want to acknowledge all former and current members of the group of Prof. Dr. Ohm for the good working atmosphere, helpfulness and not only good professional conversations. Further I want to thank Frank Albert for teaching me how to prepare and cultivate primary neurons and Rosemarie Döscher for teaching and supporting me in histochemical techniques. My thank goes to Dr. Knut Kallwellis who supervised me during the first year and who was willing to overlook and to comment my manuscript. Special thank goes to Dr. Volker Meske for always putting great confidence in me, for never getting tiered of discussing aspects of my thesis with me and for overlooking my manuscript.

I am also grateful to my friends for their constant moral support, for never getting tiered of discussing aspects of my work and for tolerating when I had only short time for visits while working on my thesis.

Last but not least I am thanking my family who always believed in me and for supporting me the whole time. They never got exhausted of being interested in my project. I am grateful to my uncle, Gerhard Holl, who supported me ever since he

heard about my great interest in the studies of biology. He gave me the opportunity to be a practical trainee in a pharmaceutical company during my early school years which had a great impact on my later decision to study biology.

In particular I want to thank René for putting up with me at any moment during this time and for his never ending support. He even made it possible for me to send off my manuscript spending an hour on top of a boat which displays only one small aspect of all the things he did for me. I also want to thank him for never giving up on me no matter what and for his great optimism during this time.

Special thanks to my mother for always standing up for me and for encouraging me at any moment of distress. Without her I would not have come that far and therefore this thesis is dedicated to her.

Table of Contents

1. Theoretical background

1.1 Rare lysosomal storage disorders

Lysosomal storage disorders are mostly due to mutations in genes encoding a single lysosomal enzyme which results in intracellular accumulation of its metabolites (Jmoudiak and Futerman, 2005). Today, over 70 lysosomal storage disorders are known (Aerts *et al.*, 2011). The major groups of hereditary metabolic storage disorders in humans are the sphingolipidoses, mucopolysaccaridoses and glycogenoses (Brady, 2006). The organelle lysosome was discovered by de Duve and colleagues in 1949 and has since been of great interest regarding their role in diseases. Lysosomes are membranous organelles, rich in hydrolases, and are responsible for the degradation of biological macromolecules. The digestive enzymes require the acidic environment provided in the lysosome in order to be active (Futerman and van Meer, 2004; Beck, 2007).

Most lysosomal storage disorders involve only a single gene (monogenic) but a variety of mutations have been described in the same gene. Owing to this, in most lysosomal disorders no genotype-phenotype correlation has yet been possible (Futerman and van Meer, 2004).

1.1.1 Gaucher's disease

Gaucher's disease is the most common sphingolipidose (Sidransky, 2004) and occurs with a frequency of 1 in 40,000–60,000 in the general population (Kacher *et al.*, 2008). The disease was described for the first time by Philippe Gaucher in 1882, who described his observations of a female patient with an enlarged spleen and not naturally occurring large cells inside the spleen, so called Gaucher cells (Futerman and van Meer, 2004). Gaucher's disease is caused by a defect in the activity of the lysosomal enzyme acid-β-glucocerebrosidase (GCase or Gba). The disease is heredity (autosomal recessive) and is mostly found among Ashkenazi Jews, with a carrier frequency of approximately 1 in 15 (Sidransky, 2004).

Gaucher's disease has been divided into three clinically distinct types, namely type I, type II and type III which differ in age of onset and in severity of the disease (Daniels *et al.*, 1982).

Type I occurs the most frequently of the three types and is often referred to as the non-neuronopathic form, as only the periphery is involved in this type of Gaucher's disease. Patients display a large variety of symptoms and some even go undiagnosed throughout their life. However, clinical manifestations often begin with splenomegaly and hepatomegaly as well as with anaemia and thrombocytopenia.

In type II, the acute neuronopathic form of Gaucher's disease, the central nervous system (CNS) is involved. This type is more stereotypic in disease development than type I. Here the impairments of neurological symptoms occur in addition to the visceral ones. In general the symptoms start with occulomotor abnormalities and are followed by brainstem involvements. Disease onset occurs already between 3 and 6 months (Pelled *et al.*, 2005) and patients die within the first 2–3 years of life (Sidransky, 2004; Jmoudiak and Futerman, 2005). Investigations of the brain from Gaucher patients did not reveal any abnormal gross histological appearance compared with normal brains. However, microscopically neuronal loss – especially in the thalamus, brain stem and occipital cortex – was observed (Oppenheim *et al.*, 2011).

Type III represents the chronic or subacute neuronopathic form of Gaucher's disease. In this case the central nervous system is involved as well as in type II, but neurological symptoms usually occur later in life. The following symptoms are involved: ataxia, abnormal eye movements, seizures and dementia. In general patients survive until their third to fourth decade of life (Sidransky, 2004; Jmoudiak and Futerman, 2005)

1.1.1.1 *Genotype / Phenotype correlation in human population*

Over 250 mutations (Hruska *et al.*, 2008) have so far been described in the gene encoding β-glucocerebrosidase. These mutations include 203 missense mutations, 18 nonsense mutations, 36 small insertions or deletions leading to either frameshifts

or in-frame alterations, 14 splice junction mutations and 13 complex alleles carrying two or more mutations (Hruska *et al.*, 2008).

Therefore a direct correlation between genotype and phenotype is largely impossible, as patients with the same genotype often show different phenotypic symptoms. There are some exceptions to this rule: The mutations N370S, L444P, IVS2 + 1G -> A, c.84insG, R463C lead in general to type I and account for over 90% of the mutant alleles found in Ashkenazi Jews and for 50–60% of non-Jewish individuals (Beutler, 1992; Sidransky, 2004; Hughes and Pastores, 2010).

1.1.1.2   The enzyme β-glucocerebrosidase

The enzyme β-glucocerebrosidase is a glycoprotein with a molecular mass that ranges from 58 to 66 kDa after glycosylation and removal of a leader sequence (Beutler, 1992). Glucocerebrosidase normally hydrolyses glucosylceramide into glucose and ceramide. Owing to the defect in the *GBA gene* and the resulting reduced activity of β-glucocerebrosidase activity found in Gaucher patients this hydrolysis occurs much less and therefore glucosylceramide accumulates in the lysosome, as described in detail in Section 1.1.1.3 (Ho, 1973). A schematic overview is given in Figure 1.
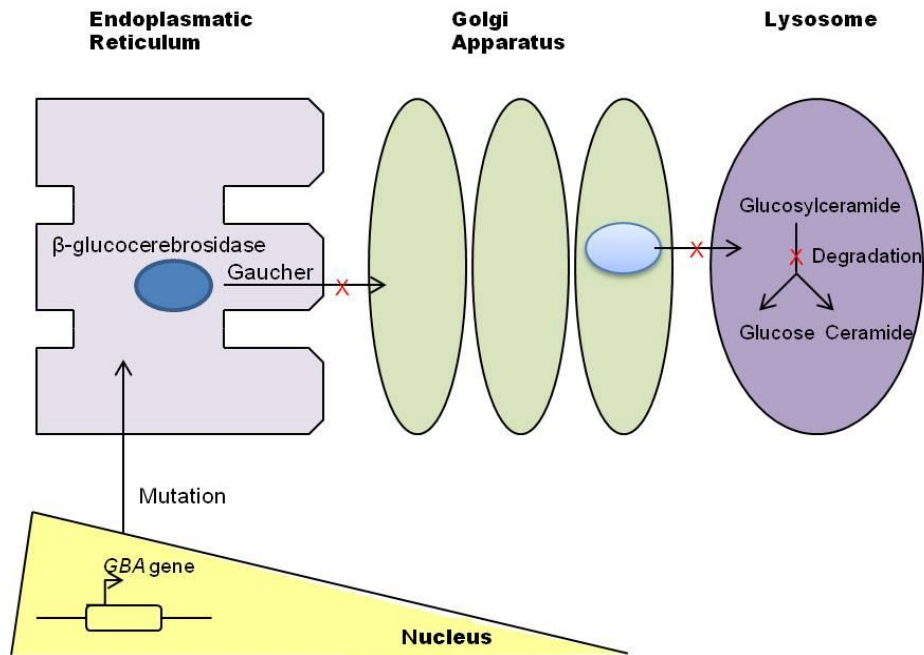
Figure 1: Schematic overview of the cause of Gaucher's disease, a mutation in the GBA gene
Mutation in the GBA gene can cause a defective transport of GCase out of the ER because of misfolding or other defects in the steps during the transport from the Golgi body to the lysosome. There arises a lack of degradation of glucosylceramide in the lysosome due to a reduced activity of glucocerebrosidase (modified after Futerman and van Meer, 2004)

Further, Ho described two different types of GCase in the human spleen in 1973: A high-molecular-weight 'acid' β-glucocerebrosidase and a 'neutral' β-glucocerebrosidase. Besides their different pH values for greatest activity, the major difference between these two isoenzymes is the membrane association of the 'acid' form (Rjinboutt *et al.* 1991); the 'neutral' form is a soluble enzyme. Owing to the fact that only the 'acid' form of glucocerebrosidase showed activity towards the substrate glucocerebroside, this from has been identified as the key player in Gaucher's disease (Ho, 1973).

The gene encoding human glucocerebrosidase is found on chromosome 1q21 (Ponce *et al.*, 2001) and consists of 11 exons. It has a total length of 7 kb (Hughes and Pastores, 2010). A pseudogene of the functional glucocerebrosidase gene has been found about 16 kb downstream. A high degree of sequence similarity has been found between the functional gene and the pseudogene. Except for the functional gene, no transcripts of the pseudogene can be translated, because no long open reading frames are found in the pseudogene (Beutler, 1992; Carstea *et al.*, 1992).

Kacher *et al.* determined the three-dimensional structure of glucocerebrosidase in 2008. The structure consists of a characteristic barrel (domain III) containing the catalytic residues and two closely-associated β-sheets (domain II). Further β-glucocerebrosidase has a third unusual small domain (domain I) containing one 3'-stranded anti-parallel β-sheet, whereas the active site of the enzyme is located in domain III. The mature glucocerebrosidase protein is composed of 497 amino acids (Hughes and Pastores, 2010).

Glucocerebrosidase also requires interactions with the lipid phosphatidylserine and the heat-stable glycoprotein saposin C. Therefore, saposin C is needed as a cofactor for glucocerebrosidase in order to hydrolyse glucosylceramide. There are also patients who show a deficiency of saposin C itself, or of its precursor protein, but who still display normal GCase activity. In all cases glucocerebroside is accumulated in the cells of these patients as well, and typical Gaucher-related symptoms are observed (Kacher *et al.*, 2008; Hughes and Pastores, 2010).

In various studies, a residual activity of glucocerebrosidase of 5–25% in patients suffering from Gaucher's disease has been detected (Daniels *et al.*, 1982). Therefore, an elevation of enzyme activity of only 15–20% of the normal level would be sufficient for clinical efficacy (Beck, 2010).

1.1.1.3 Pathological mechanisms

The most obvious effect observed due to the insufficient activity of GCase in Gaucher's disease is the accumulation of glucosylceramide in cells throughout the body. The most prominent cells under the microscope are of mononuclear phagocyte origin; these are the so-called "Gaucher cells". Gaucher cells are about 20–100 μm in diameter (Jmoudiak and Futerman, 2005; Brady, 2006). The accumulation of glucosylceramide has severe pathological consequences in Gaucher's disease as glucosylceramide is one component of cell membranes. Furthermore, it plays an important role in the pathway of complex glycosphingolipid biosynthesis and degradation (Fig. 2). Owing to the defect in GCase, glucosylceramide is accumulated intracellularly because its degradation is slow compared with that in normal cells. In

spleen obtained from all types of Gaucher's disease levels of ~30–40 mmol/kg tissue of accumulated glucosylceramide was observed (Jmoudiak and Futerman, 2005).

Even though distinct glucosylceramide accumulation is observed, it only accounts in total for less than 2% of the additional mass of the 25-fold increased size of the spleen in Gaucher patients (Jmoudiak and Futerman, 2005). Moreover, it was found that not only lysosomes predominantly accumulate glucosylceramide but also that the concentration of glucosylceramide in microsomes is 10 times greater in the brains of patients suffering from type II (Ballabio and Gieselmann, 2009).
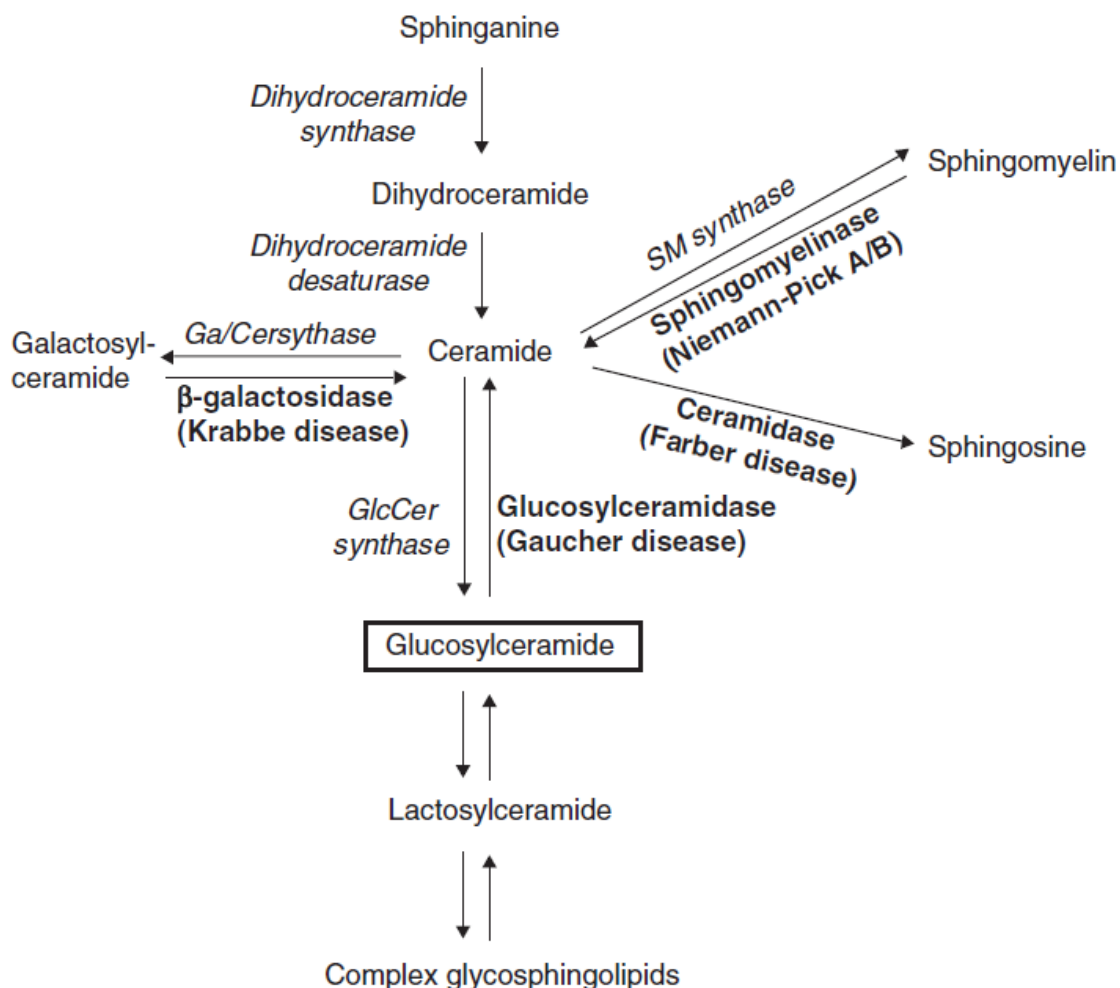
Figure 2: Overview of the metabolic importance of glucosylceramide
(Jmoudiak and Futerman, 2005)

A second substrate of glucocerebrosidase is glucosylsphingosine, which is synthesized from UDP-glucose and sphingosine. Even though the enzymatic activity

of GCase with glucosylsphingosine as substrate is less efficient than on the substrate glucosylceramide, glucosylsphingosine also seems to play an important role in brain pathology in Gaucher patients. Glucosylsphingosine may act as a possible neurotoxic agent. In type 2 patients, glucosylsphingosine reaches levels of 12.3 µmol/kg in the cerebral cortex whereas in normal brain only trace amounts (0.13 µmol/kg) are detectable (Schueler *et al.*, 2003).

Various studies have shown that the accumulation of storage material as glucocerebroside itself does not seem to be the primary cause of disease-specific symptoms in Gaucher's disease. Especially, the devastating neuronal cell death in Gaucher type II and III needs further investigation. Furthermore, the accumulation seems also to contribute to various essential secondary pathological mechanisms, as described below (Schueler *et al.*, 2003).

1) Korkotian *et al.* (1999) observed that glucosylceramide-storing neurons showed an increased calcium release from the endoplasmic reticulum in response to glutamate stimulus. Further studies by Pelled *et al.* in 2005 showed significantly enhanced calcium release via the ryanodine receptor in correlation with levels of glucosylceramide accumulation in brains from Gaucher's disease type II patients compared with brains from type III patients. Therefore, the neurodegeneration seen in Gaucher's disease type II and type III may be explained as being due to enhanced glutamate-induced neurotoxicity that leads to increased apoptosis (Ballabio and Gieselmann, 2009).

2) Another pathological mechanism was described by Bodennec *et al.* (2002), who observed that neurons from a mouse model displaying Gaucher's disease stored glucosylceramide and showed an increase in the number of axonal branch points in comparison with control mice. Furthermore, these neurons had an elevated level of various phospholipids which was due to the direct activation of phosphocholine cytidylyl transferase (CTP). CTP is the rate-limiting enzyme in the synthesis of phosphatidylcholine by glucosylceramide (Ballabio and Gieselmann, 2009).

3) Recently, the misfolding of the enzyme β-glucocerebrosidase itself has been reported to play a role in abnormalities of cellular reactions. Mutations leading to a misfolding of enzymes in the endoplasmatic reticulum would result in early degradation. Early degradation in the proteasome is believed to induce stress in the endoplasmatic reticulum. However, this mechanism is still under investigation in order to verify its involvement in Gaucher's disease type II and type III (Hughes and Pastores, 2010).

The pathology of Gaucher's disease does not seem to be only caused by the accumulated material and its resulting effects, but also by macrophage activation. For example, markers such as interleukin-1 β, interleukin 6 and tumour necrosis factor-α have been found to be elevated in serum of Gaucher patients. Further markers of alternatively activated macrophages such as chitotriosidase have also been found to be significantly increased in the serum of patients compared with in healthy individuals. This marker is commonly used to determine severity of Gaucher's disease and therefore to decide on possible treatment strategies (Jmoudiak and Futerman, 2005).

1.1.1.4 Diagnosis and therapeutic approaches

Different ways to diagnose Gaucher's disease have been developed. The gold standard diagnostic measure for Gaucher's disease is the documentation of a deficiency in β-glucocerebrosidase activity. The enzyme activity is usually assayed by using the fluorescent substrate 4-MUD (see Section 2.6.2). However, one major drawback is the lack of possible correlation between the level of residual GCase activity and the clinical phenotype. Biomarkers also play an important role in monitoring the course of disease. The best way to monitor the course of disease and to correlate it with disease severity is to use the marker chitotriosidase. Unfortunately, about 6% of Gaucher patients completely lack serum chitotriosidase activity. Moreover, this test is not standardised between different laboratories and therefore research is currently being performed to identify further biomarkers (Gupta *et al.*, 2011). Recently, a massive overproduction and secretion of the pulmonary and activation-regulated chemokine (PARC/CCL18) by Gaucher cells was observed in

Gaucher patients. In symptomatic Gaucher patients the plasma level is elevated 10- to 40-fold compared with healthy individuals. Therefore, the measurement of PARC is a good alternative method for patients who lack serum chitotriosidase (Aerts *et al.*, 2011).

Therapeutic approaches for lysosomal storage disorders can easily be divided into two groups; on the one hand treating the symptoms and on the other hand treating the cause itself.

One common treatment to address symptoms in Gaucher patients is splenectomy, the surgical removal of the spleen (Futerman and van Meer, 2004). Another way to treat patients suffering from type I is marrow transplantation, as in type I mostly macrophages are impaired. However, this form of therapy is very risky and is therefore not generally used in mildly affected patients. Unfortunately the risk of transplantation also increases with the severity of disease (Beutler, 1992). Furthermore, it is often difficult to find suitable donors for bone-marrow transplantation, there are dangers with myeloablation and the probability that recipients may require immunosuppression throughout their life (Brady, 2006).

Enzyme-replacement therapy is the most common and successful therapy used to treat the cause of Gaucher's disease type I. Initially, β-glucocerebrosidase derived from the human placenta was used. Since 1991 β-glucocerebrosidase has been produced in Chinese hamster ovary cells. Since then, this therapy has been available using a recombinant β-glucocerebrosidase which targets macrophages (Futerman and van Meer, 2004). The trade name of such a recombinant form commonly used is Cerezyme™ (imiglucerase; Genzyme Corporation). Glucocerebrosidase needs to be purified and modified by removing outer sugars to expose additional mannose residues (Beutler, 1992). After binding to the cell-surface mannose receptors the modified enzyme is endocytosed and delivered to the lysosomes to work instead of the defective enzyme. Enzyme replacement therapy leads to a reduction in organ volumes, improvement in haematological parameters and other benefits, resulting in a general improvement in the patient's quality of life. Unfortunately, enzyme-replacement therapy does not lead to improvements in type II or type III patients, as the neurological symptoms cannot be treated. This is due to the fact that the recombinant enzyme is unable to cross the blood–brain barrier, and so far no

transport mechanism has been found (Jmoudiak and Futerman, 2005). Further drawbacks of enzyme-replacement therapy are the recommended infusions every 2 weeks in order to achieve the best possible effect and the consequent high cost to the health-care system (Beutler, 1992; Tomanin *et al.*, 2012). Recently, another Gene-Activated[TM] human glucocerebrosidase (velaglucerase alpha) has been produced. Velaglucerase alfa is a secreted monomeric glycoprotein of 63 kDa and is composed of 497 amino acids. Unlike imiglucerase, velaglucerase alfa contains the native human enzyme sequence. Furthermore, velaglucerase alfa contains nine mannose units leading to an at least 2-fold greater internalisation into human macrophages than that of imiglucerase (Brumshtein *et al.*, 2010).

Another well-known therapeutic approach is the so-called substrate reduction therapy. In the case of Gaucher's disease, glycolipid synthesis is inhibited by *N*-butyl-deoxynojirimycin; this leads to a reduced production of glucosylceramide and therefore results in lower levels of accumulation. Fewer typical symptoms develop; reduced volumes of liver and spleen have been described (Futerman and van Meer, 2004; Jmoudiak and Futerman, 2005).

Further attempted therapeutic approaches include chemical chaperones, which supposedly stabilise or even reactivate improperly folded glucocerebrosidase, leading to a rescue of activity (Jmoudiak and Futerman, 2005)

So far, the most interesting and effective treatment of lysosomal storage disorders would appear to be somatic gene therapy. A variety of gene-transfer methods have been used to transfer the genetic material into disease-displaying cell-culture systems. However, unfortunately, until today the transfer to animals or even humans has been unsuccessful (Futerman and van Meer, 2004).

1.1.2 K14 lnl mouse model

In the past 30-40 years different attempts have been made to generate viable mouse models presenting the different types of Gaucher's disease. Animal models are of considerable interest, as they allow insight into the molecular mechanisms linking glucosylceramide accumulation and cellular dysfunction. Various models have been

generated by injecting a glucocerebrosidase inhibitor, by inserting different cassettes into the *GBA* gene or by using a 'single insertion' mutagenesis procedure. However, especially when the *GBA* gene was disturbed to achieve reduced GCase activity not only in the periphery but also in the brain, the mice died within hours after birth (Farfel-Becker *et al.*, 2011).

The first viable conditional mouse model of acute neuronopathic Gaucher disease was generated by Enquist *et al.* in 2007. Generating mice with reduced GCase activity was achieved by inserting a *loxP-Neo-loxP* (lnl) cassette into the *GBA* intron. In order to prevent early death of mice due to the presence of a similar skin phenotype as observed in the GCase-deficient mice before the mice were cross-bred with K14-Cre transgenic mice. This breeding led to mice showing GCase deficiency in all tissues except the skin. Cre recombinase expression is driven by the K14 promoter, which allows the recombination of glucocerebrosidase within the skin. The progression of disease in homozygous K14 knockout (ko) mice was very rapid after a symptom-free period of approximately 10 days. K14 ko mice were growth-restricted and they showed abnormal gait, hyperextension of the neck and seizures and had to be killed at about 2 weeks of age, showing end-stage paralysis. β-glucocerebrosidase is significantly reduced in K14 ko mice compared with K14 wild-type (wt) mice, but rest activity is always measured in K14 ko mice as well. Further microscopic analysis displayed normal brain architecture in K14 ko mice compared with K14 wt mice but distinctly reduced cellular density throughout the brain, and increasing numbers of apoptotic cells were revealed in K14 ko mice by using TUNEL stain. In summary, the K14 lnl mouse model shows a high degree of similarity in pathological findings as well as in clinical findings to patients with Gaucher's disease type II. Therefore, it may be considered to serve as an adequate model for gene-therapeutic approaches (Enquist *et al.*, 2007; Farfel-Becker *et al.*, 2011).

1.2 Gene therapy

Gene therapy is the direct introduction of functional genetic material into cells of the body, with the aim of therapeutic improvement. Gene therapy covers a wide range of methods to modify the nervous system; these include the delivery of genes,

sequence-targeted regulatory molecules, genetically modified cells and oligonucleotides.

The use of genetically modified haematopoietic stem cells (HSCs) to provide a permanent source of a normal enzyme could be of great interest (d'Azzo, 2003; Sands and Haskins, 2008). In general, lysosomal storage disorders are good candidates for gene therapy, as they are well characterised single-gene defect disorders. Therefore, one gene replacement would be sufficient to restore a "balanced genomic situation" (Cheng and Smith, 2003; Tomanin *et al.*, 2012). Various mouse models displaying different lysosomal storage disorders have been used for gene-therapeutic approaches (d'Azzo, 2003). Reduced storage and prolonged life span were observed in mouse models of mucolipidoses and galactosialidoses in which a murine stem cell virus-based retroviral vector was used (Matzner *et al.*, 2000; Leimig *et al.*, 2002). Furthermore, Takenaka *et al.* showed in 2000 that transplanting mice displaying Fabry's disease with mononuclear bone-marrow cells that had been transduced by a modified retroviral vector led to a decrease in disease symptoms. These results were only observed in the periphery, and not in the CNS. Overall, these studies encouraged the use of retrovirally mediated gene transfer to various stem cells (bone marrow, marrow stromal cells, mesenchymal stem cells and neural stem cells), ameliorating systemic diseases, but the effect on the CNS still needs further evaluation (d'Azzo, 2003; Bowers *et al.*, 2011).

Gene-therapeutic attempts led further to the first trials of human stem-cell gene therapies in patients suffering from Gaucher's disease. Non-ablated patients received infusions containing retrovirus (expressing human GCase cDNA) transduced HSCs from patients. Even though the gene-marked cells persisted for about 3 months, the efficiency was too low to increase the GCase activity (Schuening *et al*, 1997, Dubar *et al.*, 1998 and Rosenberg *et al.*, 2000). In order to overcome the low transduction efficiencies achieved so far by the methods described above, more and more developmental efforts are being directed to the use of different viral vectors (Table 1): lentiviral vectors such as the human immunodeficiency virus type 1 or feline immunodeficiency virus (Sands and Haskins, 2008), adenoviral vectors or adeno-associated viral vectors. Most studies so far in which AAV was used as a gene-transfer system have been successfully performed with MPSVII (Sly disease) mouse

models. Here an AAV vector expressing β-glucuronidase was injected into the striatum or cerebral spinal fluid when addressing CNS involvement (d'Azzo, 2003). Furthermore, Jung *et al.* (2001) observed an increase in enzyme activity and reduction of storage material six months after injecting a recombinant AAV-expressing human α-galactosidase into the portal vein of Fabry mice (Bower *et al.*, 2011). The first phase I clinical trial using an adenovirus for a metabolic disorder of the liver, in which one participant died, was reported in 1999 (Kremer, 2005). One of the biggest challenges facing viral vector gene delivery is the host immune response. However, in the case of AAV infection almost no innate immune response has been observed, and such immune response as occurred was mostly based on humoral response (Daya and Berns, 2008). Still, further clinical trials have been reported, with good results.

Twenty trials have been listed for lysosomal storage disorders, out of 167 clinical trials related to monogenic disease, in the Wiley Database on Gene Therapy Clinical Trials Worldwide (http://www.wiley.com/legacy/wileychi/genmed/clinical/), updated to January 2013. Summarising the different studies over the years, AAV and lentiviral vectors have emerged as the vector of choice for gene transfer to the CNS because they mediate efficient long-term gene expression with no apparent toxicity for, or strong immune response by, the recipient (Bowers *et al.*, 2011).

1.2.1 Introduction of DNA into cells

In order to perform somatic gene therapy, cells of the patient have to be genetically modified by either *ex vivo* or *in vivo* methods. Modifications would lead to constitutive expression and secretion of higher levels of the desired enzyme, and therefore these cells could become the source of the corrected enzyme in the patient (d'Azzo, 2003). In case of an e*x vivo* gene transfer, cells from the patient are isolated and modified *in vitro* by using a gene vector. Afterwards these cells are implanted back into the body of the patient. The other method is to perform an *in vivo* gene transfer, which describes the direct application of the modified gene vector into the cell or tissue of choice of the patient (Sands and Haskins, 2008).

1.2.2 Methods in gene transfer

In general two methods exist to transfer DNA into cells: viral and non-viral gene transfer. To reach long-term, stable gene expression in the CNS, viral vectors remain the most efficient vehicles and may also have the benefit of being tissue- or cell-specific (Bowers *et al.*, 2011; Tomanin *et al.*, 2012).

1.2.2.1 Viral gene transfer

Introduction of genetic material into cells by using viral vectors is termed either 'infection' or 'transduction'. Viral vectors still represent an important tool for *in vitro, ex vivo* and *in vivo* gene transfer. Different parameters such as the required duration of transgene expression, cell-type-targeted ease of vector construction and cloning capacity determine the choice of vector (Kremer, 2005; Tomanin *et al.*, 2012). An overview of the viral vectors most frequently used is given in Table 1.

Table 1: Characteristics of different viral vector systems
The table gives the most important features of the most frequently used viral vectors in gene therapy (modified after Tomanin *et al.*, 2012).

	AAV	**Adenovirus**	**Retrovirus**	**Lentivirus**
Max. size of transgene	4 kb	7–8 kb	7–8 kb	7–8 kb
Infection of non-dividing cells	Yes	Yes	No	Yes
Integration into cell genome	Yes	No	Yes	Yes
Advantages	Non-inflammation, non-pathogenicity	High titres, very high efficiency of infection	Permanent expression of transgene	Permanent expression of transgene
Disadvantages	Reduced packaging capacity	Transient expression, Immunogenicity, inflammation	Possibility of silenced transgene expression, insertional mutagenesis and oncogenesis	Endogenous recombination with other retroviral sequences and reversion to HIV, insertional mutagenesis and oncogenesis

1.2.2.2. Non-viral gene transfer

Owing to problems such as endogenous virus recombination, oncogenic effects and unexpected immune response that may occur when one is using viral vectors, non-viral vector systems are becoming of more interest in order to circumvent these problems (Niidome and Huang, 2002). Gene transfer using non-viral vectors is called transfection.

The easiest and safest method of non-viral gene transfer is to use naked DNA, which can either be injected directly into the target tissue or introduced by systemic

injection. Limitations in expression levels are inevitable, because of rapid degradation of DNA by nucleases in the serum as well as clearance of DNA by the mononuclear phagocyte system (Niidome and Huang, 2002). Improvements in the efficiency of gene transfer and expression have been achieved by developing various physical methods. Enhanced gene uptake into cells after injecting naked DNA has been achieved by an opening of the cell membrane in response to an electric field impulse, the so-called electroporation method. Electroporation can lead to long-lasting expression and is applicable to various tissues. Another method is to use a 'gene gun' to deliver the DNA directly into the target tissue or cells. Direct penetration through the cell membrane is achieved by shooting gold particles coated with DNA with the gene gun. Methods less often used, but also efficient, is ultrasound and hydrodynamic injections (Niidome and Huang, 2002).

Further non-viral methods include the use of chemical carriers. Quite a few different such techniques have been developed, but the most frequently used ones are still lipid-mediated and polymer-mediated gene transfer. Liposome-based gene delivery, based on negatively charged DNA bound to positively charged lipids, was first described by Felgner in 1987. The resulting positively charged complexes are more easily taken up by cells. Two drawbacks of non-viral gene transfer are the lower transfection efficiencies and the transience of gene expression compared with viral gene transfer (Bowers *et al.*, 2011).

1.3 Adeno-associated virus

The adeno-associated virus belongs to the *Dependovirus* genus of the human parvovirus, which is replication-deficient. AAVs have the capacity to transduce both dividing and non-dividing cells (including neurons) with the same level of efficiency (Grimm and Kleinschmidt, 1999; d'Azzo, 2003). The human AAV was discovered in 1965 as a contaminant of an adenovirus preparation (Gonçalves, 2005). AAVs are capable of transducing a wide variety of human and animal cell types; they establish long-term transgene expression primarily in tissues composed of slow-growing or post-mitotic cells (Matsushita *et al.*, 1998). As described by Monahan and Samulski in 2000, the most attractive features of this virus type are the following, which encourage the use of AAV-based vectors in human trials.

1) Capacity of latent infection through integration in the host genome

2) The lack of pathogenic or inflammatory side effects; member of this genus are not associated with human diseases

3) Stable long-term expression of transgene (Van Vliet et al., 2008).

1.3.1 Serotypes

About 50 to 90% of the human population are positive for AAV serotypes, whereas 80% of the population is specifically seropositive for AAV2 (Gonçalves, 2005; Vasileva and Jessberge, 2005). AAV2 has been detected in the human genital tract (Lai *et al.*, 2002). Table 2 below gives an overview of the different serotypes of AAVs found so far and their cell tropism.

Table 2: Overview of AAV serotypes
The table presents an overview of the different serotypes, their origin and their specific transduction site (modified after Lai *et al.*, 2002; Kremer, 2005; Büning *et al.*, 2008; Weitzman and Linden, 2011).

Serotype	Origin	Transduction site
1	Primates	Muscle, arthritic joints, heart and liver
2	Human	Muscle, liver, brain, retina and lungs
3	Human	Cochlear inner hair cells
4	Primates	Brain
5	Human	CNS, lung, eye and liver
6	Human	Muscle, heart and airway epithelium
7	Rhesus monkey	Muscle
8	Rhesus monkey	Muscle, pancreas, heart and liver
9	Primates	Spinal cord
10	Primates	Muscle
11	Primates	Muscle

Its broad host range has extended the applicability of AAV for gene therapy from preliminary animal experiments to human clinical trials (Lai *et al.*, 2002). AAVs have never been associated with any human disease. Because of this, they have the highest biosafety ratings of all gene-transfer vectors of viral origin (Grimm and Kleinschmidt, 1999; Mueller and Flotte, 2008).

1.3.2 Biology of adeno-associated viruses

AAV is a small (25 nm), non-enveloped virus consisting of a single-stranded DNA genome (Daya and Berns, 2008). AAV particles are resistant to heat and low pH and even to some detergents and solvents. Thus AAVs are particularly stable in comparison with most other viral vectors (Lai *et al.*, 2002).

1.3.2.1 Genome

AAVs are 4.7 kb linear single-stranded DNA viruses (Kremer, 2005). The structural organisation of the genome (Fig. 3) is characterised by three functional regions: two open-reading frames which are flanked by 145 nucleotide-long inverted terminal repeats (Büning *et al.*, 2008). The ITRs, acting in *cis,* play a key role as origin of replication. Proteins essential for the viral capsid (VP1, VP2 and VP3) are produced by the Cap (capsid) gene under the control of the P40 promoter located in the right ORF. Alternative splicing of the P40 transcript occurs: VP1 (87 kDa) is produced by the unspliced transcript whereas the spliced transcript produces VP2 (72 kDa) and VP3 (62 kDa). The four Rep proteins, Rep78, Rep68, Rep52 and Rep40 are produced by the Rep (replication) gene located on the left ORF. Two different promoters are required; the transcripts using the P5 promoter produce Rep78 and Rep68 whereas Rep52 and Rep40 are produced from the transcripts using the P19 promoter. In all phases of AAV's life cycle the *trans*-acting proteins Rep78 and Rep68 are important. Rep52 and Rep40 are involved in the accumulation of single-stranded viral DNA used for packaging within AAV capsids (Gonçalves, 2005; Büning *et al.*, 2008; Daya and Berns, 2008).
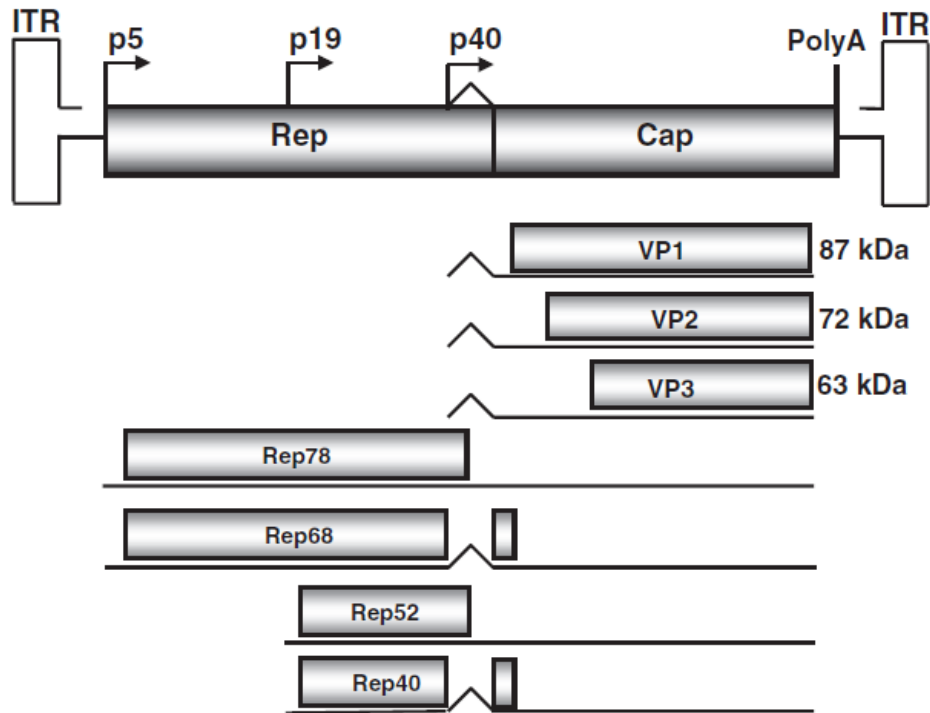
Figure 3: Genomic structure of AAVs
ORFs are flanked by the ITRs; indication of all three promoters in the map. The generation of Rep and Cap proteins is due to alternative splicing of mRNA transcripts derived from all promoters (Van Vliet *et al.*, 2008).

1.3.2.2 Viral particles

Each AAV viral particle (virion) is 20–25 nm in diameter and has an icosahedral structure. The virion is composed of 60 copies of the three viral proteins: 5-10% Vp1 and Vp2, and 80-90% of Vp3 subunits (the molar ratio is 1:1:10) (Wang *et al.*, 2011; Weitzman and Linden, 2011). VP1 and VP2 proteins share the VP3 sequence but differ from it in having additional residues at their N termini. VP1 has a unique conserved phospholipase A$_2$ (PLA2) motif, which seems to play a general role in virus infection as well as in virus escape from the endosome. Recently it has been shown that conformational changes of the virion structure during infection lead the VP1 N termini to protrude through the capsid pores, inducing the PLA2 enzymatic activity that is required for successful infection. VP2 is required neither for infection nor for assembly. The core of VP3 consists of a conserved β-barrel composed of antiparallel β-sheets. The motif is found in many different parvoviruses, but especially the interstrand loops are variable. These loops determine the serotype and therefore the receptor type used to bind to cells before infection. It has been shown that during

formation of the virion VP1 and VP2 are situated in the nuclei of infected cells whereas VP3 is nearly evenly distributed throughout the nucleus and the cytoplasm (Lai *et al.*, 2002; Gonçalves, 2005; Weitzman and Linden, 2011). Interestingly, the structural proteins for AAV assemble into empty capsids and the genome is packaged into the preformed empty capsids. During the course of infection, the number of empty viral particles decreases at the same rate as the number of DNA-containing mature virions increases. (Van Vliet *et al.*, 2008).

The differences among the capsid protein sequences result in the various serotypes as described above, leading to the use of different cell-surface receptors for cell entry. Plus and minus single strands are packaged separately into virus particles (Lai *et al.*, 2002).

1.4 Adeno-associated virus based gene transfer

AAV-based gene transfer could be a promising tool for the treatment of CNS impairments associated with lysosomal storage disorders (Sands and Haskins, 2008). An interesting feature is the alteration of tropism by pseudotyping the recombinant vectors with capsids from other AAV serotypes. AAV integrates site-specifically into the human chromosome 19 (Lai *et al.*, 2002).

1.4.1 Production systems

Traditionally, the production of recombinant AAV vectors was based on cotransfection with two further plasmids. The vector plasmid which carries the transgene expression cassette flanked by AAV-inverted terminal repeats acting in *cis* and the helper plasmid supplementing the AAV structural (c*ap*) and non-structural (*rep*) genes were cotransfected into helper adenovirus- or herpesvirus-infected cells, thus providing the necessary proteins in *trans*. Furthermore, the vector was amplified and packaged into AAV capsids giving rise to recombinant virus particles containing the transgene of interest (Grimm and Kleinschmidt, 1999; Kremer, 2005; Daya and Berns, 2008). The following drawbacks were encountered when this method was used:

1) Presence of helper virus

2) Contamination with wild-type virus was often observed

3) Large production scale which might be required to treat large populations of patients, was not possible

To overcome these problems, and in order to get rid of the adenovirus, in the mid 90´s the adenovirus-dependent coding regions (virus-associated RNAs, E4 orf6 and E2A genes) required for vector production were identified and cloned into a plasmid. Furthermore, the E1-encoded proteins, which are also needed, are supplied by the producer cells (often AAV-293 cells) (Kremer, 2005; Büning *et al.*, 2008).

In general, for gene therapy the two ORFs of the parental virus are replaced by the transgene cassette, leaving only the two ITR sequences, which are the required *cis*-acting elements. The excised proteins required can be provided in *trans*.

1.4.2 AAV infection

Viral infection is a multistep process that requires virions to pass through a series of barriers (receptor binding, cell entry, intracellular trafficking, endosomal release, viral uncoating or nuclear entry) before delivering the genome into the nucleus for replication (Büning *et al.*, 2008).

AAV2 virions contact the cell membrane several times before being internalised by the interaction with the cellular receptor heparin sulfate proteoglycan or the fibroblast growth factor 1. The interactions are further enhanced by various coreceptors, of which six are known so far (Daya and Berns, 2008). The docking site on the viral capsid has been mapped to amino acids 585–588, with two relevant arginine residues at positions 585 and 588 (Weitzman and Linden, 2011).

 AAV trafficking after transfection is not understood in all details, but it seems likely that the virions are endocytosed into clathrin-coated vesicles. The endosomal acidification triggers conformational changes of the viral capsid, leading to exposure of previously hidden regions. This region is the N terminus of VP1, which is required for endosomal escape (Gonçalves, 2005; Büning *et al.*, 2008). For intracellular trafficking and cellular signalling the protein Rac1 and the phosphatidylinositol 3-

kinase pathway are required (Daya and Berns, 2008). Mobilisation of AAV2 into the nucleus was shown to be supported by MG-132, a strong inhibitor of chymotrypsin-like activity of the proteasome (Wang *et al.*, 2011). Once the AAV has entered the nucleus there are two distinct and interchangeable pathways of its life cycle that it can follow: the lytic or the lysogenic pathway. The lytic pathway develops in cells that are also infected by a helper virus, whereas the lysogenic pathway is established in cells in the absence of any helper virus. When an AAV infects a human cell alone, the gene-expression programme is auto-repressed, and latency ensues by preferential integration of the viral genome into a region of roughly 2 kb on the long arm of human chromosome 19, as mentioned above (Gonçalves, 2005). The single-stranded genome of AAV must be converted into a double strand for transcription (Lai *et al.*, 2002). It has been found that the conversion of the single-strand DNA vector genome into a double-stranded DNA is the rate-limiting step in transduction (McCarty, 2008). Rep activities are essential for DNA replication steps as they inhibit cell proliferation. AAV2 gene expression is tightly regulated through the repressive effects of cellular factors and the viral Rep protein. The Rep proteins can mediate both activation and repression of AAV transcription (Weitzman and Linden, 2011). Afterwards the AAV needs to be uncoated before it is integrated into the host genome and expression of the transgene is possible.

1.5 Blood–brain barrier

The blood–brain barrier (BBB) plays a central role in regulating the chemical microenvironment of the CNS by preventing simple diffusion of most small molecules and proteins from the bloodstream into the brain (Spencer and Verma, 2007). Furthermore, under physiological conditions the BBB ensures a constant supply of nutrients (oxygen, glucose and other substances) for brain cells and guides inflammatory cells to respond to the changes of local environment (Persidsky *et al.*, 2006). The blood-brain barrier consists of three sites; cerebral capillary endothelium, choroid plexus epithelium and arachnoid membranes (Rapoport, 1996). Each consists of tight junctions (zonulae occuldens) and transport between microvascular endothelial cells and low vesicular transport which build the physical barrier of the blood-brain barrier (Pardridge, 2005; Bowers *et al.*, 2011). Moreover, the brain

microvascular endothelial cells interact closely with other components of the neurovascular unit (astrocytes, basement membrane, pericytes and neurons). The brain microvascular endothelial cells perform essential biological functions – including barrier, transport of micronutrients and macronutrients, receptor-mediated signalling, leukocyte-trafficking and osmoregulation – and are situated at the interface between the blood and the brain. 99% of the BBB endothelium is enveloped by astrocytes, which interact with endothelial cells and therefore induce and modulate the development of the BBB. Endothelial cell proliferation, survival, migration, differentiation and vascular branching are regulated by the association of pericytes to blood vessels. Tight regulation of the microcirculation and the tissue it supplies is required for a high level of neuronal activity and for the dynamic nature of their metabolic requirements. The extracellular matrix of the basement membrane also interacts with the cerebral microvascular endothelium and is involved in the maintenance of tight junctions. Tight junctions are composed of the integral transmembrane proteins, occcludins, claudins and junctional adhesion molecules (Persidsky *et al.*, 2006).

Specialised transporter systems present on the luminal and abluminal membranes of the endothelial cells tightly regulate the molecular traffic in and out of the CNS. Exceptions to the rule are some (2%) small molecules (size of 400–500 Da) such as oxygen and carbon dioxide gases and also some lipid-soluble proteins, which can freely diffuse across the cellular membranes. As a result, most gene-transfer vehicles are efficiently excluded by the blood–brain barrier (Pardridge, 2005; Bowers *et al.*, 2011). The blood–brain barrier transporters are classified into three groups: carrier-mediated transporters, active efflux transporters and receptor-mediated transporters (Pardridge, 2005). The transport of almost all larger proteins to the CNS occurs by receptor-mediated transcytosis. The well-characterised blood–brain barrier receptors are as follows:

1) Low-density lipoprotein receptor
2) Transferrin receptor
3) Insulin-like growth factor receptor

So far, gene delivery by viral vectors has been found to be mediated by stereotactic injections into the CNS, which results only in localised gene expression. Therefore,

owing to the size of the human brain, too many injections would be required to allow widespread expression. A major challenge for the treatment of brain disorders is to overcome the blood–brain barrier to deliver therapeutic macromolecules to the whole brain. Different approaches to target these proteins to the CNS across the blood–brain barrier are required for treating neural degenerative conditions by using blood–brain barrier receptors (Spencer and Verma, 2007).

1.5.1 Low-density lipoprotein receptors as possible transport mechanism

The low-density lipoprotein receptor (LDLR) family is a cell-surface transmembrane glycoprotein that recognises extracellular ligands and internalise them for degradation by lysosomes. Naturally, LDLRs play a crucial role in cholesterol homeostasis (Hussain *et al.*, 1999; Spencer and Verma, 2007). About 10 different receptors, which are expressed in a tissue-specific manner and primarily bind apolipoprotein complexes, make up this family (Spencer and Verma, 2007). All members of the family share four major structural modules: the cysteine-rich complement-type repeats, epidermal growth factor precursor-like repeats, a transmembrane domain and a cytoplasmic domain. The complement-type repeats comprise about 40 amino acids, containing six cysteine residues per repeat, and constitute a ligand-binding motif. The members of the LDLR family are transmembrane glycoproteins containing large extracellular domains; while the intracellular domains are comparatively short (Hussain *et al.*, 1999).

In general, apolipoproteins bind lipids in the bloodstream and target them for lysosomal degradation by binding to LDLR on the cell surface of the target cell, which leads to an endocytosis of the complex. The receptors bind their ligands with high affinity. In the LDLR family, receptors display negative charges on their surfaces and their ligands present positive charges. The most prominent members of the apolipoproteins are apolipoprotein B (ApoB) and apolipoprotein E (ApoE). The conversion to an early endosome and the resulting lower compartmental pH lead to a release of the apolipoprotein complex and to a recycling of the receptor (Spencer and Verma, 2007). The transport of the apolipoprotein complexes form the endoplasmatic reticulum to the Golgi seems to be the rate-limiting step in transport (Twisk *et al.*, 2000). Expression of all members of the low-density lipoprotein receptors are

regulated by hormones and growth factors (Hussain *et al.*, 1999). At the blood-brain barrier apolipoproteins are bound by LDLRs and are transcytosed into the abluminal side of the blood-brain barrier, where they are taken up by neurons and/or astrocytes (Spencer and Verma, 2007). Therefore, LDLRs are of great interest as transporting systems to cross the blood-brain barrier in gene therapy. In order to exploit this possibility, proteins for gene therapy are fused with apolipoproteins to form complexes that are able to bind to LDLRs. Such complexes are expected to make the transport of proteins across the blood–brain barrier possible.

1.6 Biology of cortical organotypic brain slice cultures

Organotypic brain cultures were originally developed by Gahwiler in 1981, providing a three-dimensional model of functional brain tissue (Lossi *et al.*, 2009). Organotypic brain-slice models offer the following unique advantages:

1) Maintenance of the morphological cryoarchitecture of the tissue
2) and therefore the interactions of several cell types of the brain tissue being studied (such as glial-neuronal cells)
3) Maintenance of neuronal activities with intact functional local synaptic circuitry
4) Maintenance of tissue-specific cell connections
5) The possibility of use for studying viral life cycles
6) More ready manipulation than is allowed by organ culture
7) The possibility of use for studying some immune functions (Benbrook, 2006; Cho *et al.*, 2007; Lossi *et al.*, 2009).

In summary, organotypic slice cultures represent a complex multi-cellular *in vitro* environment (Murphy and Messer, 2000; Cho *et al.*, 2007; Su *et al.*, 2011). For this reason they represent a step between monolayer cultures and *in* vivo models (Benbrook, 2006; Cavaliere and Matute, 2011). They have become a powerful tool for studying cell damage in various neuropathological states (Su *et al.*, 2011). Furthermore, they have already been used as models for stroke, epilepsy, neuronal injury and neuroprotection (Staal *et al.*, 2011).

Several different methods have been developed to maintain thin slices of brain tissue in order to keep them alive in long-term cultures. In general, best results were achieved when using animals at postnatal days 3–9 to prepare organotypic slice cultures. The advantage of using brain tissue of such young animals is that this yields viable and healthy cultures owing to the high degree of plasticity and resistance to mechanical trauma during slice preparation. Post-natal slice cultures can be maintained *in vitro* for days to weeks, during which developmental maturation of brain tissue continues *ex vivo* (Cho *et al.*, 2007). Most of the studies to characterise organotypic brain-slice cultures have been performed on samples from the hippocampus, as this is the ideal model to study synaptic connections. In order to overcome the lack of studies of the cortical neuronal changes following the culture of whole-brain slices, Staal *et al.* (2011) investigated cell survival as well as the cellular and protein expression alterations of whole-brain-slice cultures from mice of different ages (neonates, young and mature adult mice). These experiments also illustrated the significant vulnerability of long-term culture of slices derived from neonates. De Simoni *et al.* (2003) showed that organotypic slices cultured for 1, 2 or 3 weeks *in vitro* were developmentally equivalent to brain slices dissected on post-natal day 14, 17 or 21. This equivalence was shown by the number of primary branches, the total length of neurons, the outgrowth of apical dendrites, and spine density. The existing basic synaptic connections at early ages become progressively elaborated to form mature synaptic networks which largely mimic the endogenous developmental changes in the brain during the first few weeks after birth (Cho *et al.*, 2007).

1.7 Aim of this study

Gaucher's disease is a rare lysosomal storage disorder caused by a defect in the gene coding for β-glucocerebrosidase. This defect results in reduced GCase activity leading to an accumulation of the storage material glucosylceramide. Three clinical types of Gaucher's disease have been described; in type I only the periphery is involved, whereas in type II and type III also the CNS is involved, leading to a much earlier death of patients than in type I. In recent years increasing attention has been paid to developing gene-therapeutic approaches in order to find possible ways to transport therapeutic enzymes across the blood–brain barrier.

The aim of the present study was to develop adeno-associated vectors for proof-of-principle experiments in order to find a possible therapeutic approach to treat Gaucher's disease type II patients. AAVs were planned to be developed that express a transgene (*lacZ* as reporter gene and *hGCase* as transgene) fused to the gene expressing the low-density binding domain of ApoB. The transfection efficiency of the vectors developed and their expression potential as well as the activity of the transgene expressing β-glucocerebrosidase were to be investigated and evaluated. Using a fusion protein with ApoB was thought to be useful in overcoming the blood–brain barrier when testing the AAVs in K14 animals. However, the animal experiments planned in this study were cancelled owing to transport and breeding problems. Instead, a model which presents a situation between the *in vitro* and the *in vivo* situations was to be established. Therefore, cortical organotypic brain-slices from K14 mice were to be used to provide a model for Gaucher's disease type II. Proof-of principle experiments were to be performed in the established cortical organotypic brain-slice cultures by transducing them in two different ways using the developed AAVs. The investigations conducted in this study were part of the research programme of the BMBF consortium "Innovative Gene & Cell Therapy for Gaucher Disease Type 2."

My own investigations were split into the following steps:

1) Characterisation of K14 lnl mouse model
2) Establishment of a GCase activity assay
3) Cloning of adeno-associated viral vectors
4) Testing and evaluating the cloned vectors in fibroblasts and primary neurons

5) Packaging of viruses by using AAV-293 cells and testing transduction efficiency of lacZ transduced AAV-HT1080 cells

6) Establishment and characterisation of cortical organotypic brain-slice cultures as Gaucher's disease type II model

7) Proof-of-principle experiments on differently packed AAV2s by evaluating their efficiency in cortical organotypic brain-slice cultures.

2. Animals, Materials and Methods

2.1 Animals and animal housing

K14 lnl mice (supplied by Genzyme Co., USA) were housed in cages and fed with standard rodent pellets and water *ad libitum.* Animals were kept in a climate- and light-controlled room (temperature 22 ± 0.5 °C; relative humidity between 50% and 60%; 12-hour light/dark cycle). Breeding of K14 lnl mice is only possible with heterozygous mice, as the homozygous mice die within two weeks. Breeding was controlled at the FEM (Forschungseinrichtung für Experimentelle Medizin; situated at Bayer Schering AG, Berlin). All K14 ko and wt mice were used for experiments at an age of 8–10 days if not otherwise stated. All standard guidelines of the Animal Care Committee of the Senate of Berlin were strictly followed and the number of killed animals was reported annually.

2.2 Materials

2.2.1 Chemicals and reagents

All standard chemicals and reagents were purchased from Merck, Roth and Sigma-Aldrich unless indicated otherwise.

4-Methylumbelliferyl- β-D-glucopyranoside	Sigma
β-Mercaptoethanol Ampicillin	Stratagene
Agarose	Carl Roth
Camptothecin	peQLab
Chloroform	Carl Roth
Complete Proteinase Inhibitor Cocktail	J.T. Baker
Conduritol B epoxide	Roche Diagnostics.
Ethidium bromide	Sigma

Glycine	Merck
Kanamycin	Serva E.
Luria–Bertani (LB) Agar	Carl Roth
Luria–Bertani (LB) Media	Carl Roth
Low-melting agarose	Carl Roth
Magnesium chloride ($MgCl_2$)	peQlab
Magnesium sulfate heptahydrate ($MgSO_4 \cdot 7H_2O$)	Roboklon
Methanol	Merck
N-(2-Hydroxyethyl)piperazine-N`-2-ethane sulfonic acid (HEPES)	J.T. Baker
Protein Hydrolysate NZ-amine AS	Serva E.
Non fat dried milk powder	Sigma
Normal goat serum	AppliChem
Sodium bicarbonate ($NaHCO_3$)	Vector Laboratories
TEMED	Riedel de Haen
Tetracycline	Carl Roth
Triton X-100	Carl Roth
Rotiphorese Gel 40	Merck
Yeast extract	Carl Roth

2.2.2 Oligodeoxynucleotides

Table 3: Oligonucleotides purchased from TIBMOLBIOL
Primer names, length (bp), sequences, melting temperature (Tm) and orientation – either sense (se) or anti-sense (as) – are given. Names indicate the respective target genes.

Name	Sequence (5' – 3')	bp	Tm (°C)	Primer type
β-globin Fwd	attctgagtccaagctaggc	20	52.9	se
Cre for 14	ttcccgcagaacctgaagatg	21	60.2	se
Cre rev 14	tcccaagaaatgccagattacg	22	58.8	as
GCEcoRVneu	atagatatcggccggatccgccatgtctgc	30	68.2	se
GCHINDIII.rev	gtgaagcttggcctctcttccgggtcagc	29	69.7	as
GCWT.for	tgttccccaacacaatgctcttt	23	61.2	se
GCWT.rev	tctgtgactctgatgccaccttg	23	60.2	as
hGHpolyA Rev	tagaaggacacctagtcaga	20	46.1	as
Neo.new.rev	aagacagaataaaacgcacgggtg	24	62.2	as
pQE-TriSysF	gttattgtgctgtctcatcattt	23	51.6	se
pQE-TriSysR	tcgatctcagtggtatttgtga	22	52.9	as

2.2.3 Enzymes

Table 4: Enzymes used in this study
Enzyme names, restriction sites for restriction enzymes, and manufacturers are given.

Name	Restriction Site	Company
Proteinase K		Carl Roth
Restriction enzymes		Fermentas
AfeI (Eco47III)	AGCGCT	
BamHI	GGATCC	
EcoRI	GAATTC	

EcoRV (Eco32I)	GATATC	
HindIII	AAGCTT	
KpnI	GGTACC	
T4 DNA ligase		Fermentas
Taq DNA polymerase		Roboklon
Thermosensitive alkaline phosphatase		Fermentas

2.2.4 Antibodies

Table 5: Antibodies
This table gives information on the type of antibody (monoclonal or polyclonal), the species it was derived from, the application (IF = immunofluorescence, IHC = immunohistochemistry, WB = western blot) and the manufacturer.

Antibody	Application	Company
Goat anti-mouse Alexa Fluor 488	IF	Molecular Probes
Goat anti-rabbit Alex Fluor 546	IF	Molecular Probes
Goat anti-rabbit Alexa Fluor 488	IF	Molecular Probes
Goat anti-rabbit Alexa Fluor 546	IF	Molecular Probes
Goat anti-rat Alexa Fluor 488	IF	Molecular Probes
Monoclonal mouse antibodies		
anti-human 8E4 (β-glucocerebrosidase)	IF, WB	Genzyme Corporation
anti-GFAP	IF, WB	Sigma
anti-HA Taq	If, WB	Sigma
anti-Map2	IF, WB	Synaptic Systems
anti-NeuN	IF, WB	Chemicon
anti-Synaptophysin 1	IF, WB	Synaptic Systems
Monoclonal rat antibodies		

anti-CD68	WB	AbD serotec
Peroxidase labelled anti-goat	WB	Vector Laboratories
Peroxidase labelled anti-mouse	WB	Vector Laboratories
Peroxidase labelled anti-rabbit	WB	Vector Laboratories
Polyclonal rabbit antibodies		
anti-GAPDH	WB	Synaptic Systems
anti-Glucocerebrosidase	IF, IHC, WB	Sigma

2.2.5 Kits

AAV2 Helper-Free System	Agilent Technologies
Amaxa Mouse Neuron Nucleofector Kit	Lonza
Beta-Galactosidase Staining Kit	Promo Kine
Gene Jet Gel Extraction Kit	Fermentas
jetPEI® DNA transfection reagent	Polyplus transfection
LDH-Cytotoxicity Assay Kit II	Abcam
Pierce BCA Protein Assay Kit	Thermo Scientific
Pure Link Quick Plasmid Miniprep Kit	Invitrogen
QIA filter Maxi Kit (EndoFree)	Qiagen
QIA quick PCR Purification Kit	Qiagen

2.2.6 Cell culture reagents

2-Mercaptoethanol	GIBCO
B27 Supplement (serum free)	Invitrogen
N,N-Dimethylformamide (DMF)	Merck
DMEM Media, 4.5 g/l glucose, sterile	Invitrogen

Dimethylsulfoxide   Sigma

GlutaMax1 (100x)   Invitrogen

Foetal bovine serum (FBS; heat-inactivated)   Invitrogen

Hank´s salt solution with Ca^{2+}, Mg^{2+} Biochrom

Hank´s salt solution without Ca^{2+}, Mg^{2+} Biochrom

HYLO Glue 111   Maston-Domsel

Neurobasal media (-L Glutamine)   Invitrogen

Normal horse serum   Invitrogen

Penicillin/Streptomycin (10,000U/1,000 µg/ml)   Invitrogen

Poly-D-Lysine   Sigma

RPMI Media 1640   Invitrogen

Typan Blue stain (0.4%)   Sigma

X-Gal   Carl Roth

2.2.7 Bacterial strains

Table 6: Bacterial strains
This table gives information on the genotype of the different bacterial strains used in the present study and their origin.

Genotype of bacteria	Origin
E. coli M15 [pREP 4](NalS, StrS, RifS, Thi-, Lac-, Ara+, Gal+, Mtl-, F-, RecA+, Uvr+, Lon+)	Received from J.L. Körner
E. coli XL 10-Gold Ultracompetent Cells (TetrΔ(mcrA)183 Δ(mcrCB-hsdSMR-mrr)173 endA1 supE44 thi-1 recA1 gyrA96 relA1 lac The [F' proAV lac1qZΔM15 Tn10 (Tetr) Amy Camr])	Stratagene

2.2.8 Plasmids

Table 7: Plasmids used in this study
Name, size (kb), use and origin of each plasmid used in this study are given.

Plasmid name	Size (kb)	Use	Origin
pAAV.CMV_sGBA_HA_ApoB	6.5	Cloned vector for AAV2 production and GCase expression	Own work
pAAV.MCS	4.6	Shuttle vector for AAV2 production	Agilent Tech.
pAAV.LacZ	7.3	Control vector for viral titre measurement	Agilent Tech.
pAAV.RC	7.3	Required for AAV2 production	Agilent Tech.
pFB.CAG_sGBA__ApoB	8.8	Second vector for AAV2 production and GCase expression	Provided by N. Jäschke
pFB.CMV_sGBA	7.9	Isolation of *GCase* cDNA	Provided by N. Jäschke
pHelper	11.6	Required for AAV2 production	Agilent Tech.
pQE-TriSystem	5.8	Used for in-between cloning step	Qiagen
pQE-TriSystem_hGC	7.7	Isolation of gene of interest	Own work

Graphic maps of plasmids used for cloning in this study are given in Section 11.2 unless indicated otherwise

2.2.9 Cells

AAV-293 cells	Agilent Tech.
AAV-HT1080 cells	Agilent Tech.
Fibroblasts derived from an healthy individual, gender and age unknown	Provided by M. Swierczek
Fibroblasts derived from a Gaucher patient of either type II or III, gender and age unknown	Provided by M. Swierczek

2.2.10 Other materials and equipment

96-well plate (Rotilab®-Micotestplates; F-Profil)	Carl Roth
ABC Kit	Vector Laboratories
Amersham Hyperfilm ECL	GE Healthcare
Binocular (Olympus SZX9)	Olympus Optical Co.
BioNate3	Thermoscientific
Cell culture dish (10 cm^2)	BD Falcon
Cell culture flasks (25 cm^2, 75 cm^2, 175 cm^2)	BD Falcon
Cell culture plates (6- and 12-well)	Sarstedt
Cell scraper	Sarstedt
Cell Strainer 70µm	BD Bioscience
Citrate buffer	DAkO Diagnostics
Cryostat	Carl Roth
Direct PCR Tail	peQLab
Drigalski spatula	Carl Roth
dNTP-mix	Carl Roth
ELISA Reader (ELX 800 Universal MicroPlate Reader)	Bio-Tek Instruments
Electrophoresis apparatus (Power Pac 300)	Bio Rad

Entellan	Merck
Eppendorf centrifuge (5804R)	Thermoscientific
Falcon tubes (15 ml and 50 ml)	BD Bioscience
Freezer	
–20 °C	Liebherr Comfort
–80 °C	DanYo
GeneRuler 100bp DNA ladder (ready-to-use)	Fermentas
GeneRuler 1kb DNA ladder (ready-to-use)	Fermentas
Histoacryl glue	Aesculap
Hydromount	National Diagnostics
Immobilon PVDF membrane	Millipore
Incubator (Nuaire TS Autoflow)	Nuaire
Instruments (sterile)	Aesculap
Inverted microscope (Olympus IX70)	Olympus Optical Co.
Cryo tubes	VWR International
Laminar Air	Heraeus Instruments
Marker Spectra^{TM} Multicolor Broad Range	Thermoscientific
Nucleofector	Lonza
Nucleopore Track-Etch membrane (25mm, 8µm)	Whartman
Neubauer improved cell-counting chamber	Carl Roth
Object slides (Superfrost)	R. Langenbrinck, Labor & Medizintechnik
Pipette tips	Eppendorf
PCR tubes (Multi®-Ultra Tubes 0.65ml)	Carl Roth
Stainless steel blades	Campden Instruments
Sonificator (UP 100 H)	Hielscher Technology
Synergy 2	BioTek

Thermomixer compact	Eppendorf
Thermocycler (T3 Thermocycler)	Biometra
Raven Incubator	LTE Scientific
Reaction tubes (0.5/ 1/ 2ml)	Eppendorf
UV-Light (HITACHI CCD-KP161)	Campden Instruments
Vibratome (Integraslice 7550MM)	Campden Instruments
Water bath (GFL 1083)	Gesellschaft für Labortechnik
Western Blot; blotting chamber	Bio Rad
Western Blot Fixative (PP X-Omat Lo)	Kodak
Western Lightning® Plus-ECL	Perkin Elmer
Western Blot; gel chamber (Mini Protean 3 Cell)	Bio Rad
Western Blot Developer (X-Omat Ex11)	Kodak

2.3 Genotyping of K14 lnl mice

2.3.1 Lysis of tail biopsies

Tail biopsies from P1-P3 old K14 lnl mice were lysed with 200 µl of Direct PCR tail buffer with 5 µl of Proteinase K at 55 °C, 1400 rpm in a Thermomixer compact until the tail was fully lysed. For inactivation of the enzyme Proteinase K the samples were heated to 85° C for 15 min. Samples were cooled to 4 °C before use in the polymerase chain reaction.

2.3.2 Lysis of embryonic K14 lnl mouse brain

A small piece of embryonic (E15-E16) cerebella mouse brain was transferred into a 1.5 ml reaction tube containing 0.5 ml of lysis buffer. Resuspending the brain was performed by pipetting it up and down until all pieces were dissolved. The sample was incubated for 5 min at 55 °C, at 1400 rpm in a heating block (Thermomixer

compact). Afterwards the samples were heated to 100 °C for 10 min in order to destroy the activity of the enzyme Proteinase K. The DNA was used in the following PCR amplifications.

<u>Lysis Buffer:</u> 10 mM Tris-HCl, 100 mM NaCl containing 10 mg/ml Proteinase K (freshly added)

2.3.3 Polymerase chain reaction (PCR) of tail biopsies and mouse brain

Two different genes (GC and Cre) were assayed by PCR to determine the genotype of each K14 lnl mouse. The DNA used in the PCR reaction was extracted by lysis of tail biopsies (2.3.1) or the mouse embryonic brain (2.3.2). In order to amplify the GC gene a set of three primers was used: GCwt.fwd, GCwt.rev and Neo.new.rev. Sequences and amplification temperatures are given in Table 3. A set of two primers, Cre for 14 and Cre rev 14, was used to amplify the Cre gene.

Each PCR reaction had a total volume of 30 µl and contained 10 x Puffer A, 2.5 mM MgCl$_2$ (stock: 25 mM MgCl$_2$), 1 µl DNA, 0.5 µM of each primer (stock: 10 µM), 200 µM of dNTP mix and 0.75 U Taq Polymerase (stock: 5 U/µl) in ddH$_2$O.

PCR amplification was run in the Thermocycler (T3 Thermocycler) following the protocol given in Table 8 and Table 9 as recommended by Genzyme Co.

Table 8: PCR programme to amplify the GC gene

Steps in PCR amplification	Temperature	Time
1. Initial denaturation	94 °C	2 min
2. Denaturation	94 °C	30 sec
3. Annealing	61 °C	30 sec
4. Extension (Repeating steps 2-4 for 35 cycles)	72 °C	1 min
5. Final extension	72 °C	8 min

Table 9: PCR programme to amplify the Cre gene

Steps in PCR amplification	Temperature	Time
1. Initial denaturation	94 °C	2 min
2. Denaturation	94 °C	1 min
3. Annealing	56 °C	1 min
4. Extension (Repeating steps 2-4 for 35 cycles)	72 °C	1 min
5. Final extension	72 °C	5 min

The amplified PCR products were analysed by Gel electrophoresis (2.3.4). In case of the GC gene two different fragments were possible, the wt fragment at 837 bp or the ko fragment at 413 bp identifying the genotype of each mouse. In case of the Cre gene either a fragment was visible at 300 bp or none at all. This information was

required for breeding K14 lnl mice and for their use in further experiments as described in Section 2.1.

2.3.4 Agarose gel electrophoresis

PCR products were analysed by agarose gel electrophoresis. Each PCR sample was mixed with 3 µl of DNA sample buffer and 10–30 µl of sample was loaded onto a 1.1% agarose gel (1 x TBE, 1.1% agarose and 3.5 µl EtBr). Either a 100 bp or a 1 kbp DNA ladder was run in parallel in order to be able to estimate the size of each PCR product. Electrophoresis was run at 90 volt for 10 min and afterwards constantly at 100 volt for further 30–40 min depending on the size of amplified PCR product. The bands identifying the amplified PCR products were visualised under UV light.

TBE buffer: 10.8 g Tris base, 5.5 g boric acid, 0.8 g EDTA in 1 l dH$_2$O

DNA sample buffer: 5 g saccharose, 25 mg bromphenol blue in 10 ml 1 x TBE

2.4 Immunohistochemistry

One aspect of this work was to characterise the K14 lnl mouse. This was also done by immunohistochemical staining as described in the following sections. Therefore, K14 lnl mice at the age of 7, 11 or 14 days were decapitated, and the brain was isolated and fixated in a 4% PFA solution for one night at 4 °C. Thereafter, brains were washed in dH$_2$O overnight before being processed further.

4% PFA: 10 g PFA was dissolved in 125 ml dH$_2$O at 70 °C, 1 drop of 0.5 N NaOH was added after the PFA was clear, and the mixture was cooled and filtered. Finally 125 ml 2 x PBS (pH 7.4) was added

2.4.1 Paraffin embedding and slicing

Paraffin embedding was performed as routinely done in our laboratory. In brief, each brain was placed in a cassette and went through an ascending alcohol series,

chloroform, a chloroform–histo wax mix and finally into histo wax which was changed 4 times before embedding. Paraffin wax was kept at about 60 °C to keep it fluid. Each brain was orientated in the same direction in a stainless specimen holder in order to keep the same plane for sectioning. Keeping the same plane is important for comparison of different brains after staining. Thereafter, each brain was embedded with paraffin wax inside the specimen holder. Each paraffin block was trimmed to an optimum cutting surface, leaving a small edge of paraffin around the tissue. Sections were cut at 10 µm and transferred with a tiny brush to a water bath at 50 °C in order to flatten the sections before positioning them on an objective slide for further processing.

2.4.2 HE staining of paraffin sections

HE staining is often used to obtain a first overview staining of different tissues. Haemalm is used to colour the nuclei of cells in blue, and eosin to colour various structures in pink. Staining was performed according to standard techniques. Sections were deparaffinised in the following series: 3 x 5 min xylol, 2 x 5 min 100% EtOH, 2 x 5 min 96% EtOH, 1 x 70% EtOH, 2 x 5 min dH_2O. Sections were incubated for 7–10 min with haemalm staining solution in the dark before being rinsed under water for 20–30 min depending on the intensity of blue colour development. Subsequently, sections were incubated with eosin staining solution for 3–5 min, washed with dH_2O, and differentiated in 70% alcohol before being dehydrated in a rising alcohol series and mounted in Entellan. All sections were examined under the light microscope.

Haemalm staining solution: 1g haemalm was dissolved in 1 l dH_2O, 0.2 g sodium iodate, 50 g kalinite, 50 g chloral hydrate, 1 citric acid were added and the mixture filtered

Eosin staining solution: 0.5% from eosin stock solution in 200 ml dH_2O in a glass cell, with addition of 2–3 drops of acetic acid

Eosin stock solution: 1% aqueous solution

2.4.3 Nissl staining of paraffin sections

In this study Nissl staining was used especially to compare the presence and distribution of neurons in K14 ko mouse brains compared with K14 wt mouse brains. In general, Nissl staining is used to stain the cell body, especially the endoplasmatic reticulum.

Sections were deparaffinised as described above (Section 2.4.2) before being incubated in Nissl staining solution for 30–50 min in a water bath. Thereafter, sections were differentiated in a rising alcohol series, cleared in xylene and mounted with Entellan before being examined under the light microscope.

<u>Nissl staining solution:</u> 1 part of stock solution and 19 parts of 1 x PBS

<u>Nissl staining stock solution:</u> 0.2% aqueous solution

2.4.4 Immunoperoxidase staining of paraffin sections

Before the staining procedure, sections need to be "baked" for 60 min in an oven before being deparaffinised in the following series: 3 x 5 min Xylol, 2 x 5 min 100% EtOH, 2 x 5 min 96% EtOH, 1 x 70% EtOH, 2 x 5 min dH_2O. Further processing accorded to standard techniques. In brief, sections were incubated with citrate buffer (DAKO buffer), endogenous peroxidase was blocked with 1% H_2O_2 in 1 x PBS, sections were washed 3 x 5 min in 1 x PBS and unspecific binding was prevented by incubating the slices in blocking solution for 1 hour at RT. Incubation with primary antibody against β-glucocerebrosidase (dilution 1:200) or against GFAP (dilution 1:400) for 2 nights at 4 °C was carried out. Thereafter, sections were washed again for 3 x 5 min in 1 x PBS before being incubated with 1:250 diluted biotiniylated anti-rabbit secondary antibody (Table 5) in 1 x PBS for 1 hour at RT. After repeated washing (3 x 5min in 1 x PBS), sections were incubated with ABC for 30 min in the dark at RT. Sections were washed again and stained for approximately 5 min with DAB staining solution and nickel enhancer. Sections were washed for 5 x 10 min in 1 x PBS before being dehydrated in alcohol and cleared in xylene. Sections were mounted with Entellan. Control experiments included preabsorbtion of the primary antibodies. All stainings were examined under the light microscope.

Blocking solution: PBS, 10% normal serum, 0.5% from 10% Triton X-100 solution

Antibody solution: PBS, 1% normal serum, 0.1% from 10% Triton X-100 solution, specific antibody

DAB staining solution with nickel enhancer: PBS, 1% DAB, with dropwise addition of 1% $CoCl_2$ and 1% NH_4NiSO_4 before starting the reaction by addition of 0.3% H_2O_2

2.5 Methods in molecular biology

2.5.1 General conditions for bacterial cultures

Depending on the different applications, such as cloning, transformation or plasmid isolation, a variety of *E. coli* strains (Table 6) were used in this work.

All *E. coli* strains were cultivated either in LB broth or on LB agar plates. Plasmids used in this work contained the resistance gene against *Amp*, which makes it possible to select positive single colonies that contain the plasmid. The end concentration of *Amp* was 100 µg/ml. A second selectivity is given by the antibiotic resistance of the bacterial strain itself. Table 10 gives information about the resistance of the various bacterial strains used in this study and the end concentrations of antibiotics used for their selection.

Table 10: Bacterial strains and their antibiotic resistance
The table gives information on and concentration of antibiotic required for each bacterial strain used in this study.

Bacterial strain	Antibiotic resistance	End concentration
E. coli M15 [pREP4]	Kanamycin	25 µg/ml
E. coli XL-10 Gold Ultracompetent cells	Tetracycline	12.5 µg/ml

Luria–Bertani broth: 25 g Luria–Bertani broth in 1 l dH$_2$O, autoclaved at 120 °C for 35 min. Storage at 4 °C.

LB-agar: 40 g Luria–Bertani agar in 1 l dH$_2$O, autoclaved at 120 °C for 35 min. Storage at 4 °C.

2.5.2 Creation of TSS-competent *E. coli* M15 [pREP4]

E.coli bacteria are not able to take up spontaneously foreign DNA from different sources. Therefore various methods exist to make the *E.coli* cells competent to take up the foreign DNA. In this work *E. coli* M15 [pREP4] bacteria were made competent by the TSS-method.

To prepare an overnight culture, one colony of *E. coli* M15 [pREP4] bacteria was picked in 10 ml of LB broth containing kanamycin and incubated in a glass reaction tube at 150 rpm, 37 °C. Next morning 2 ml of the overnight culture was used to inoculate 200 ml of LB broth, and bacteria were grown at 150 rpm, 37 °C to an optical density of OD$_{600}$ = 0.5. Thereafter the bacterial suspension was centrifuged at 1200 g, 4 °C for 10 min and the pellet was resuspended on ice in 20 ml TSS medium. The bacterial suspension in TSS medium was stored in 100 µl aliquots at –80 °C.

TSS medium: 42.5 ml LB broth, 5 g PEG-800, 2.5 ml DMSO and 1.25 ml MgCl$_2$ (2 M stock, pH = 6.5)

2.5.3 Heat-shock transformation of various *E. coli* strains

Changing the genetic background of bacterial cells by the introduction of genetic material by bacterial plasmids is called transformation. In this study, transformation of different bacterial strains (see Table 6) depending on the experimental condition was performed by the heat-shock method. An aliquot of 50–100 µl of competent *E. coli* was thawed on ice. Working with XL-10 ultracompetent cells, these bacteria require incubation with 2 µl of β-mercaptoethanol for 30 min on ice, while gently mixing the reaction tube every 10 min. Besides this intermediate step for the XL-10 bacteria, thawed bacteria were mixed with the required amount of DNA (5–10 µl ligation mix or

1–500 ng plasmid DNA) and incubated for 20 min on ice. Thereafter bacteria were heat-shocked for 45 sec at 42 °C in a heating block (Thermomixer compact). This is the critical step during transformation and caution must be taken not to prolong the heat-shock impulse. Thereafter the transformed bacteria were incubated for further 2 min on ice before adding 1 ml of pre-warmed LB medium to the bacteria and incubating the mixture at 150 rpm, 37 °C, for 60 min in the Thermomixer. 100–200 µl of the culture, depending on the bacterial strain, were streaked out with a Drigalski spatula onto an agar plate containing the required antibiotics (see Table 10) and cultivated overnight at 37 °C in an incubator (Raven incubator).

Plates containing single colonies of bacteria which were not immediately used for further experiments could be stored at 4 °C.

2.5.4 Preparation of plasmid DNA

For further analysis positive clones were picked by sterile toothpicks to inoculate either 10 ml LB medium or 100 ml LB medium containing specific antibiotics. Cultures were grown either in an orbital shaker at 150 rpm or in a water bath at 250 rpm

The Pure Link Quick Plasmid Miniprep Kit, following the instruction manual, was used for analytical plasmid preparation. 'Mini' preparation was sufficient in order to verify transformation events or for performing further intermediate cloning steps.

Plasmids required for further cloning experiments or for transfection experiments were isolated with QIA filter Maxi Kit (EndoFree) following the instruction manual.

2.5.5 Determination of DNA concentration

The DNA concentration of plasmids isolated after 'mini' or 'maxi' plasmid preparation was determined by using a photometer (BioNate3; wavelength 260 nm).

2.5.6 Digestion of DNA with restriction enzymes

Restriction enzymes (restriction endonucleases) are generally used to digest DNA at specific restriction sites and therefore lead to either a linearisation of plasmids or to fragmentation of DNA. This method is often used in order to isolate a gene of interest from an already existing vector or to verify the results of ligation/cloning experiments. Each restriction digest of a total volume of 10–60 µl contained 1–5 µg of plasmid DNA, 5–10 units of restriction enzyme (Table 4) and 10 x fast digest buffer in dH$_2$O. The reaction mixture was incubated for 1 hour at 37 °C in a heating block (Thermomixer compact). Thereafter, the DNA fragments were visualised by gel electrophoresis for analysis as described in Section 2.3.4.

In order to get rid of any disturbing buffers after digesting vector DNA, the samples were purified by using the QIA quick PCR Purification Kit as described by the manufacturer.

To prepare DNA fragments for further cloning experiments, DNA was separated by gel electrophoresis at constant 90 V. The required DNA fragment was isolated from agarose gel by using the Gene Jet Gel Extraction Kit, following the instruction manual.

2.5.7 Dephosphorylation of DNA vectors

In order to prevent recirculation of digested vector DNA during ligation experiments a thermosensitive alkaline phosphatase was used. For dephosphorylation reaction, 50 µl of eluted vector DNA (QIA quick PCR Purification Kit), 3 units of Alkaline phosphatase (AP) and 10 x AP buffer in dH$_2$O were mixed and incubated at 37 °C for 1 hour and the reaction was stopped by heating to 65 °C for 15 min in a heating block (Thermomixer compact).

The samples were purified with the QIA quick PCR Purification Kit following the instruction manual in order to prevent any disturbing reaction due to remaining buffers during the following ligation experiments.

2.5.8 Ligation of DNA fragments

For ligation experiments the enzyme T4 DNA ligase was used. The T4 DNA ligase catalyses the ligation by forming a phosphodiester bond between the 3'-hydroxy and 5'-phosphate groups. The only requirement is that the two strands must be compatible with each other. For ligation, the DNA to be inserted must be in a molar ratio of 5:1 or 15:1 to the linearised dephosphorylated vector, depending on the experimental conditions. The total concentration of linear vector DNA should be at least 20 ng. In addition, 1 unit of T4 DNA Ligase and 10 x T4 DNA ligase buffer are required. The reaction mixture was topped up with dH_2O to a total volume of 20 µl. The reaction sample was incubated for 1 hour at 22 °C in a heating block (Thermomixer compact). The reaction was stopped by heating the sample to 65 °C for a further 10 min.

2.5.9 Sequencing

Sequencing was performed by Dr. Martin Meixner. Specific primers required for sequencing are given in Table 3, (except for the standard sequencing primers required, which were added by Dr. Meixner). The resulting sequences were determined by using the NCBI BLAST tool (http://www.ncbi.nlm.nih.gov/BLAST).

2.6 Methods in protein biochemistry

2.6.1 Verification of proteins

2.6.1.1 Extraction of proteins by cell lysis

In order to extract proteins, the total brain and organotypic slices were homogenated, whereas cultivated cells were harvested and lysed in a buffer afterwards.

The total mouse brain or cortical organotypic brain-slices were homogenised in 400 µl of lysis buffer on ice, by using a potter. In the case of cultivated cells, cells were washed with ice cold PBS and afterwards harvested with a cell scraper into 400 µl lysis buffer on ice. The suspension was sonicated at 100% amplitude, 0.5

cycles (ten times). Thereafter the samples were centrifuged at 1000 g, 4 °C for 5 min. After centrifugation, 25 µl of the supernatant was mixed with 4x sample buffer and incubated at 95 °C for 5 min in a heating block for denaturation. The rest of the supernatant was transferred to a new 1.5 ml reaction tube for storage at –20 °C until further experiments were performed.

<u>Lysis buffer:</u> PBS, 0.2% Triton X-100, 1 x Complete Proteinase Inhibitor Cocktail (Stock: 25 x)

<u>PBS:</u> 9.1 mM $Na_2HPO_4*7H_2O$, 1.7 mM NaH_2PO_4, 150 mM NaCl in 1 l dH_2O; adjustment to pH 7.4 with NaOH

<u>4 x Sample buffer:</u> 4 ml H_2O, 1 ml Tris base (stock 0.5 M), 0.8 ml glycerine, 1.6 ml SDS (stock: 10% SDS solution), 0.2 ml bromphenol blue (stock 3% bromphenol blue solution) and 400 µl β-mercaptoethanol

2.6.1.2 Extraction of proteins by freeze-thaw cycle

Cultivated cells were washed with ice-cold PBS and then harvested by using a cell scraper. Each sample went through three cycles of freezing and thawing. In order to do this, each sample was shock-frozen in liquid nitrogen for about 30 sec and thawed at room temperature. The lysed samples were centrifuged at 10,000 g at 4 °C for 10 min. The supernatant was stored at –20 °C until further use.

2.6.1.3 Determination of protein concentration with BCA test

The bicinchoninic acid (BCA) assay was used for colorimetric determination of the total protein concentration of a sample.

The sample was diluted (total brain 1:10, cells and slice cultures 1:3) in lysis buffer. The reaction was performed in a 96-well plate. For this purpose 10 µl of each diluted sample or standard sample was pipetted into sample wells in triplicate. The BCA standard was used in a concentration range of 0–1000 µg/ml. 100 µl of BCA solution was added to each well before incubating the sample plate in an incubator for 30 min

at 37 °C. After incubation, the plate was measured in an ELISA reader at a wavelength of 562 nm and the results transferred to an Excel datasheet for calculation.

<u>BCA solution:</u> 50 vol BCA buffer + 1 vol CuSO$_4$ solution

(50 parts Reagent A + 1 part Reagent B)

<u>BSA standard:</u> 2 mg/ml (w/v) BSA stock in dH$_2$O

2.6.1.4 Western blot

Gel electrophoresis was performed to separate protein mixtures and to analyse them. The methods used corresponded to standard protocols.

The amount of acrylamide in the resolving gel is based on the protein to be analysed and is usually between 7.5% and 12%. In the stacking gel above the resolving gel, the acrylamide concentration is 5%; this is used to "stack" the proteins and allow them to migrate to the resolving gel independently of their molecular weight.

Protein samples were thawed and heated to 60 °C for 5 min in a heating block before applying them at a concentration of 1–4 µg to the wells by using a Hamilton syringe. The protein concentration varied according to the experimental question and the type of material. Electrophoresis was started with a voltage of 90 V DC until all samples migrated through the stacking gel to the resolving gel. Afterwards the voltage was changed to 110 V for 60–90 min, depending on the degree of separation required.

<u>Gel buffer 1:</u> 45.41 g Tris base, 1 g SDS in 250 ml dH$_2$O; pH adjustment to 8.8 with 1 N HCl

<u>Gel buffer 2:</u> 15.14 g Tris base, 1 g SDS in 250 dh$_2$O; pH adjustment to 6.8 with HCl

<u>10 x Elpho-buffer:</u> 30.3 g Tris base, 144 g glycine in 1 l dH$_2$O

> 1 x Elpho-buffer: Dilution of 10 x stock buffer with dH$_2$O and addition of 10% SDS

After separation, the proteins were transferred onto a PVDF- membrane (Immobilon) using the semidry blotting method according to standard techniques at constant 15 V for 50 min.

Blotting buffer: 5.8 g Tris base, 2.9 g glycine, 3.7 ml from 10% SDS stock solution, 200 ml methanol in 1 l dH$_2$O

Proteins on the membrane were blocked in blocking buffer for 1 hour at room temperature before being incubated with the primary antibody. Afterwards the membrane was transferred into a 15 ml Falcon tube containing the required primary antibody (see Table 11) in 3 ml of 1:3 with TBST-diluted blocking buffer and incubated at 4 °C on a rolling shaker overnight.

10 x TBST: 48 g Tris base, 17.4 g NaCl, 20ml Tween in 2 l dH$_2$O

    1 x TBST: Dilution of 10 x stock buffer with dH$_2$O, adjust pH to 7.4

Blocking buffer: 10% dried milk powder in 1 x TBST, adjust pH to 7.4

On the next day, membranes were washed for 3 x 10 min in 1 x TBST, the secondary antibody (Table 11) was added in 20 ml 1 x TBST and membranes were gently shaken for 1 hour at RT. After the incubation time the membrane was washed again as before.

Table 11: Primary and secondary antibodies used for western blots
The table gives the concentration used for each antibody used in western blotting and their species of origin. For information on manufacturers see Table 5.

Antibody	Species	Dilution
Primary antibodies		
8E4	Mouse	1:3000
β-glucocerebrosidase	Rabbit	1:1000

CD68	Rat	1:2000
GAPDH	Rabbit	1:2000
GFAP	Mouse	1:2000
HA-Taq	Mouse	1:3000
Map-2	Mouse	1:5000
Synaptophysin 1	Mouse	1:5000
Secondary antibodies IgG Ab, peroxidase labelled Mouse Rabbit Rat		1:4000

Proteins were visualised by enhanced chemiluminiescence (ECL). The membrane was incubated in 3 ml of detection solution (solutions 1 and 2 were mixed 1:1) in the darkroom before exposure of a film for 10 sec to 2 min. In order to develop the film it was incubated in developing solution for about a minute, washed with dH_2O, placed into the fixing solution for another 1–2 minutes and washed again before being hung up to dry. The membrane was used for Coomassie staining (see Section 2.6.1.5). Developed films were scanned and assessed.

2.6.1.5 Detection of proteins on PVDF membrane with Coomassie staining

The proteins detected on the membrane with the western blot method can be visualised by Coomassie staining. After the film had been successfully developed (see Section 2.6.1.4), the membrane was washed once in 1 x TBST to remove the detection solution. Thereafter the membrane was incubated in a staining solution with gentle shaking of the membrane for 30 min at RT. Thereafter, the membrane was

incubated in a de-staining solution until the background and possible protein bands were visible again. For storage the membrane was dried.

<u>Staining solution:</u> 4 tablets of Serva blue G in 100 ml ethanol, 125 ml dH$_2$O, 25 ml acetic acid

<u>De-staining solution:</u> 250 ml dH$_2$O, 250 ml methanol, 50 ml acetic acid

2.6.2 GCase activity assay

The reduced activity of the enzyme β-glucocerebrosidase is the key feature in Gaucher's disease. The activity of the enzyme differs enormously in healthy individuals compared with patients suffering from Gaucher's disease. Therefore the measurement of the activity of this enzyme plays a key role in this study and was used in different parts of this study such as for the characterisation of K14 lnl mice pups, establishment of cortical organotypic brain-slice cultures of K14 lnl mice as well as after transduction experiments of K14 ko organotypic slice. The assay as performed in this study was based upon a previously developed GCase activity assay (Fink e*t al.*, 1989), with slight modification.

The protein concentration, depending on experimental material, varied between 2 and 10 µg in 15 µl of extraction buffer. For each protein concentration, two assay samples (A = destroyed enzyme and C = native enzyme) were required. At the beginning of this study, while establishing this assay, a third sample B (as sample C, but additionally containing CBE) was used. CBE is a specific inhibitor of the enzyme β-glucocerebrosidase. CBE was used to verify the specificity of the substrate, 4-MUD, for the native enzyme GCase used in this assay. Sample A was incubated at 90 °C for 5 min in a heating block in order to destroy the native enzyme. In case of sample B 60 µl CBE (320 µM end concentration) were added, whereas the same volume of extraction buffer was added to sample A and C. All samples were vortexed and incubated at 37 °C for 45 min. Thereafter 30 µl of the substrate 4-MUD (0.6 mM end concentration) was added to each sample, and the mixtures were vortexed and incubated at 37 °C for a further 2 hours. The reaction was stopped by adding 105 µl stop-solution (0.4 M end concentration) to each sample with vortexing. The samples

were either stored overnight at 4 °C or measured at once. Each sample was pipetted in triplicate into a 96-well plate. The plate was measured at a wavelength of 365 nm/445 nm in a specific plate reader (Synergy 2). Measured values are given in relative fluorescence units and were transferred into an Excel datasheet and evaluated. The background fluorescence (A), destroyed enzyme, was subtracted from that of sample C in order to obtain the real fluorescence intensity. The relative GCase activity was used for comparing samples of different experiments with each other.

<u>Extraction buffer:</u> 50 mM di-potassium hydrogen phosphate 3-hydrate in dH$_2$O, pH adjustment to 5.9 before adding 1.5% Triton X-100

<u>4-MUD Substrate:</u> 15 mM 4-Methylumbelliferyl β-D-glucopyranoside in extraction buffer

<u>CBE Inhibitor:</u> 400 µM Conduritol B epoxide in extraction buffer

<u>Stop-solution:</u> 0.8 M NaOH and 0.8 M glycine in dH$_2$O

2.7 Biological models: Cell cultures and cortical organotypic brain-slice cultures

2.7.1 Cultivation of cells

In this study a variety of cell types (see Section 2.2.9) and primary neuronal cells (see Section 2.7.6) were used to address different experimental questions.

Fibroblasts from a Gaucher's disease (Fig. 18) patient and from healthy individual as well as primary neurons from K14 ko mice were used to test different types of vectors for GCase activity before packing them into AAV2 particles.

AAV-293 cells (Fig. 25A) are derived from common human embryonic kidney HEK293 cells which have been transformed by adenovirus type 5. These cells were used to produce AAV2 particles.

AAV-HT1080 cells (Fig. 26B) represent a human fibrosarcoma cell line. These cells were used to determine the efficiency of virus transduction and to calculate the titre of each viral supernatant produced.

Culture media:

Fibroblasts: DMEM, 10% FCS and 1% Pen/Strep

AAV-293 and AAV-HT1080: DMEM, 10% heat-inactivated FCS, 2 mM GlutaMax1

All cells used in this work were cultivated in cell-culture flasks (15 cm^2, 75 cm^2 and 175 cm^2) in an incubator at 37 °C and 5% CO_2 content. For different experiments depending on the experimental question, cells were either grown in 10 cm^2 cell-culture disks or on 12-well cell-culture plates.

2.7.2 Passaging of cells

Every 2–3 days, the confluency of cells was observed. Cells were passaged at 80% confluency, except for AAV-293 cells, which have to be passaged at 50% confluency. For passaging, cells were washed with PBS and incubated with a trypsin-EDTA solution until adherent cells detach, which can be observed under an inverted microscope. Detachment of cells was stopped by adding complemented growth medium and the required number of cells was transferred into new cell-culture flasks, dishes or plates.

2.7.3 Freezing and thawing of cells

Eucaryotic cells can be cryopreserved, thawed and re-cultured again. For cryopreservation, growth media was aspirated from cells cultivated in a 75 cm^2 flask. Cells were washed once with PBS, incubated with a trypsin-EDTA solution under observation for 1–3 minutes at RT for detachment. Detachment of cells was stopped by adding pre-warmed growth medium to the flask. Cells were transferred into a

15 ml Falcon tube and centrifuged at 200 g for 10 min at RT. The pellet was resuspended in freezing medium. 1 ml of cell suspension was transferred into 2 ml cryo tubes and cooled down at 1 °C per min in a –80 °C freezer. From the next day on they were stored in a tank filled with liquid N_2.

Cryopreserved cells were thawed for 1–2 min at RT before resuspension in 10 ml pre-warmed growth medium and centrifugation at 200 g for 3 min at RT. The pellet, containing the collected cells, was resuspended in fresh growth medium and transferred into cell-culture flasks. The flask contained twice as much growth medium as had been used for resuspension of the pellet. For cultivation, cells were placed into an incubator at 37 °C and 5% CO_2.

<u>Freezing medium:</u> 50% DMEM, 40% heat-inactivated FCS, 10% DMSO

2.7.4 Counting cells with Neubauer improved haemocytometer

Counting of cells is important when passaging or cryopreserving cells. Counting is performed after trypsinsation, centrifugation and resuspension of the cell pellet. For counting, 10 µl of cell suspension was mixed with 50 µl of Trypan blue and 40 µl of growth medium. In the case of dead cells the dye is able to enter the cell, leading to a blue staining observed under the microscope, whereas living cells do not take up the dye as their cell membrane is intact. The haemocytometer (after Neubauer) was loaded with the cell–dye mixture and examined under the inverted microscope. Unstained cells were counted in all 4 squares (each square consisting of 16 small squares).

The cell number was determined as follows: Each big square consists of an area of 1 mm^2, with a height of 0.1 mm. Therefore the formula was used:

$$\frac{\text{Number of cells}}{\text{4 fields}} * 10 * 10^4 = \text{cell number/ml}$$

2.7.5 jetPEI® transfection of fibroblasts

Fibroblasts from a Gaucher patient (M.G. fibroblasts) and from a healthy individual were cultivated as described in section 2.7.1 and used to test various vectors (Table 7) used in this study. Transfection was performed by using the jetPEI® transfection reagent and following the method described in the instruction manual. The day before transfection, 200,000 cells were seeded per well in a 12-well plate. Cells were 50–70% confluent on the next day, and the medium was replaced by 1 ml of fresh growth medium. For transfection, 2 µg of plasmid DNA was diluted with 150 mM NaCl to a final volume of 50 µl and vortexed. Subsequently, 2 µl of jetPEI® reagent was diluted with 150 mM NaCl to a final volume of 50 µl and vortexed. It was important to add the 50 µl of jetPEI® solution to the 50 µl plasmid DNA solution and not the other way around; otherwise, the efficiency would be reduced, as stated by the manufacturer. The mixed solution was vortexed immediately and incubated for 20 min at RT before 100 µl of the jetPEI®–plasmid DNA mix was added dropwise to the cells. The plate was gently swirled before being incubated for another 48 hours at 37 °C and 5% CO_2. Afterwards, cells were harvested and processed as described in section 2.6.1.1 and were analysed either by western blotting (section 2.6.1.4) or the GCase activity assay (section 2.6.2).

2.7.6 Primary neuronal cell cultures

2.7.6.1 Preparation of primary neurons from embryonic mouse brains

Primary neuronal cell cultures are only able to grow on material which is coated with poly-D-lysine (PDL). The PDL powder was dissolved in 50 ml sterile water to produce a stock solution of 5 mg/ml, and aliquots of 1 ml were stored at –20 °C. A working solution (80 µg/ml) of PDL was used to coat either 6- or 12-well plates with 1 ml or 2 ml of PDL solution; for immunofluorescence, sterile glass plates were placed inside the well, and for assays and nucleofection these were omitted. The PDL solution was left inside the well overnight at RT and the plates were washed three times with sterile dH_2O the next morning. After washing, plates were dried for at least 1 hr on the clean bench at RT until being used.

Mouse embryos of age 15–16 days (E 15-16) were used to prepare and cultivate primary neuronal cells as described by Brewer *et al.* (1989). The pregnant K14 +/- mouse was killed by cervical dislocation and the abdomen cleaned with 70% v/v alcohol/water. The abdominal cavity was opened with large scissors without cutting into the muscle layer beneath. Another pair of scissors was used to open the muscle layer to obtain access to the uterus. Forceps was used to take out and transfer the embryos to a Petri dish, filled with ice-cold Hank's solution, under the laminar-flow hood. The embryos were decapitated and transferred into another Petri dish. Beneath binoculars, the brain was prepared under semi-sterile conditions. A very small pair of scissors was used to open the cranium carefully through the foramen magnum up to the orbit. A fine spoon was used to take out the brain. Two very sharply pointed pairs of forceps were used to separate the cerebellum and the cerebrum, to separate the two hemispheres, to take off the thalamus and to free both hemispheres from any residual meninges. A small part of the cerebellum was used for lysis (section 2.3.2) and genotyping afterwards (section 2.3.3), as only K14 wt and -/- embryos were of interest in this study. Both hemispheres were kept in 5 ml DMEM media on ice while the PCR was running. After genotyping and identifying the embryos required, both hemispheres were transferred with a glass Pasteur pipette upside down into a 15 ml Falcon tube. The hemispheres were washed once with ice-cold Hank's solution. Thereafter the hemispheres were triturated in 2 ml of Hanks solution w/o Mg^{2+} and Ca^{2+} using three glass Pasteur pipettes of different thickness and incubated on ice for 5 min. The supernatant was transferred to a new 15 ml Falcon tube and centrifuged at 80 g, 4 °C, for 5 min. The cell pellet was resuspended in growth medium. Cells were plated out into various cell culture vessels. The cells were then incubated at 37 °C, 5% CO_2 until primary neurons were used for a variety of experiments. The medium was changed once a week if not otherwise stated.

<u>Growth media:</u> Neurobasal media, 2% B27 Supplement, 1% Pen/Strep and 1% 50 mM GlutaMax

2.7.6.2 Nucleofection of primary K14 ko neurons

In this study, the plasmids (Table 7) used were not only tested for GCase enzyme activity and expression in M.G. fibroblasts as described in section 2.7.5 but were also

tested in primary neurons from K14 ko embryos. Nucleofection was performed by using the Amaxa® Mouse Neuron Nucleofector® Kit following the instruction manual if not otherwise stated.

For nucleofection experiments, primary neurons were prepared as described in section 2.7.6.1 until the identification of genotypes of each mouse pup. After identifying K14 ko embryos, both hemispheres of these embryos were washed with Hank's solution, which was discarded afterwards. The hemispheres were triturated using three glass Pasteur pipettes, of different thickness, in 1.5 ml of Medium 1. The cell suspension was incubated on ice for 5 min before the supernatant was transferred to a fresh 15 ml Falcon tube. The cell suspension was centrifuged at 80 g, 4 °C, for 5 min. The supernatant was discarded and the cell pellet resuspended in Medium 1. Cells were counted in a Neubauer improved cell chamber (section 2.7.4). The cell suspension was split into 1.5×10^6 cells per nucleofection in each 1.5 ml reaction tube; the tubes were centrifuged again at 80 g, 4 °C. Each cell pellet was resuspended very carefully in 100 µl Nucleofector solution. Incubation should not continue for longer than 15 min, as otherwise increased cell death may occur during nucleofection (Instruction manual). Either 2 µg of pMaxGFP® DNA (positive control), provided by the manufacturer, or 3 µg of vectors to be tested were added to the cell-nucleofector solution mix. The DNA/cell/nucleofector solution mixture was transferred to the cell provided and placed in the Nucleofector device. Programme 0-005 was chosen for nucleofection. Thereafter, 500 µl of pre-warmed Medium 1 was added to the cell without resuspending the solution. Nucleofected cells were carefully transferred by using a Pasteur pipette into one well of a 12-well plate and incubated at 37 °C and 5% CO_2. 4 hours after incubation, the medium was replaced by 750 µl Medium 2a and the cells replaced in the incubator. Following another 24 hours of incubation, the medium was replaced by 1 ml of Medium 2. The medium was exchanged once a week until the nucleofected cells were analysed by western blotting (section 2.6.1.4), subjected to the GCase activity assay (section 2.6.2) or stained by Immunofluorescence.

Medium 1: RPMI, 10% FCS

Medium 2: Growth medium for primary neuronal cells

Medium 2a: Medium 2 supplemented with 5% FCS

2.7.6.3 Immunofluorescence staining

Verifying successful nucleofection and the efficiency rate was performed by using cells nucleofected with pMax. The control vector, supplied by the manufacturer, expresses GFP in positively nucleofected cells. Furthermore, the antibody Map2 was used to stain neurons in order to verify the cell specificity of the nucleofector solution supplied. Nucleofected cells were cultivated for one week before the growth medium was discarded and cells were washed with ice-cold PBS. The cells were fixed with 4% PFA at RT for 15 min. Cells were washed again for 3 x 10 min with PBS before incubation with lysis buffer for 30 min at RT. In order to prevent unspecific binding, cells were incubated with blocking buffer for 1 hour at RT before being incubated with the primary antibody overnight at 4 °C. The following dilutions for antibodies were used: GFAP 1:300, Map2 1:400 in 1:5 diluted blocking buffer. On the next day, cells were washed again for 3 x 10 min with PBS before being incubated with the secondary antibodies (Table 5: dilution 1:400) in PBS for 1 hour at RT. Thereafter cells were washed again 3 x 10 min with PBS before covering the glass plates with a small drop of Hydromount and placing them upside down onto an objective slide. Each staining was examined under a fluorescence microscope (Olympus IX70).

Lysis buffer: PBS, 0.3% Triton X-100

Blocking buffer: Lysis buffer, 5% normal serum

2.7.7 Cortical organotypic brain-slice cultures

The disadvantage of using primary neuronal cell cultures is the fact that – compared with brain tissue – they lack any extracellular matrix, neuronal connectivity and protein expression as well as the interactions between neurons and glia cells. To overcome these disadvantages, experiments were performed with set-ups similar to the *in vivo* situation. Therefore cortical organotypic brain-slice cultures (Yamamoto et al., 1989 and 1992) were used, which is a very complex *in vitro* model.

For preparation of cortical organotypic brain-slice cultures, 8–9 day old (P8–9) K14 wt or ko pups were decapitated. The brain was isolated under sterile conditions beneath the laminar flow hood. The cranium was opened by using very tiny sharp scissors to

cut through the foramen magnum up to the orbit. The brain was taken out by using a fine spoon and transferred into a Petri dish containing ice cold 1 x Krebs buffer. Each brain was transferred into a small plastic form which was two-thirds filled with warm 4% low-melting agarose. The brain was swirled around with a 200 µl pipette tip in order to ensure that the brain was fully enclosed with agarose. The agarose block enclosing the brain was allowed to set fully on ice. The hardened agarose block was trimmed with a scalpel, leaving an edge of approximately 2 mm around the brain tissue. Each cut brain block was glued with histoacrylamide onto the sample plate. The sample plate was transferred into a specific tray, which was filled with ice-cold 1 x Krebs buffer situated in the vibratome (Fig. 4).

Figure 4: Vibratome used to cut cortical organotypic brain-slices

Cortical slices of thickness 400 µm were cut with a stainless steel blade at a rate of 26 mm/sec. Slices were carefully transferred by using two spatulas into small Petri dishes, filled with ice cold 1 x Krebs buffer, situated on an ice plate. After about 5–8 slices per mouse brain had been collected, each slice was transferred with two spatulas onto the membrane (Nucleopore Track-Etch Membrane, 25 mm, 8 µm pore size). The membrane was placed with the shiny side upside down on top of 2 ml of

ice-cold growth medium in a 6-well cell-culture plate. The slices were cultivated for 2–14 days in an incubator at 37 °C, 5% CO_2 until further experimental use. A schematic drawing of a cultured cortical organotypic brain-slice is shown in Figure 5.
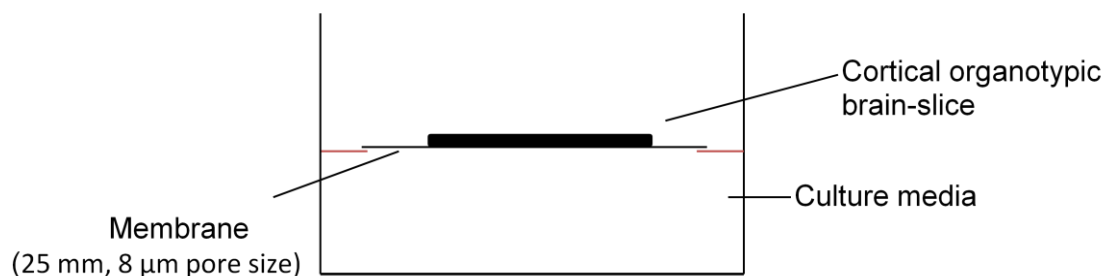
Figure 5: Schematic drawing of an organotypic slice in culture
The position of the slice on top of the membrane in a 6-well plate is shown; showing that there is no contact between the slice and the growth medium.

Protein extraction was performed as described in Section 2.6.1.1 and was used either for comparison of GCase activity (Section 2.6.2) in slices of K14 ko to K14 wt mice or to analyse their cultivation conditions using different cell-specific markers by western blotting (Section 2.6.1.1). Finally, cortical organotypic brain-slice cultures were used to test various vectors packed into AAV2 viral particles (Section 2.8.2) by transduction experiments (Section 2.9).

10 x Krebs buffer: 1.26 M NaCl, 25 mM KCl, 12 mM NaH_2PO, 12 mM $MgCl_2$ * $6H_2O$, 25 mM $CaCl_2$ * $2H_2O$, autoclaved at 1 bar for 35 min , stored at 4 °C

1 x Krebs buffer: 450 ml Milli Q water (autoclaved), 50 ml 10 x Krebs buffer, 0.99 g glucose, 1.05 g $NaHCO_3$, sterile-filtrated and stored at 4 °C

4% Low-melting agarose: 2 g low-melting agarose in 50 ml 1 x Krebs buffer, kept in a water bath at 50 °C until use

Growth media: 50% DMEM, 25% heat-inactivated HS, 25% Hank´s with Ca^{2+}/Mg^{2+}, 1% P/S, 6.5 mg/ml glucose

2.7.7.1 Cell viability staining with calcein

Calcein staining was used to determine cell viability in cortical organotypic brain-slice cultures. Calcein can be transported through cell membranes in living cells. Calcein is a fluorescent dye with an excitation maximum at 495 nm.

Calcein staining was performed after slices had been cultured (see Section 2.7.7) for either 2 or 4 days. The medium was exchanged before addition of 2.5 µM of calcein staining solution to the medium. The cortical organotypic brain-slices were cultured at 37 °C, 4% CO_2, for further 60 min. Thereafter the medium was aspirated before the slices were examined under the fluorescence microscope (Olympus IX70).

2.8 Adeno-associated viral methods

In this work AAV2 particles were used to identify their potency for gene therapy in K14 lnl mice, depending on the vector with which they were packed. Working with AAV serotype 2 was based on the original aim of this work to develop a gene therapy for Gaucher's disease type II using the K14 mouse model. AAV2 specifically infects heart-muscle and liver cells. Especially, infecting heart-muscle cells played an interesting part in our strategy, as these cells divide very slowly (slow turnover) and could therefore be used as depot organ for continuous production of the fusion protein (human GCase + LDLR domain). During this work the strategy had to be slightly changed because of breeding problems, and attention was therefore concentrated on testing packed AAV2 particles in an *ex vivo* model for Gaucher's disease type II (see Section 2.7.7).

The AAV2 Helper-Free System was used following the instruction manual. The advantage of this system is the production of infectious recombinant human AAV-2 virions without the requirement for a helper virus such as the Herpes simplex virus (see Section 1.4.1).

The Helper free system requires the pHelper plasmid which supplies the most important gene products to produce infective AAV particles. PHelper is co-transfected with the AAV2 shuttle vector (pAAV.MCS), including the gene of interest and pAAV.RC, into AAV-293 host cells. The pAAV.RC plasmid expresses the r*ep* and *cap*

genes in *trans* required for virus production. The AAV-293 cells stably express the adenovirus E1 gene (Instruction manual, Agilent Technologies).

The plasmids pAAV.CMV_sGBA_HA_ApoB (pAAV.hGC), pFB.CAG_sGBA_ApoB (pFB.CAG) and pAAV.LacZ were separately packed into AAV2 particles. The first two plasmids encode the gene product for the enzyme β-glucocerebrosidase fused to the ApoB binding domain and the HA taq. The plasmid pAAV.hGC cloned in this study is under the control of the CMV promoter. The plasmid pFB.CAG, a kind gift of N. Jäschke, was under the control of the CAG promoter. The plasmid pAAV.LacZ plasmid was used as positive control for viral particle production and indirect titre measurement

2.8.1 Generating transient AAV2 producing cells via transfection

The general standard techniques to cultivate AAV-293 cells are described in Section 2.7.2. For transfection experiments, AAV-293 cells were plated in 10 ml growth medium into 10 cm^2 cell-culture dishes and cultivated at 37 °C, 5% CO_2, for 48 hours. The instructions recommend 70–80% confluency of cells on the day of transfection. This confluency was achieved when plating 2 x 10^6 cells per dish 2 days before transfection.

All three plasmids required for transfection were thawed on ice. 10 µg of each plasmid (pHelper, pRC and either the pAAV expression plasmid (pAAV.hGC or pFB.CAG) or pAAV.LacZ) was mixed in a 2 ml reaction tube. 1 ml of 0.3 M $CaCl_2$ solution was added to the plasmids and gently mixed. For a negative transfection control, one of the three vectors required was omitted. A second 2 ml reaction tube was filled with 1 ml of 2 x HBS. The 1.03 ml DNA/$CacCl_2$ mix was added dropwise to the HBS solution and mixed by inversion. Immediately, drops of the DNA/$CaCl_2$/HBS mixture were applied to the plate of AAV-293 cells, which was gently swirled to distribute the DNA evenly in the medium. The transfected cells were returned for cultivation at 37 °C, 5% CO_2, for 6 hours. After 6 hours, the medium was replaced by 10 ml fresh growth medium and the plate return to the incubator for a further 66–72 hours.

CaCl$_2$ solution: 0.3 M CaCl$_2$ aqueous solution, sterile filtration

2 x HBS: 280 mM NaCl, 1.5 mM Na$_2$HPO$_4$, 50 mM HEPES; adjustment of pH to 7.10 with NaOH

2.8.2 Producing AAV2 viral stocks

After transfection, AAV-293 cells were monitored for virus production. This event can be observed under the light microscope because of phenotypic changes of AAV-293 cells. The most prominent sign of viral production is the colour change of the growth medium from red to orange/yellow compared with the negative control (non-transfected) plate.

The time required for the production of viral particles is in general 3 days after transfection. AAV-293 cells were harvested with a cell scraper into the growth medium. Taking the growth medium as well increases the yield of viral particles. The cell suspension was transferred into a 15 ml Falcon tube and four rounds of freezing in a dry-ice ethanol bath and thawing at room temperature were performed. After the last thawing cycle, the cell suspension was centrifuged at 10,000 g for 10 min at RT. The supernatant (viral stock) was transferred into a new 15 ml Falcon tube. The viral stock was either cryo-preserved or used immediately for transduction experiments.

2.8.3 Cryopreservation of viral supernatants

AAV2 viral stocks can be cryopreserved at –80 °C and stored for up to one year (instruction manual). The viral stock was stored in cryotubes in aliquots of 0.250 ml, 0.5 ml or 1 ml. Aliquots of viral stocks required for various transduction experiments were thawn on ice and used immediately.

2.8.4 AAV2 transduction and viral titre measurement

In general, transduction describes the transfer of foreign DNA into a cell by viral infection. The marker gene *lacZ* was used to determine the viral titre of produced viral stocks. Titre measurement of viral stocks was performed in AAV-HT1080 cells which were cultivated as described in Section 2.7.2.

2.8.4.1 Indirect viral titre measurement in AAV-HT1080 cells

Two days before transduction, AAV-HT1080 cells were plated at a cell density of 150 000 cells in 1 ml growth medium into a 12-well cell-culture plate. Before transduction, 0.2 ml AAV permissive medium was added per well and cells were further incubated for another 4 hours. Thereafter, the medium was completely aspirated and diluted viral stocks were added in triplicate. The primary stock was diluted 100-fold with growth medium. A 5-fold serial dilution in 2.5 ml was performed from this 100-fold dilution. The dilution series was performed from 2×10^{-3} to 8×10^{-5} in L-DMEM medium. Triplicates of each dilution were added in a volume of 0.5 ml to each well of AAV-HT1080 cells. A negative titre control, containing no viral particles, was run in parallel. The cells were incubated at 37 °C, 5% CO_2 for another 2 hours. During this incubation time, the culture plates were gently swirled at 30 min intervals. After the incubation period, 0.5 ml of pre-warmed H-DMEM medium was added per well and the incubation was prolonged for a further 40-48 hours.

DMEM growth medium: DMEM, 10% heat-inactivated FCS, 2 mM L-glutamine

AAV permissive medium: DMEM growth medium supplemented with 4.8 µM Camptothecin (1 mM Stock in PBS from the original 10 mM Stock in DMSO)

L-DMEM medium: DMEM, 2% heat-inactivated FCS, 2 mM L-glutamine

H-DMEM medium: DMEM, 18% heat-inactivated FCS, 2 mM L-glutamine

2.8.4.2 Histochemical LacZ confirmation via X-Gal staining

β-galactosidase is often applied to determine transduction efficiencies and was also used in this work in order to perform indirect viral titre measurement. β-galactosidase is encoded by the LacZ gene and catalyses the hydrolytic cleavage of 5-bromo-3-indoyl-β-D-galactopyranoside (X-Gal) which leads to a blue staining. Due to the blue staining, cells successfully transduced by the LacZ coding AAV2´s can be specifically identified.

β-galactosidase staining was performed following the instruction manual. Transduced cells were washed once with 1 x PBS and incubated with 500 µl / well of fixing buffer for 15 min at RT. Thereafter cells were washed twice with 1 x PBS and incubated for 2–4 hours with freshly prepared 1 x X-Gal solution in a volume of 500 µl / well. The staining solution was aspirated and 1 x PBS was added to each well before the stained cells were examined under the microscope and photographs were taken for documentation.

All dilutions of the viral stock used for titre measurement were examined under the light microscope with a 20 x objective. The dilution of the viral stock, which had about 10% positive cells per viewing field, was used to determine the transfection efficiency and to calculate the titre of the viral stock. For each well of the triplicate, 5 fields were chosen randomly, and in these fields blue cells and the total number of cells were counted. An example of such a data set obtained by the counting procedure is shown in Table 12.

Table 12: Counting of positively transduced AAV-HT1080 cells with AAV2 particles expressing LacZ

AAV-HT1080 cells were transduced with three different dilutions of AAV2 particles expressing LacZ in triplicate. Dilution displaying 10% positive cells using a 20 x objective of a light microscope was chosen to determine the titre. The table gives the numbers of positively blue stained cells and the total number of cells for each randomly chosen field. Five fields in total were chosen for each triplicate. The last lane gives the average of counted cells.

Well 1		Well 2		Well 3	
Blue cells	**Total cells**	**Blue cells**	**Total cells**	**Blue cells**	**Total cells**
22	53	25	61	15	71
7	30	12	50	17	32
12	35	7	27	7	22
17	42	15	32	32	71
8	15	7	20	5	21
13.2	33	13.2	28	15.2	43.4

The average numbers of cells counted in all 5 fields of each triplicate were determined. Finally, the average mean of triplicates was determined for blue-stained cells as well as for the total number of cells. The following formula was used to determine the transduction efficiency:

$$\text{Transduction efficiency} = \frac{\text{Average number of blue stained cells}}{\text{Average number of all cells}} \times 100$$

The following formula was used to determine the titre of viral stocks produced by indirect measurement of LacZ expression:

$$\frac{IFU}{ml} = \frac{(\text{Average number of blue stained cells per field})\times(597 \text{ fields per well})}{(0.5ml)\times(\text{dilution factor})}$$

The total number of fields when using a 20 x objective is derived as follows:

The radius of a standard 20 x objective = 0.45mm

The area per field = 0.045 cm x 0.045 cm x 3.1415 = 6.36×10^{-3} cm^2

The area of the well of a 12-well plate = 3.8 cm^2

Therefore:

$$\text{The total number of fields per well} = \frac{3.8 \ cm^2}{6.36 \times 10^{-3} \ cm^2}$$

1 x X-Gal solution: Freshly diluted in 25 x X-Gal Stock with staining buffer and discarded after use; 25 x X-Gal stock can be stored at –20 °C

2.9 AAV2 transduction of K14 ko cortical organotypic brain-slice cultures

K14 ko cortical organotypic brain-slice cultures of the cerebrum were used to determine GCase activity and expression after the transduction with AAV2 particles. These particles were packed with various vectors as described in section 2.8 above.

Preparation and cultivation conditions of cortical organotypic brain-slice cultures have already been described in section 2.7.7. For the present experimental question, slices were cultivated at 37 °C, 5% CO_2, for one day. On the following day (12–16 hours later), the medium was fully replaced with 1 ml of AAV-permissive slice growth medium and incubated at 37 °C, 5% CO_2 for four hours. Camptothecin is often used as adenovirus superinfection to accelerate the limiting step of conversion of a single-stranded virus to double-stranded, whereas otherwise the virus only relies on cellular

replication factors for synthesis of the complementary strand (McCarthy et al., 2001 and Lai et al., 2002). This conversion is required for gene expression to occur. The medium was aspirated and slices were transduced with AAV2 particles in two different ways. Either 1 ml of diluted AAV stock was added directly to the well, or 40 µl of undiluted AAV stock was added directly on top of the slice. Slices were incubated for 2 hours at 37 °C. For clarity, Fig. 5 shows a schematic drawing of cultured slices. In addition, parallel-treated non-transduced slices were incubated as a negative control. After transduction the plate was returned into the incubator for a further two hours and gently swirled every 30 minutes. Thereafter, 1 ml of freshly prepared slice growth medium was added to each well and slices were returned to the incubator and cultivated for another 2, 4 or 7 days until analysis.

Slice growth medium: DMEM, 25% FCS, 25% HBSS, 1% Pen/Strep, 6.5 mg/ml glucose

AAV permissive slice growth medium: Slice growth medium supplemented with 4.8 µM camptothecin (1 mM Stock in PBS from the original 10 mM stock in DMSO)

Diluted AAV viral stocks: 500 µl AAV diluted in 2ml of slice growth medium

GCase activity in transduced K14 ko slices was analysed and compared with analogous results from non-transduced slices. Proteins were extracted as described in Section 2.6.1.1 and the GCase activity assay was performed as previously described in Section 2.6.2.

Furthermore the expression of the human GCase of transduced K14 ko organotypic slices was analysed by western blotting (see Section 2.6.1.4.) In order to detect the produced fusion protein, the antibody mouse anti-HA Taq was used.

2.9.1 LDH cytotoxicity measurement of transduced slices

The lactate dehydrogenase kit was used in order to investigate whether the transduction of cortical organotypic slices with AAV2 particles leads to any cytotoxic effect. Cell death or cytotoxicity due to elevated plasma membrane damages can

often be determined. Classically, the enzyme lactate dehydrogenase is used as it is present in all cell types throughout the body. LDH is a very stable enzyme, but owing to damage of plasma membrane, it is rapidly released into the culture medium. Slices transduced by adding viral particles into the medium itself were not analysed as this might have led to false positive results. Therefore, only slices directly transduced were investigated. Following the instruction manual, samples of growth media of transduced as well as non-transduced organotypic slices were collected for comparison. The high control, required in order to determine cytotoxicity, was produced by saturating the slice with the growth medium (supplemented with Triton X-100) and incubation overnight at 37 °C. Samples were measured in triplicate. The cytotoxicity (%) of each sample was calculated by the following formula.

$$\text{Cytotoxicity (\%)} = \frac{\text{(Test Sample - Low Control)}}{\text{(High Control - Low Control)}} \times 100$$

2.10 Vector program

The vector sequences of the plasmids used and cloned in the present study were created and documented by using the program SnapGene. The plasmid maps of the vectors and schematic drawings were created by using the program SnapGene as well.

2.11 Statistical analysis

In this work the most important aspect was the explorative evaluation of data sets to characterise and compare the two different vectors pAAV.CMV_sGBA_HA_ApoB and pFB.CAG_sGBA_ApoB, expressing human GCase, in different experimental set-ups. Furthermore, the transduction efficiency of AAV2-produced particles containing either of these two vectors was evaluated. Their GCase-dependent benefit in organotypic slice cultures was evaluated as well. Statistical analysis was performed by using Microsoft Excel. In the first step the mean of a specific data set was

calculated; then the standard error and the standard error of the mean were determined. To determine whether two data sets were significantly different from each other the Student's t test was used. This test compares the mean of two different data sets. Excel differentiates between different types of this test; in this study type 2 was used as it is appropriate for comparing the means of two data sets that have similar variances. Statistical significance was considered to be given if $p^* < 0.05$ or $p^{**} < 0.01$, as obtained by Student's t test. Subsequent results were evaluated in a descriptive manner and therefore no further statistical analysis was required.

3. Results

3.1 Characterisation of K14 lnl mouse model

The major aim of this work was to establish a possible gene-therapeutic approach for Gaucher's disease type II.

For this purpose, the K14 lnl mouse model displaying Gaucher's disease type II was characterised. Breeding of K14 lnl mice proved to be very difficult and resulted in low numbers of knockout mice, approximately 1–2 of 30 pups in total. Moreover if litters were too large, the weakest pup, being generally the knockout, was often killed by the female, thus further reducing the number of animals available for experiments. Breeding was one reason which led to the decision to establish an *ex vivo* model representing Gaucher's disease type II using K14 lnl pups. Moreover, only one mouse brain resulted in 5-8 slices, which made it possible to perform more experiments. The use of cortical organotypic brain-slices revealed the characteristics of the disease in a model which represented a possible situation compared with the situation *in vivo*.

Genotyping the K14 lnl mice (Figure 6) was one major aspect, as only heterozygous mice can be used for breeding (see Section 2.1). Only K14 knockouts which have the Cre gene are able to survive and therefore were used for the different experiments performed in the present study. The K14 wt mice which were also positive for Cre were used as controls.

73
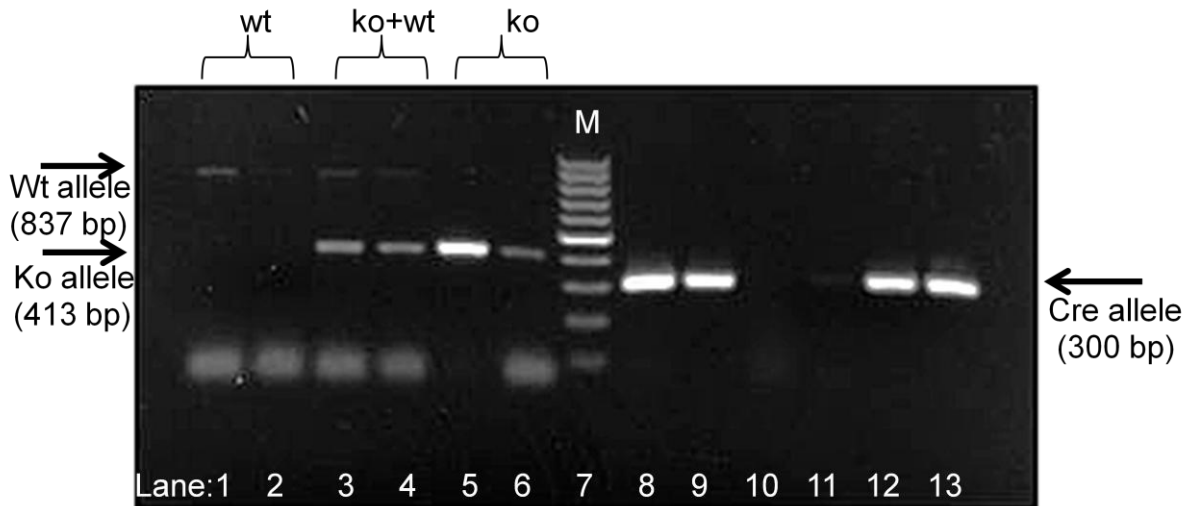
Figure 6: Genotyping of K14 lnl mice via PCR and analysis on agarose gel
The GC wt fragment (837 bp) is shown in lanes 1–4, GC ko fragment (413 bp) is shown in lane 4-6. The possible Cre fragment (300 bp) is shown in lanes 8 and 9 and lanes 12 and 13. The 1 kb marker was loaded onto lane 7.

K14 lnl pups were split into three different groups, for characterisation, depending on their symptoms at the stage of disease. The first group comprised K14 lnl pups aged 7 days (Figure 7A). At this first stage of disease, defined as the symptom-free stage, the most obvious difference was the growth-restriction of K14 ko mice compared with their K14 wt siblings. The next group comprised mice around the age of 11 days (Figure 7B), at this stage the following symptoms occurred in ko mice: cramping when touched, abnormal gait and hyperextension of the neck. The third group comprised mice at the end stage of disease, defined at the age of 13 days: here seizures occurred spontaneously, and most mice were dehydrated. At this stage mice had to be killed immediately.
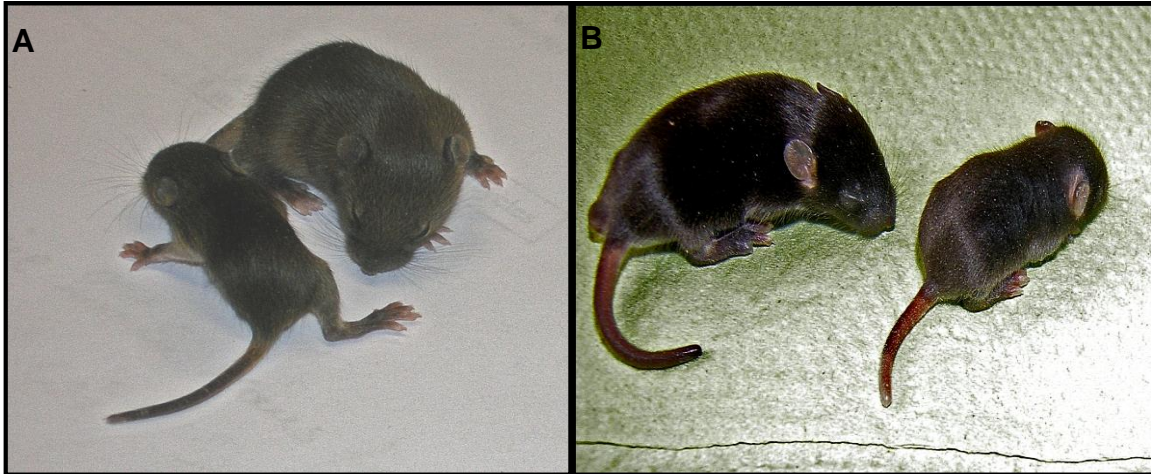
Figure 7: K14 lnl mice pups
Both pictures show mice pup pairs of the same litter. The left picture shows a ko (left) and a wt (right) mouse of the age of 7 days and the right picture a wt (left) and a ko (right) mouse at the age of 11 days.

3.1.1 Histological analysis of K14 mouse brains

The histological analysis (see Section 2.4) was performed to investigate whether there are differences in the density of neurons and the staining of either β-glucocerebrosidase or GFAP.

The Nissl staining (see Section 2.4.3) performed on frontal paraffin sections from brains derived from K14 ko mice (P11 (Fig. 8E) shows generally a gross normal brain architecture compared with control mice (P11 (Fig. 8A) as far as it can be seen by Nissl staining. Neuronal loss in the cortex (Fig. 8F) and cerebellum (Fig. 8H) of K14 ko mice compared with control mice (Figs. 8B and 8D) can be observed. Especially in the cortex shown in Figures 8C and 8G, which are taken from 8B and 8F and shown at higher magnification (represented by a square), the loss of large pyramidal neurons in the cortical layers (Fig. 8G) in K14 ko mice could be shown.
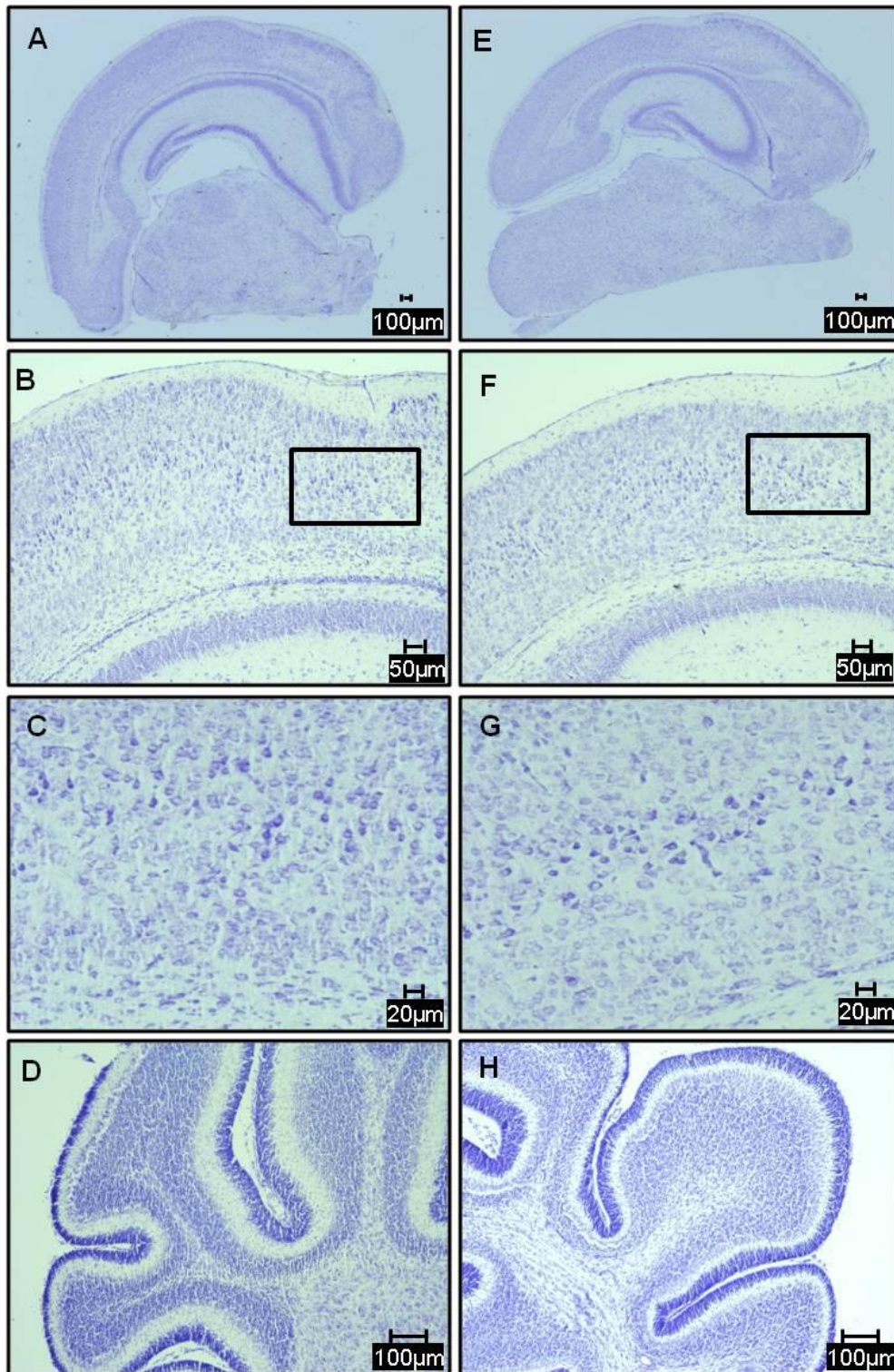
Figure 8: Nissl staining of K14 lnl mice brain
Nissl staining in K14 wt mice (A–D) and K14 ko mice (E–H) at the age of 11 days. Normal brain architecture was displayed in ko mice (E) compared with wt mice (A) (magnified 50 times). Neuronal loss was observed in the cortex (F) and cerebellum (H) (magnified 200 times). Higher magnifications of the black frame in B and F are shown in C and G to show the loss of large pyramidal neurons in K14 ko mice (G). The cerebellum is displayed at pictures D and H using (magnified 500 times).

In K14 ko mice astrogliosis occurs during the course of disease. Therefore, GFAP expression in K14 mice brains was compared with the GFAP expression in brains of K14 wt mice. In Fig. 9, as an example, GFAP staining is shown in the cortex of frontal paraffin sections derived from brains of K14 lnl mice at different ages (P7 and P14). These two groups were chosen as they present the stages of the beginning of disease (Figs. 9A and 9B) and the end stage of disease (Figs. 9C and 9D) in K14 lnl mice. Astrogliosis was seen in K14 ko mice at P7 (Fig. 9B) as well as at P14 (Fig. 9D) compared with control mice of the same age (Figs. 9A and 9C). GFAP expression in K14 ko mice was increased in the brain of older mice (Fig. 9D) compared with the expression level in younger mice (Fig. 9B).
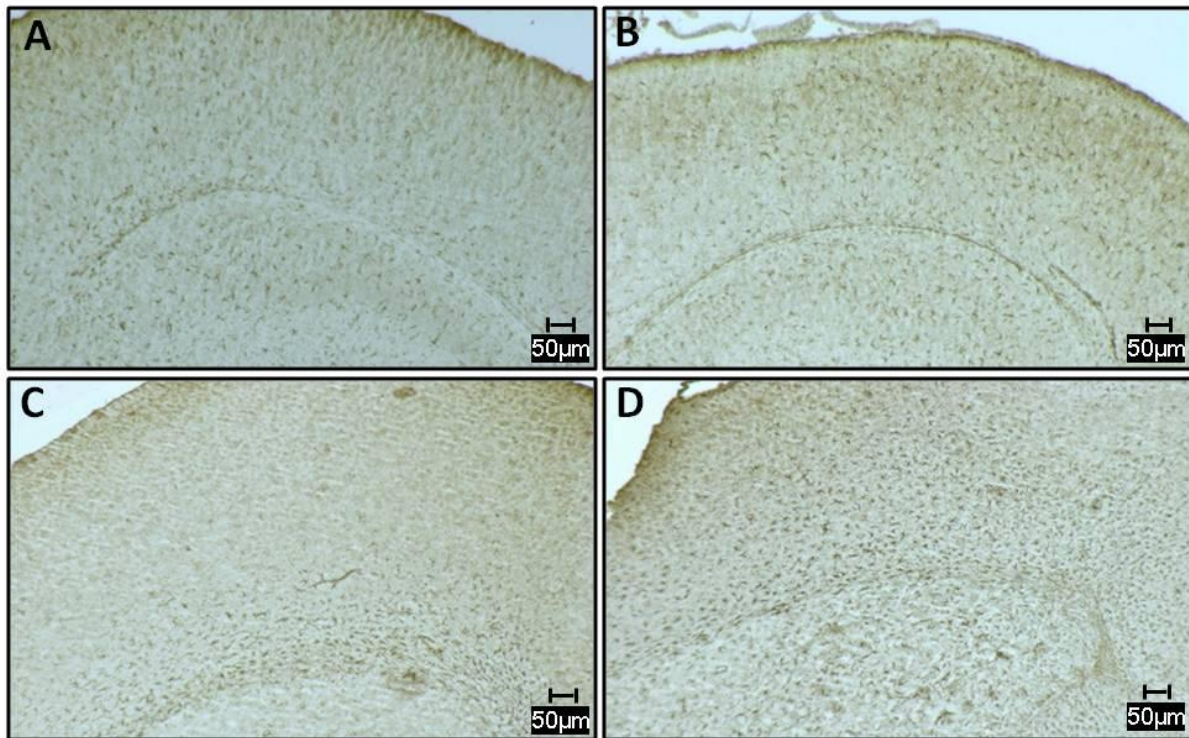
Figure 9: GFAP staining of K14 lnl mice brain at different developmental stages
GFAP staining (magnified 200 times) of frontal sections of the cortex of K14 lnl at the age of 7 days (A and B) and 14 days (C and D). Astrogliosis was observed in K14 ko (B and D) compared with K14 wt mice (A and C).

The deficiency of the enzyme glucocerebrosidase, the most important aspect of this mouse model, was also observed by staining using frontal paraffin sections of K14 lnl mice. The β-glucocerebrosidase staining (brown) underlined with HE staining (blue)

was compared between the hippocampus (Figs. 10A - 10D) as well as the cortex (Figs. 10E - 10H) of K14 lnl mice. Again, 7-day-old (Figs. 10A and B, E and F) as well as 11-day-old (Figs. 10C and 10D, 10G and 10H) K14 lnl mice were used. In general glucocerebrosidase is found in every cell of the brain. GCase staining was less in K14 ko mice, at both developmental stages, in the hippocampus (Figs. 10B and 10D) as well as in the cortex (Figs. 10F and 10H) compared with K14 wt mice (Fig. 10; hippocampus, A and C; cortex, E and G).
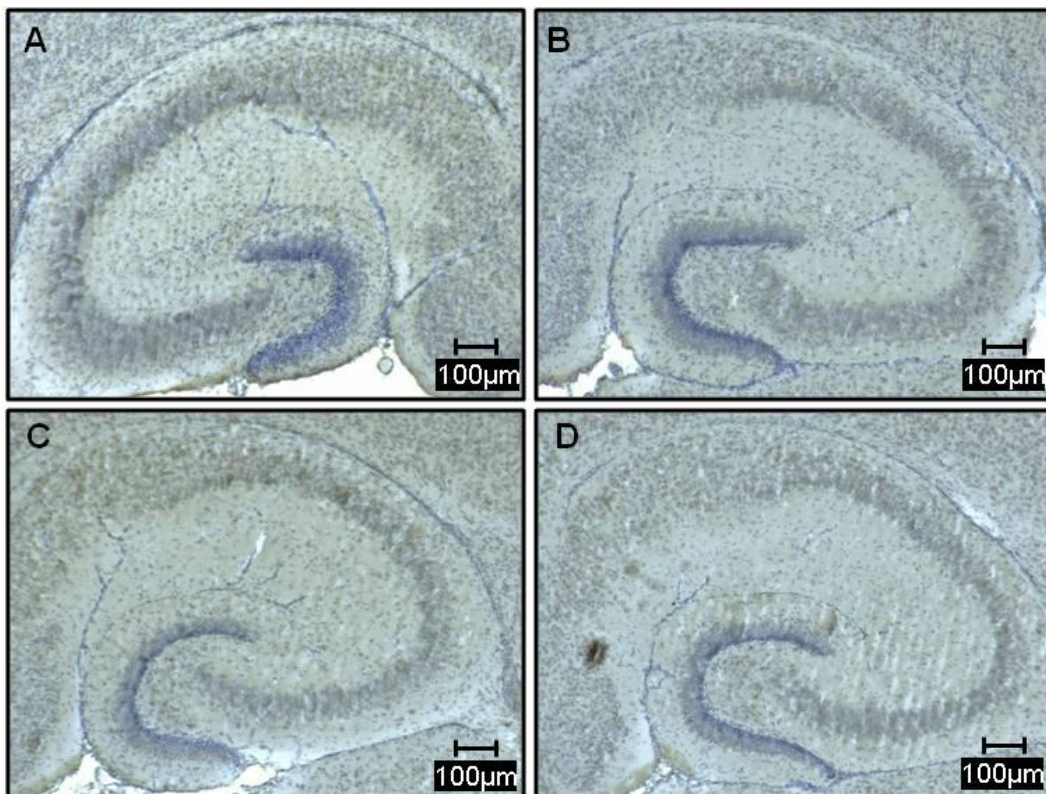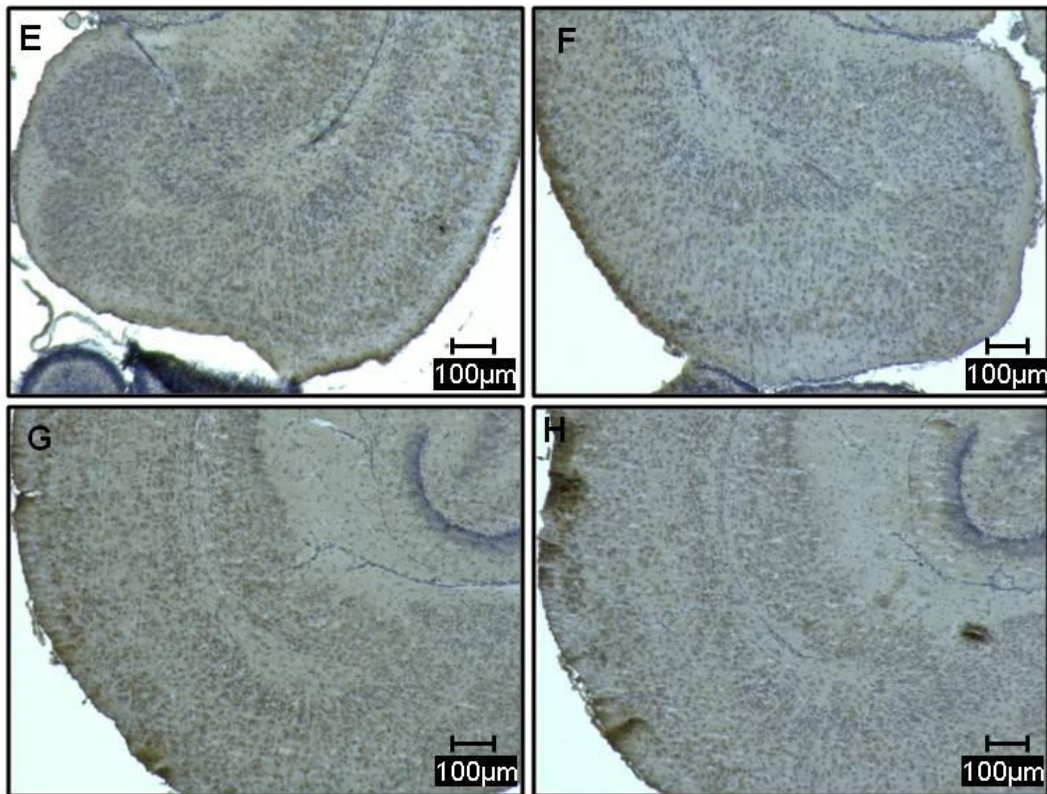
Figure 10: β-glucocerebrosidase staining of K14 lnl brains
Staining (magnified 200 times) of the hippocampus (A–D) and the cortex (E–H) of K14 lnl mice at 7 (A–B, E–F) and 14 days (C–D, G–H) of age. Less GCase staining was seen in K14 ko mice in the hippocampus (B, D) as well as in the cortex (F, H) compared with the K14 wt mice (hippocampus, A and C; cortex, E and G) at both developmental stages.

3.1.2 Relative β-glucocerebrosidase activity in K14 lnl mice brains

Gaucher's disease type II is caused by the reduced enzyme activity of the lysosomal enzyme β-glucocerebrosidase and resultant damages. By using a specific established assay (see Section 2.6.2) it was possible to determine the relative GCase activity in K14 brains (cerebellum and cerebrum).

Figure 11 and Figure 12 show the relative GCase activity measured at the different developmental stages (P7, 11 and 14) in the cerebellum and the cerebrum, respectively, of K14 lnl mice. The activity measured at each time point was compared in between K14 ko mice and K14 wt mice.

In Fig. 11 the relative GCase activity in the cerebellum (0.33 ± 0.14) was significantly decreased (Student's t test; $p < 0.01$) compared with the activity measured in K14 wt mice (1 ± 0.16) in the group of 7-day-old mice. Furthermore, the relative GCase activity was also significantly reduced (Student's t test; $p < 0.05$) in the cerebellum of

K14 ko mice at the ages of 11 days (0.39 ± 0.12) and 14 days (0.46 ± 0.22) compared with the activity measured in the cerebellum of K14 wt mice (P11: 1 ± 0.24; P14: 1 ± 0.12).
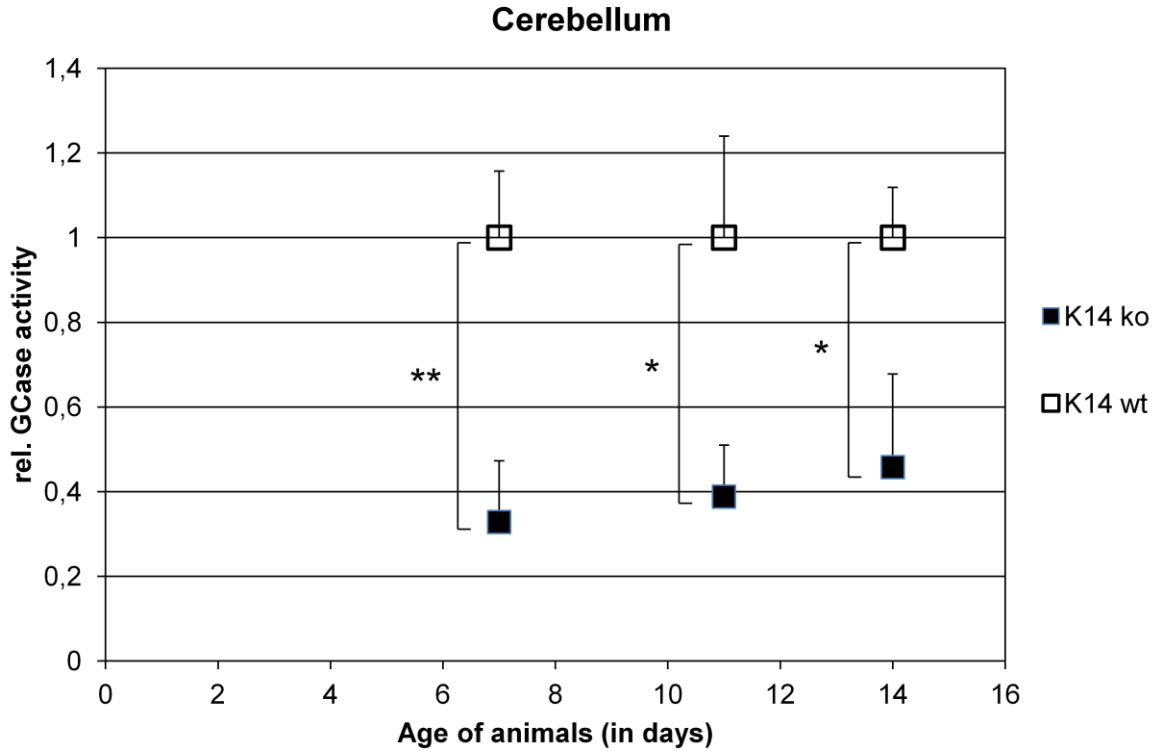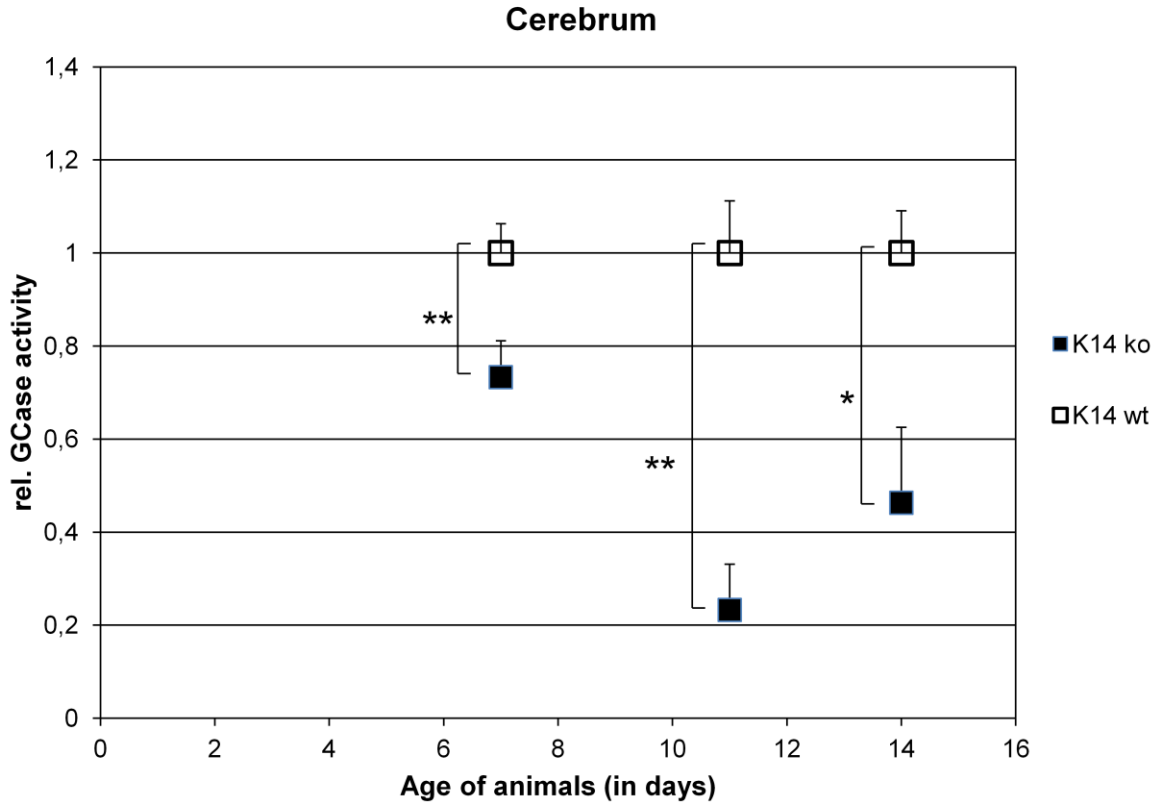

Figure 11: Relative GCase activity in the cerebellum of K14 lnl mice
Samples of homogenised cerebellum of 7-, 11- or 14-day-old K14 ko or K14 wt mice were examined for their activity in conversion of the substrate 4-MUD. Significantly decreased relative GCase activity was observed at all stages of disease in K14 ko mice compared with K14 wt mice of the same age. Data shown are means ± SD of 3 animals per group. All data were subjected to Student's *t* test; * $p < 0.05$; ** $p < 0.01$.

In Fig. 12 the relative GCase activity was also significantly ($p < 0.01$) reduced in the cerebrum of 7-day-old (0.73 ± 0.07) as well as in 11-day-old (0.23 ± 0.09) K14 ko mice compared with K14 wt (P7: 1 ± 0.06; P11: 1 ± 0.11). The last group, comprising 14-day-old K14 ko mice, also showed a significantly reduced ($p < 0.05$) GCase activity (0.46 ± 0.16) compared with K14 wt mice (1 ± 0.09).

Figure 12: Relative GCase activity in the cerebrum of K14 lnl mice
Samples of homogenised cerebrum of 7-, 11- or 14-day-old K14 ko or K14 wt mice were examined for their activity in conversion of the substrate 4-MUD. Significantly decreased relative GCase activity was observed at all stages of disease in K14 ko mice compared with K14 wt mice of the same age. Data shown are means ± SD of 3 animals per group. All data were subjected to Student's t test; * $p < 0.05$; ** $p < 0.01$.

3.2 Cloning vectors expressing the transgene β-glucocerebrosidase, packaging into AAV2 particles and an e*x vivo* model of Gaucher's disease type II

3.2.1 Cloning of an adeno-associated vector expressing human β-glucocerebrosidase

Two different vectors were used in this work, pAAV.CMV_sGBA_HA_ApoB (pAAV.hGC; Fig. 17A) and pFB.CAG_sGBA_ApoB (pFB.CAG; Fig. 17B) in order to produce viral AAV2 particles which were under the control of either CMV or the CAG promoter. The common feature of both vectors is the cloned gene of interest: the LDLR-binding domain, which was fused to the human cDNA coding the therapeutic transgene β-glucocerebrosidase.

A few different attempts were required before the gene of interest was finally cloned into the pQE TriSystem vector and from there on into the required shuttle vector pAAV.MCS to produce the AAV2 virus particles. A variety of attempts were made to use PCR amplification after designing specific primers with additional restriction sites. However, the cloning of PCR fragments is in general not a method of choice, as these fragments are very unstable. Another major drawback in producing PCR fragments is the primer's efficiency. In this work the designed primers did not show the efficiency that would be required to allow the use of the amplified PCR fragments for further cloning. However, the pQE TriSystem vector was good to be used as subcloning vector when digesting the gene of interest as described below.

3.2.1.1 Subcloning into the pQE TriSystem vector

The vector pFB.CMV_sGBA (see Section 11.2) was digested with the restriction enzymes EcoRI and KpnI to isolate a 1906 bp-long insert representing the β-glucocerebrosidase gene and the LDLR binding site. The Insert has an EcoRI sticky end at the 5' site and a KpnI sticky end at the 3' site. In order to be able to clone the digested gene of interest into the pQE TriSystem vector, it was also digested with EcoRI and KpnI and dephosphorylated to prevent any self-annealing steps afterwards.

The gene of interest was ligated into the prepared pQE TriSystem vector by sticky-end ligation in the 5' -> 3' orientation. The resulting vector pQE TriSystem_hGC had a size of 7706 bp (plasmid not shown). The reaction products from two different ligation set-ups were heat-shock transformed into *E. coli M15,* and in total 5 clones from each ligation were picked and analysed by restriction digestion (Fig. 13). All clones were tested to be positive, for the gene of interest, as a fragment of 1906 bp was digested with EcoRI and KpnI and visualised on an agarose gel. Clone 4 of 1:15 ligation mix was used for maxi plasmid preparation and sequencing of the insert (see Section 2.5.9).
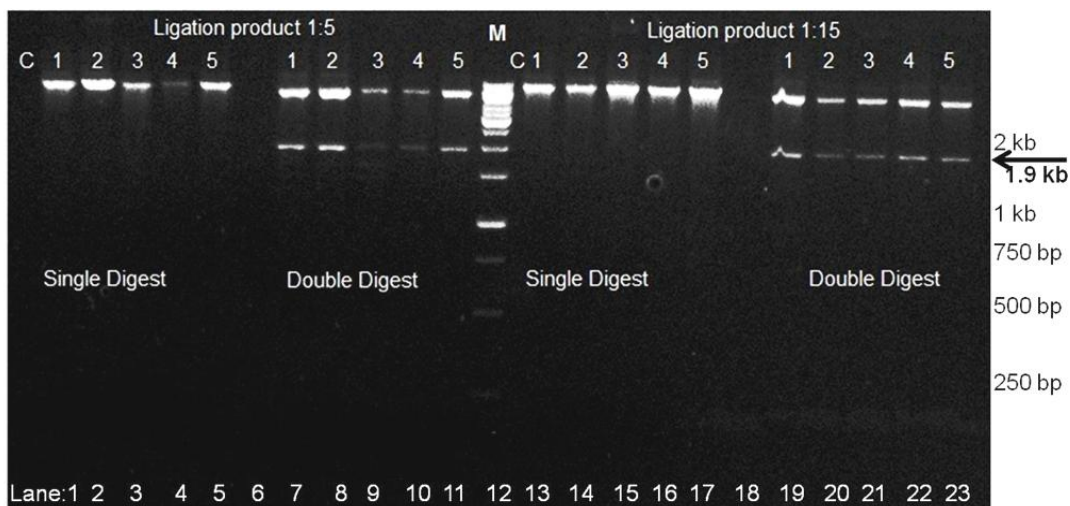
Figure 13: Digested *E. coli M15* clones after heat-shock transformation
Two different ligation mixes (1:5 and 1:15) were used to ligate the prepared gene of interest into the pQE TriSystem vector by using competent *E. coli* M15. Five clones of each mix were used either for a single digest with EcoRI for linearisation (7706 bp) or for a double digest to verify the cloning event; the gene of interest is indicated with an arrow (1906 bp). In lane 12, the 1 kb marker was applied; the most important sizes are indicated on the right side of the picture.

After sequencing, the sequence of the cloned vector pQE TriSystem_hGC was compared with the original glucocerebrosidase sequence derived from the donor vector pFB.CAG by aligning both sequences using BLAST. The alignment revealed a homology of 97%. Therefore this vector was used for the final cloning steps to construct pAAV.CMV_sGBA_HA_ApoB.

3.2.1.2 Cloning of pAAV.CMV_sGBA_HA_ApoB

For cloning the vector pAAV.CMV_sGBA_HA_ApoB the gene of interest (coding human GCase and LDLDR signal sequence) was isolated by restriction digestion with EcoRI and HindIII from the subcloning vector pQE TriSystem_hGC. Digestion resulted in a 1914 bp fragment. The Insert consisted of an EcoRI sticky end at the 5' site and a HindIII sticky end at the 3'site. The adeno-associated vector pAAV.MCS was digested with the enzymes EcoRI and HindIII as well.

The gene of interest was ligated by sticky-end ligation in the 5' -> 3' orientation into the pAAV.MCS vector, resulting in the vector pAAV.CMV_sGBA_HA_ApoB with a total size of 6514 bp (Fig. 17). Again two different ligation mixes (1:5 and 1:15) were

transformed by heat-shock transformation into *E. coli XL-10* (see Section 2.5.3). Afterwards 4 clones from each transformation experiment were picked and digested with EcoRI and HindIII (Fig. 14). All clones showed positive results and the gene of interest are indicated by an arrow (1914 bp fragment). Clone 2 (ligation product 1:5) was picked for maxi plasmid preparation and sequencing.
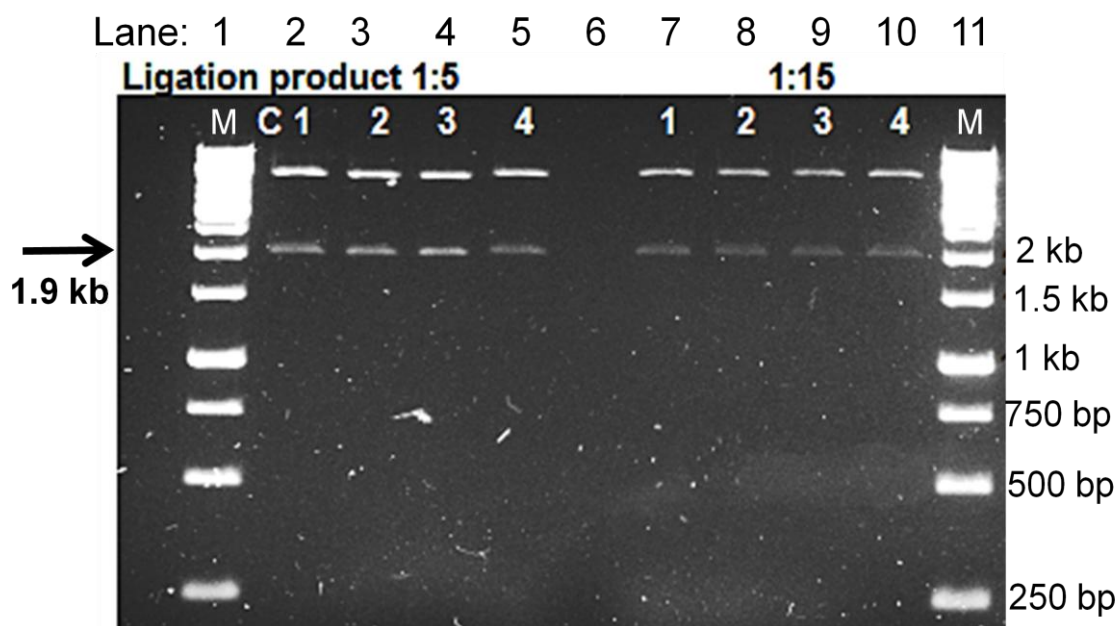
Figure 14: Control digests of transformed *E. coli XL-10*
Four clones from each ligation set after transformation into *E. coli XL-10* were picked for analysis by restriction digest with EcoRI and HindIII. Fragments of 1914 bp (arrow indicating the cloned gene of interest) and 4600 bp were visualised. In lanes 1 and 11, the 1 kb marker was applied; the most important sizes are indicated on the right side of the picture.

In order to verify the presence of the gene of interest in the cloned isolated vector pAAV.hGC of clone 2 sequencing was performed. The alignment of the sequence of pAAV.hGC with the sequence of human GCase revealed a homology of 100%. Figure 15 shows part of the performed alignment, whereas the full alignment is found in Section 11.3.

Figure 15: Part of the alignment of the sequences of pAAV.hGC and the human GCase
'Query' represents the sequence of pAAV.hGC and 'Sbjct' the sequence of the human GCase.

Figure 16 shows a part of the sequence alignment performed of the cloned pAAV.hGC and the shuttle vector pAAV.MCS, performed in order to verify the presence of the backbone. The sequence homology was found to be 96% (see Section 11.3).

Figure 16: Verification of pAAV.MCS backbone by alignment with the sequence of pAAV.hGC
'Query' represents the sequence of pAAV.hGC sequence and 'Sbjct' the sequence of the backbone vector pAAV.MCS

All sequencing results verified the presence of the transgene β-glucocerebrosidase in the cloned pAAV.hGC vector (Fig. 17A). Therefore this vector and pFB.CAG were

tested for GCase enzyme activity and expression in two different cell systems, Gaucher patient fibroblasts and primary neurons derived from K14 ko mice.
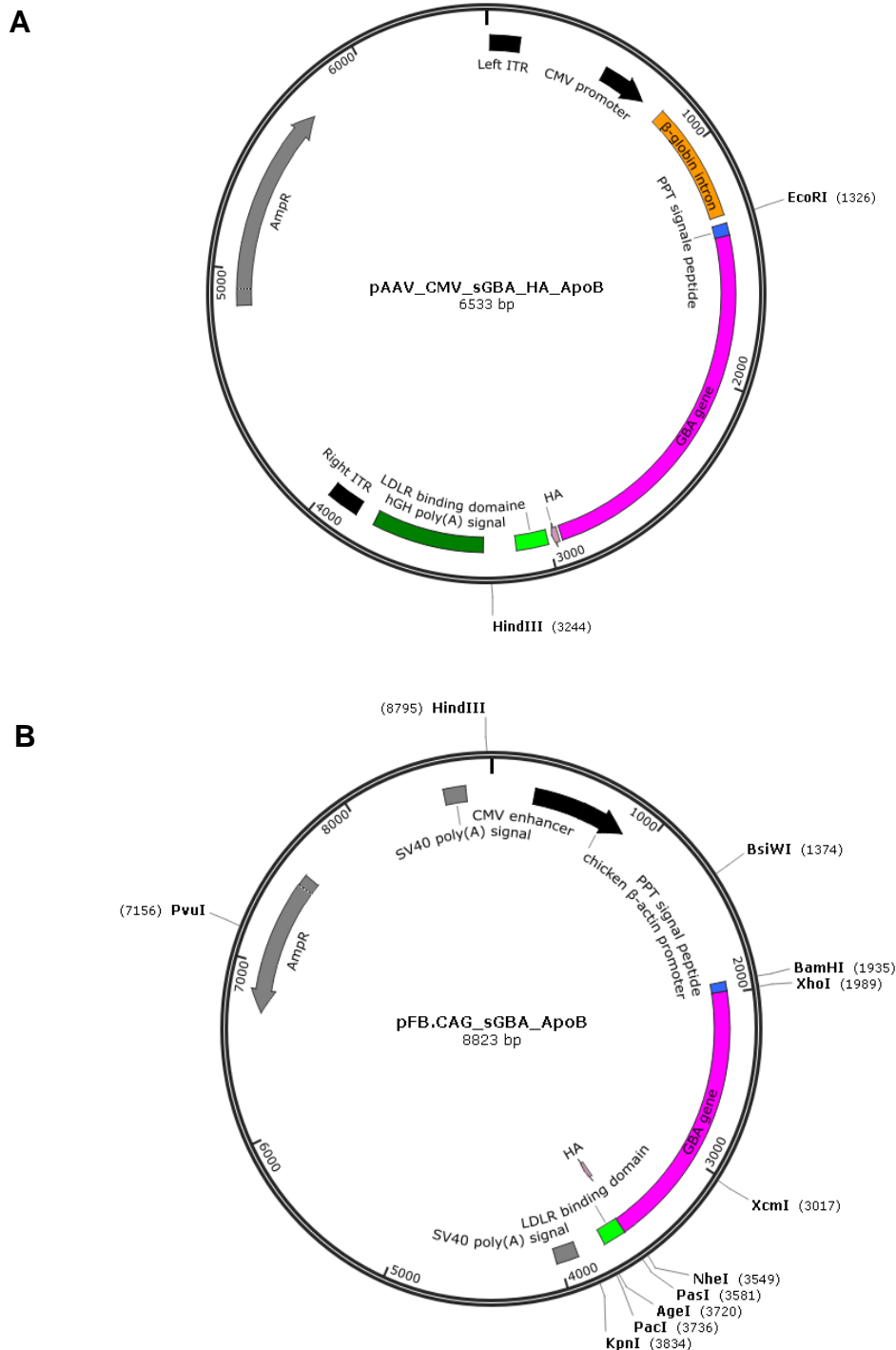
Figure 17: Schematic overview of pAAV.hGC and pFB.CAG
A: Graphic of pAAV.hGC; GBA gene: *β-glucocerebrosidase gene*; LDLR: low-*density-lipoprotein receptor signal sequence*; hGH polyA: *human growth hormone poly A signal*; AmpR: *ampicillin resistance gene*; CMV promoter: *cytomegalovirus*; ITR: *internal repeats*. B: Graphic of pFB.CAG. Similar features as described for A, except the promoter: CAG: *combination of CMV early enhancer element and chicken beta-actin promoter*.

3.2.2 Analysis of pAAV.CMV_sGBA_HA_ApoB and pFB.CAG_sGBA_ApoB

In this work the gene of interest was verified according to the enzyme activity of the transgene β-glucocerebrosidase. Both vectors mentioned above were compared after transfecting them into two different cell systems, i.e., either fibroblasts derived from a Gaucher patient or primary neurons derived from K14 ko embryos.

3.2.2.1 Measurement of GCase activity and expression in fibroblasts

In order to find out whether pAAV.hGC and pFB.CAG actually express an active form of β-glucocerebrosidase, both vectors were used to transfect fibroblasts (Figure 18) from a Gaucher patient.
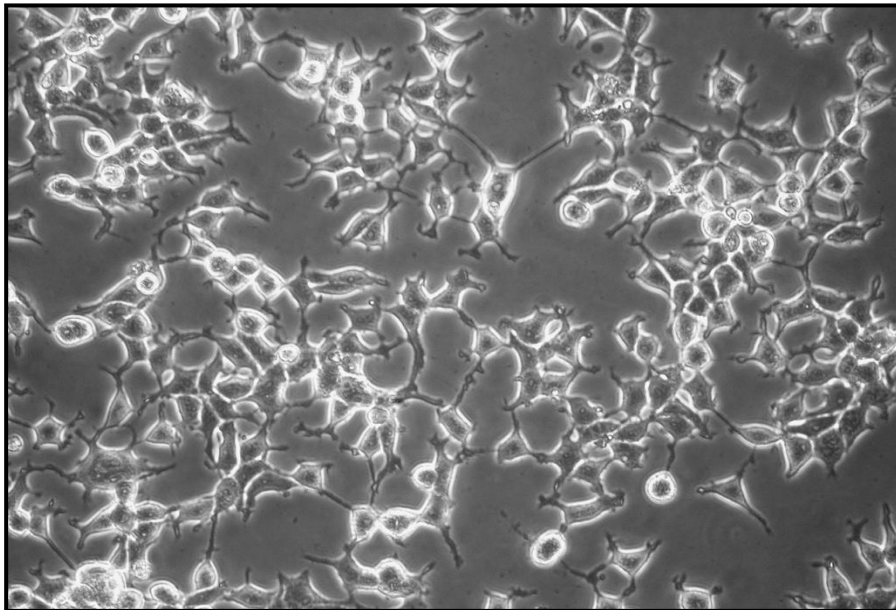
Figure 18: Fibroblasts from a Gaucher patient in culture, 20 x objective

The activity of GCase of transfected fibroblasts was determined by measuring the conversion rate of 4-MUD using the GCase activity assay (Section 2.6.2). As shown in Figure 19, the GCase activity was significantly ($p < 0.01$) increased in transfected M.G fibroblasts with either pAAV.hGC (2.77 ± 0.75) or with pFB.CAG (3.03 ± 0.65) compared with untreated M.G. fibroblasts (1 ± 0.35). Furthermore, the transfection of

M.G. fibroblasts with both vectors led to the same GCase activity level as found in fibroblasts from a healthy individual (2.69 ± 0.42). The GCase activity in fibroblasts of a healthy individual was also significantly (p < 0.01) increased compared with untreated M.G. fibroblasts.
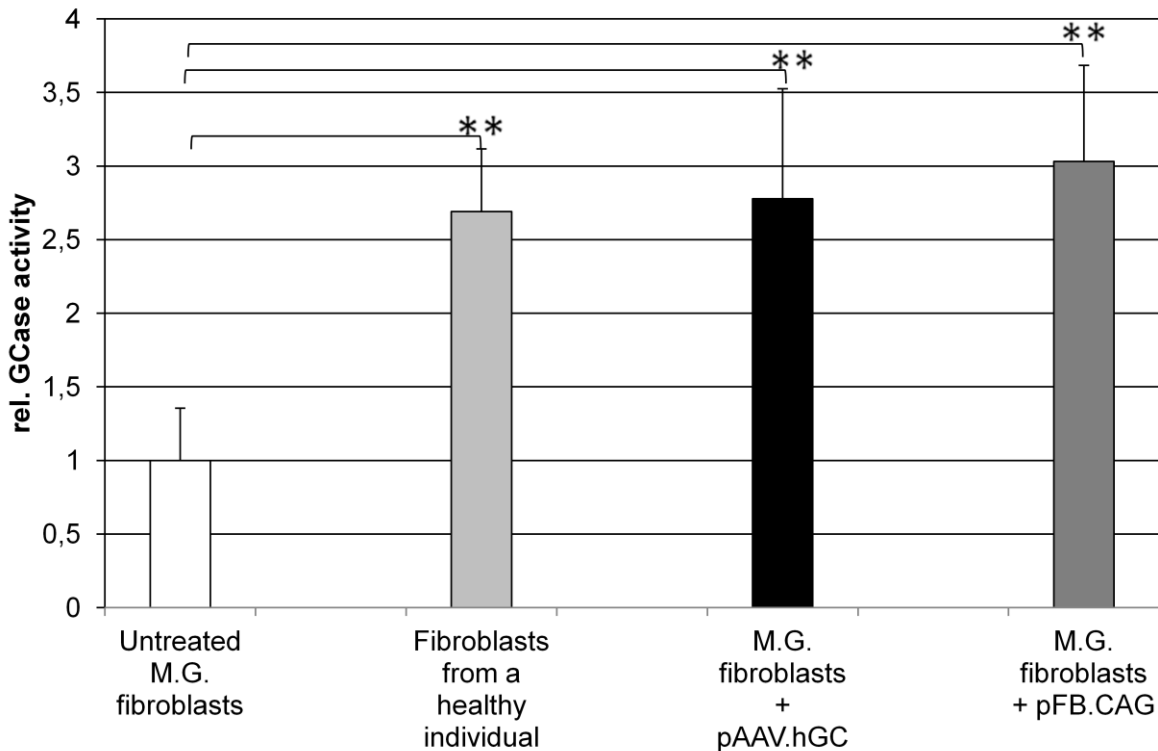

Figure 19: Measurement of relative GCase activity in lysates of fibroblasts
Transfected M.G. fibroblasts with either pAAV.hGC or pFB.CAG showed significantly increased relative GCase activity compared with untreated M.G. fibroblasts. However, no difference was seen compared with fibroblasts from a healthy individual. Data shown are means ± SD from 10–15 fibroblast cultures per group. All data were subjected to Student's *t* test; **$p < 0.01$.

Further analysis was performed by measuring GCase activity in the media of transfected M.G. fibroblasts compared with untreated M.G. fibroblasts and fibroblasts derived from a healthy individual. This was done because the gene of interest was believed to code for a secretable form of β-glucocerebrosidase. Figure 20 shows significance ($p < 0.01$) in the case of transfecting M.G. fibroblasts with either pAAV.hGC (11.91 ± 2.23; p < 0.01) or pFB.CAG (12.99 ± 0.12; $p < 0.05$) compared with untreated M.G. fibroblasts (1 ± 0.21). The increase of GCase activity was even 12 times as great as in the untreated M.G. fibroblast. GCase activity was also

significantly ($p < 0.01$) increased in the media of transfected M.G. fibroblasts compared with the activity measured in the media from fibroblasts of a healthy individual (4.72 ± 0.45).
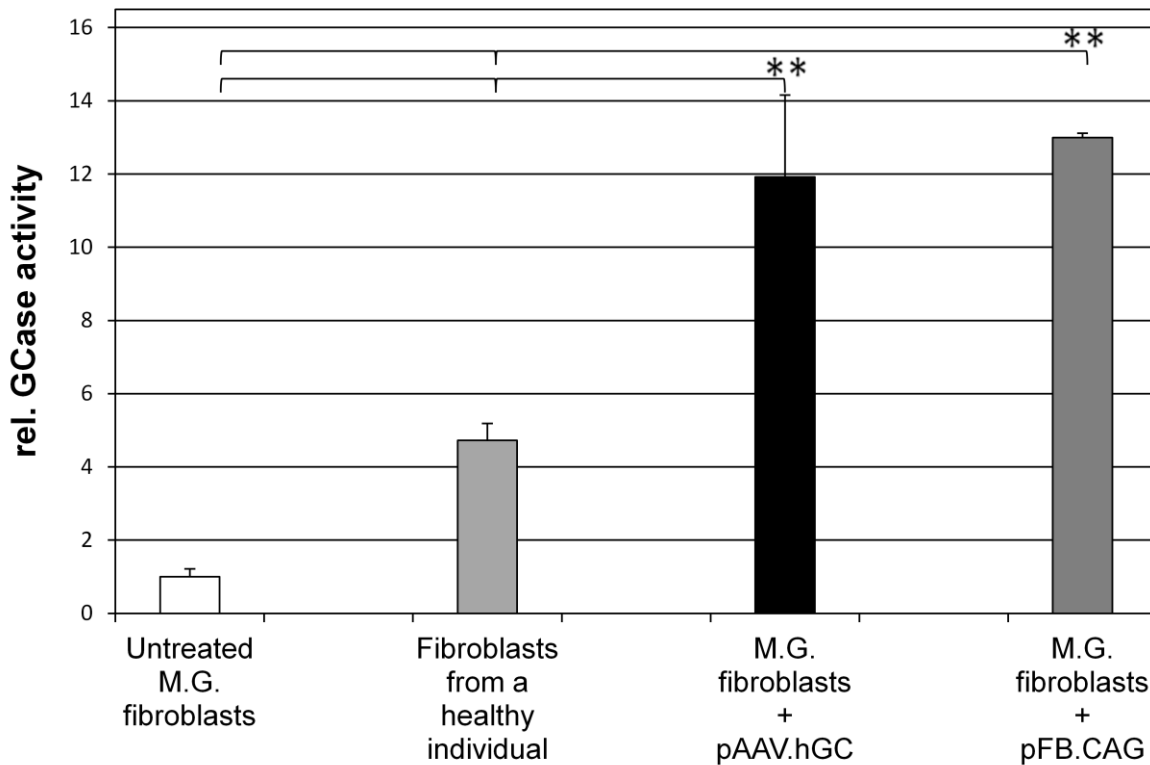

Figure 20: Measurement of relative GCase activity in the media of transfected fibroblasts
Increased GCase activity was measured in M.G. fibroblasts transfected either with pAAV.hGC or pFB.CAG compared with untreated M.G. fibroblasts and fibroblasts from a healthy individual. Data shown are means ± SD of 3 cultures per group. All data were subjected to Student's t test; ** $p < 0.01$.

The protein level of β-glucocerebrosidase was determined by western blot separation using the HA-Taq to detect the fusion protein in the lysate of M.G. fibroblasts. Figure 21 shows one example in which the antibody against HA-Taq was used to detect the fusion protein. Positive results were obtained, as in both cases detection was possible for M.G. fibroblasts transfected with either pAAV.hGC or pFB.CAG. Here the original vector pFB.CMV was also used to transfect M.G. fibroblasts as positive control for the gene of interest. No detection of the fusion protein was possible in samples from non-transfected M.G. fibroblasts.
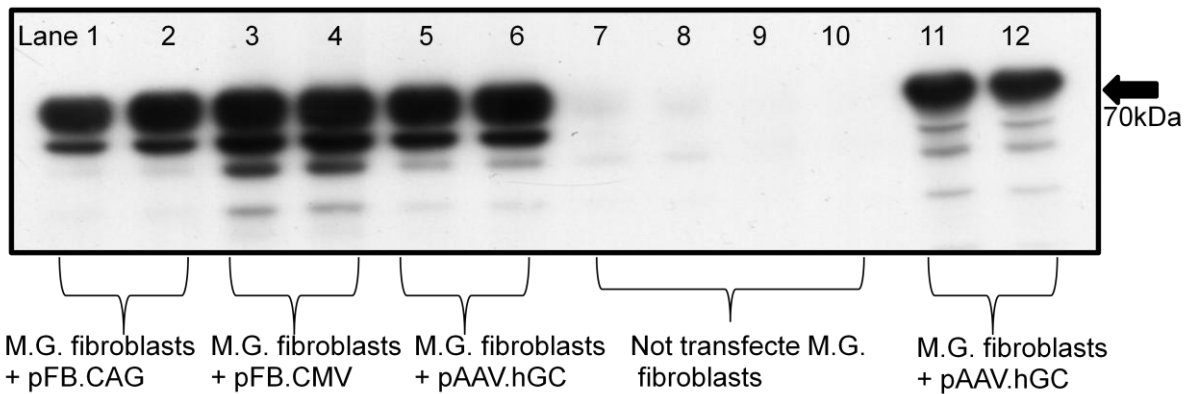
Figure 21: Detection of the fusion protein using HA-Taq by Western blot
2 µg of protein of each sample was loaded onto a separate lane. The antibody against the HA-Taq was used to detect the fusion protein of transfected M.G. fibroblasts with pFB.CAG (lanes 1 and 2) or pAAV.hGC (lanes 5 and 6 and lanes 11 and 12) in comparison with non-transfected M.G. fibroblasts (lanes 7–10). As a positive control, M.G. fibroblasts were transfected with the original vector pFB.CMV (lanes 3 and 4).

3.2.2.2 GCase activity in K14 primary neurons

Verification of both vectors was further performed in primary neurons derived from K14 embryos. First, primary neurons from K14 wt and K14 ko mice were cultivated and GCase activity measured and compared. Knockout K14 embryos were cultivated to compare relative GCase activity in general. After one week of cultivating primary neurons, cells were harvested, processed and the same protein concentration was used for GCase activity assay. The relative GCase activity of lysates of neurons derived from K14 ko embryos (0.28 ± 0.09) was significantly ($p < 0.05$; Student's t test) decreased compared with neurons derived from K14 wt embryos (1 ± 0.11), as shown in Figure 22. These results are in line with data from whole-brain analyses (Figs. 11 and 12).
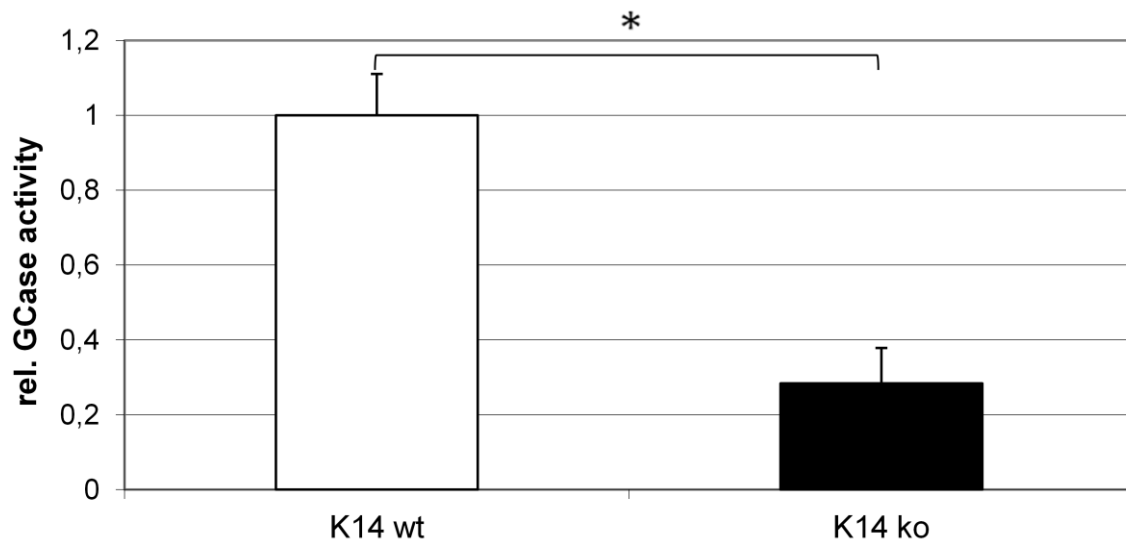
Figure 22: Comparison of relative GCase activity between neurons derived from K14 wt and K14 ko mouse embryos
Relative GCase activity was significantly decreased in neurons from K14 ko embryos compared with K14 wt embryos. Data shown are means ± SD of primary neuron cultures from 3 different mice per genotype. All data were subjected to Student's *t* test; *$p < 0.05$.

Primary neurons from K14 ko mouse embryos were used for nucleofection with pAAV.hGC and pFB.CAG. For verification of successful nucleofection of primary neurons and to determine the efficiency, primary neurons were first transfected with pMaxGFP[®]. PMaxGFP[®] encodes green fluorescent protein (Fig. 23A). Nucleofected cells were also stained with Map2 antibody, a neuronal marker to verify the specific cell type (Fig. 23B). Figure 23C shows positively nucleofected primary neurons of K14 knockout mice. The transfection efficiency of neurons using the Nucleofector Kit (see Section 2.7.6.2) was determined to be about 60% after counting cells that were positive for green fluorescent protein.
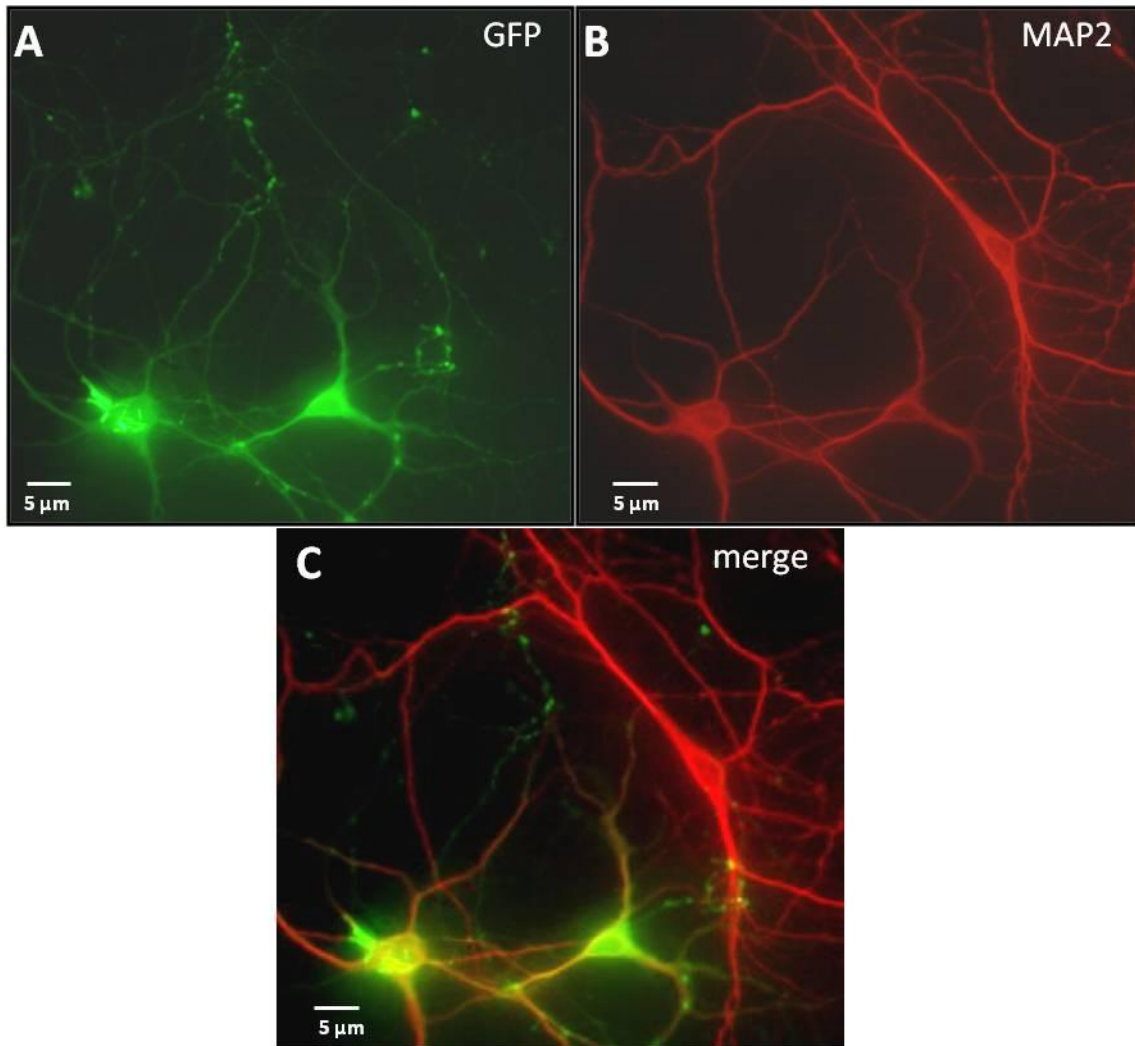
Figure 23: Successfully nucleofected primary K14 ko neurons with pMaxGFP®
A: View field showing positively nucleofected neurons with pMaxGFP® encoding green fluorescent protein. B: Same view field as A; Map2 staining of neurons. C: Merged picture of A and B, showing that the positively nucleofected cells are neurons.

After establishing the method of nucleofection of primary neurons with pMaxGFP®, further experiments were performed using pAAV.hGC and pFB.CAG to nucleofect primary neurons of K14 ko embryos. Figure 24 shows the significant ($p < 0.05$; Student's t test) increase in relative GCase activity after the nucleofection of primary neurons from K14 ko embryos with pAAV.hGC (1.66 ± 0.32) compared with GCase activity of non-nucleofected (1 ± 0.51) primary neurons from K14 ko embryos. Nucleofection with pFB.CAG (1.51 ± 0.3) also led to an increase of relative GCase activity compared with non-nucleofected primary neurons; this increase was not significant.
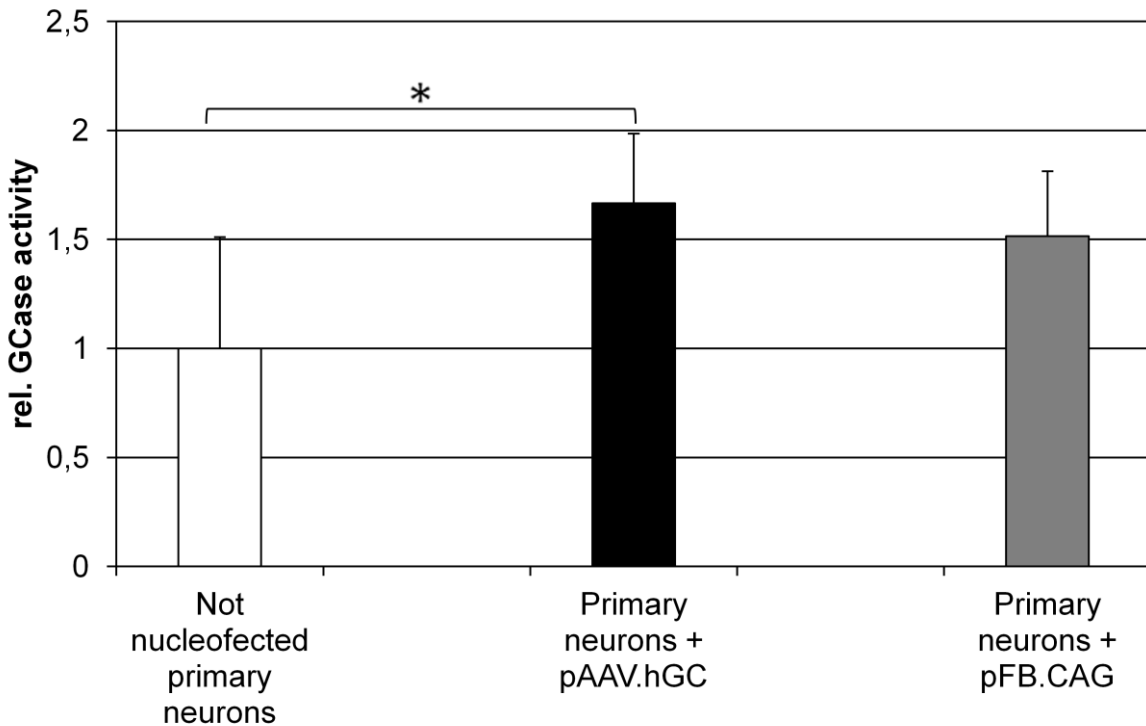
Figure 24: Relative GCase activity after nucleofection of primary neurons derived from K14 ko embryos
pAAV.hGC nucleofection led to a significant increase in relative GCase activity compared with control. The nucleofection with pFB.CAG also led to an increase in relative GCase activity. Data shown are means ± SD of GCase activity of cultured primary neurons derived from 4–8 different K14 ko mice per group. All data were subjected to Student's *t* test; *$p < 0.05$.

3.2.3 Production of AAV2 particles expressing the marker gene LacZ

3.2.3.1 Generation of AAV2-producing AAV-293 cells

Both vectors investigated above were cloned in order to express human GCase in transduced cells. In order to allow transduction into different cell types, these vectors had to be packed into viral particles.

The AAV-293 cell line was used as a viral-particle-producing cell line. Initially the plasmid (pAAV.LacZ) coding the *nLacZ* gene was used to determine the transfection efficiency and transgene expression of the viral particles produced.

The production of viral particles can be observed by colour change of the media, but also through phenotypic changes, as shown in Figure 25. Sometimes viral particle production makes cells appear rounder and they become detached from the bottom

of the cell culture dish and can be observed as free-floating cells (Fig. 25B). These can be harvested in the medium as described in Section 2.8.2 to confirm that all the viral particles produced are present in the supernatant after centrifugation.
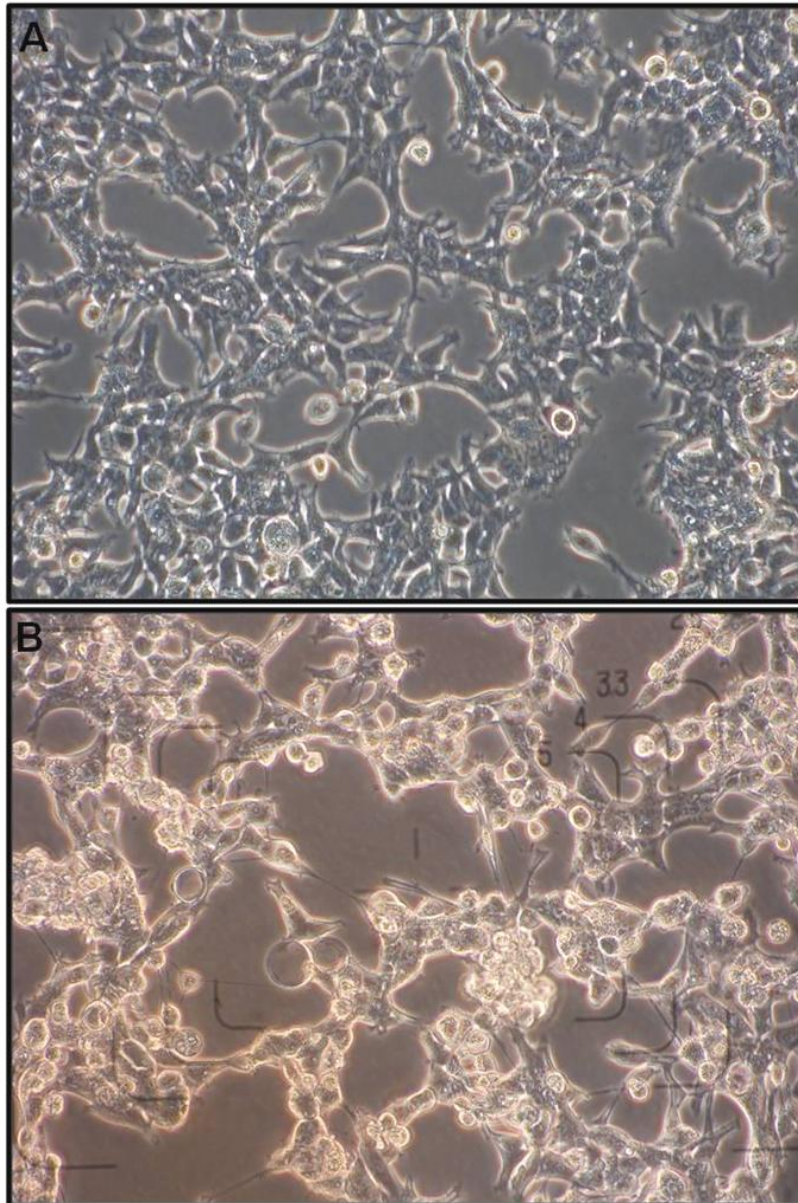

Figure 25: AAV-293 cells
A: AAV-293 cells before transfection. B: AAV-293 cells after transfection with pAAV.LacZ.

3.2.3.2 Analysis of AAV2 virus particles in AAV-HT1080 cells

After the successful production of AAV2 viral particles in AAV-293 cells, AAV-HT1080 cells were used to detect the transduction efficiency and viral titre of the viral stocks

produced. The presence of the reporter gene *nLacZ* was detected by X-Gal staining (Fig. 26) in AAV-HT1080 cells containing AAV2 particles packed with plasmids coding for the reporter gene. 'Positive' stained cells appear blue, while cells transduced with the negative control remain unstained. The negative control was produced by either substituting the pHelper or pRC for transfection of AAV-293 cells.
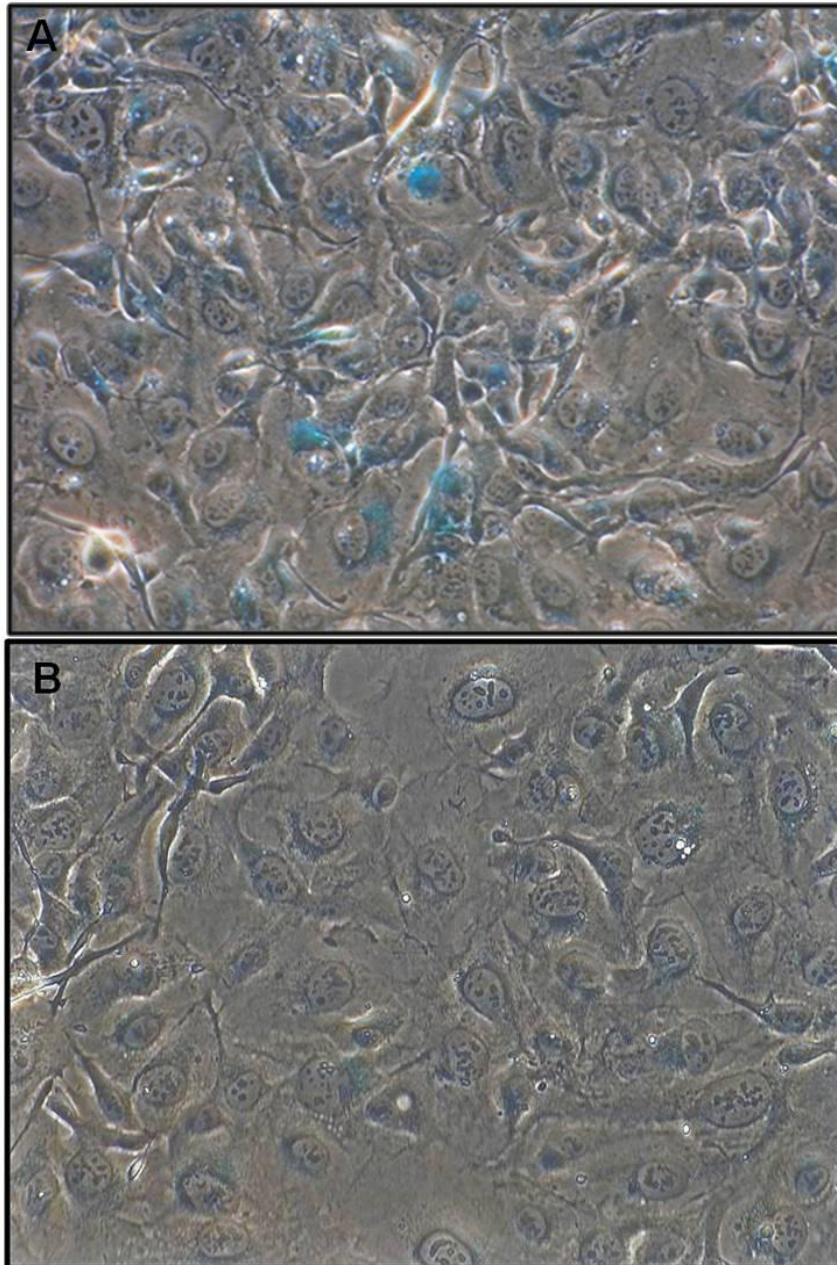

Figure 26: Transduction of AAV-HT1080 cells
A: AAV-HT1080 cells transduced with AAV2 particles packed with plasmid expressing *nLacZ*. 'Positive' cells were stained blue by X-Gal staining (20 x objective). B: AAV-HT1080 cells transduced with negative control; no blue-stained cells were observed.

The results obtained for the transduction efficiency of different viral supernatants produced in the present study are summarised in Table 13. The mean transduction efficiency of the AAV2-produced viral particles was found to be 45.2%.

Table 13: Transduction efficiency of AAV2-produced viral supernatants
Left column, name and production date of each viral supernatant; right column, transduction efficiency determined by X-gal staining in %.

Viral supernatants	Transduction efficiency
AAV2_LAcZ (10.08.12)	36.4
AAV2_LacZ (31.08.12)	49.7
AAV2_LacZ (16.09.12)	47.0
AAV2_LacZ (22.09.12)	47.7

3.4.3 Viral titre determination in AAV-HT1080 cells

In order to be able to determine the titre of each viral supernatant produced in AAV-293 cells, X-Gal staining was also used for indirect titre measurement of AAV-HT1080 cells transduced with LacZ-packed AAV2 particles. The titre of the viral supernatant pAAV.LacZ (production date: 31.08.2013) was determined to be 8.3×10^6 IP/ml. The differently packed AAV2 particles obtained on this day were used for all further transduction experiments performed. The indirect titre was determined for viral titres produced on different days (see Table 14) which are stored at -80 °C until further usage.

Table 14: Viral titre of AAV2 supernatants
Left column: Date, name and production date of each viral supernatant; right column: titre given in IP/ml.

Viral supernatants	Infectious particles per ml
AAV2_LAcZ (10.08.12)	8.3×10^6
AAV2_LacZ (31.08.12)	8.9×10^6
AAV2_LacZ (16.09.12)	11.9×10^6
AAV2_LacZ (22.09.12)	10.9×10^6

3.2.4 Characterisation of cortical organotypic brain-slices as an *ex vivo* model for Gaucher's disease type II

In vitro systems, such as cell cultures of one cell type differ quite substantially from the *in vivo* situation. Therefore, one major goal of the present study was to establish an *ex vivo* model, displaying the disease Gaucher's disease type II and coming closest to the actual *in vivo* situation. Therefore the organotypic slice culture of the cerebrum (see Fig. 27) from K14 pups was established. The characterisation of this model was performed by using knockout as well as wild-type pups of the K14 lnl mouse model for comparison.
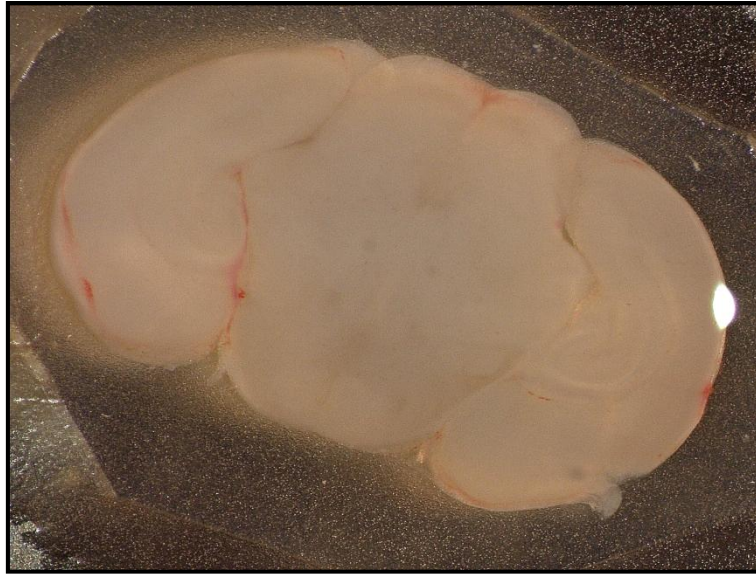
Figure 27: Cortical organotypic brain-slice culture of the cerebrum
Brain slices were prepared from K14 P8-9 pups; DIV 5.

3.2.4.1 Cell composition of organotypic K14 lnl brain slice

The main aim of this analysis was to find out whether there are any differences in the cell composition in slices derived from K14 ko mice compared with slices derived from K14 wt. The cell composition was analysed by comparing the protein expression detected with different cell markers by western blotting. GFAP was chosen for astrocytes, synaptophysin for neurons and CD 68 for activated microglia. Slices were harvested after periods of culturing varying from 1 day to 18 days. For later experiments only one week of incubation was of interest. Before actually comparing the expression of protein detected by different cell markers, protein concentration had to be adjusted. To make it possible to rely on the same protein concentration being present in each sample, each sample was adjusted by GAPDH protein expression (Fig. 28A). GAPDH is a housekeeping gene; therefore, it is often used for protein concentration adjustment. Slices from K14 wt / ko cultures were harvested at different time points in culture. Figure 28 shows an example of western blots for each cell marker used: for all cell markers, no significant differences between K14 wild-type and K14 knockout slices were observed.
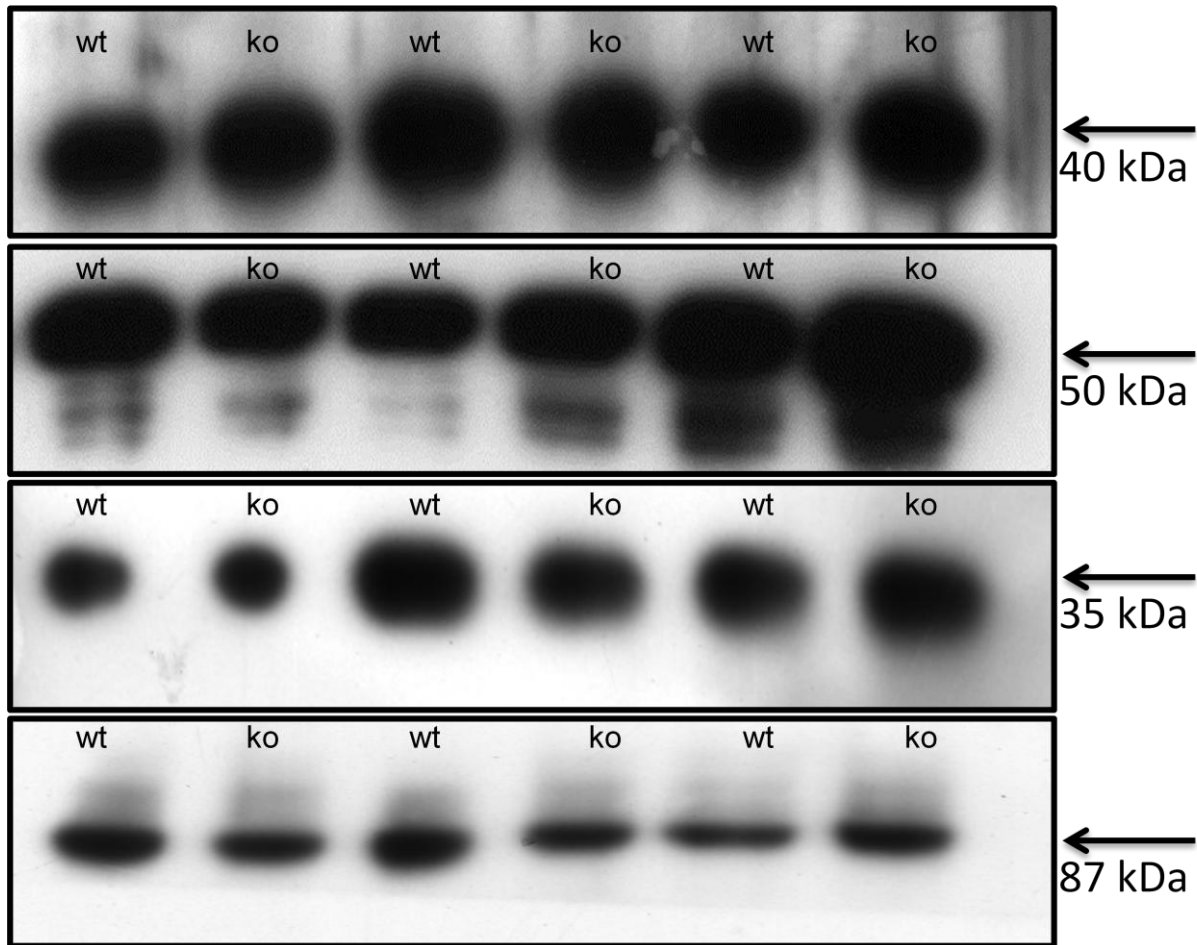
Figure 28: Comparison of K14 wt with K14 ko slices using various cell-specific markers
A protein concentration of 2 µg was used for each sample to be analysed. Alternately, samples from K14 wt and K14 ko slices were loaded onto the gel. Results at various time points after culturing the slices were compared. As examples, DIV1 (lanes 1 and 2), DIV3 (lanes 3 and 4) and DIV5 (lanes 5 and 6) are shown for each cell marker. A: GAPDH as housekeeping gene; to adjust the loading volume of each sample; B: GFAP as marker for astrocytes; C: synaptophysin as marker for neurons; D: CD68 as marker for activated microglia.

Figure 29 shows the statistical analysis of the western blot data set. For each time point, the result from slices of K14 wt mice was set to 100%. The protein expression detected using GFAP (Fig. 29A) was slightly increased in slices from K14 ko mice compared with slices from K14 wt mice. The greatest increase was observed on Day 7 in culture. However, these differences were not significant (Student´s t test). No difference was seen in the protein expression detected by synaptophysin (Fig. 29B) between slices from the two genotypes of K14 mice. Further, CD68 (Fig. 29C) showed a slight decrease in protein expression of slices from K14 mice compared

with slices from K14 wt mice but this increase was also not significant (Student´s t test).
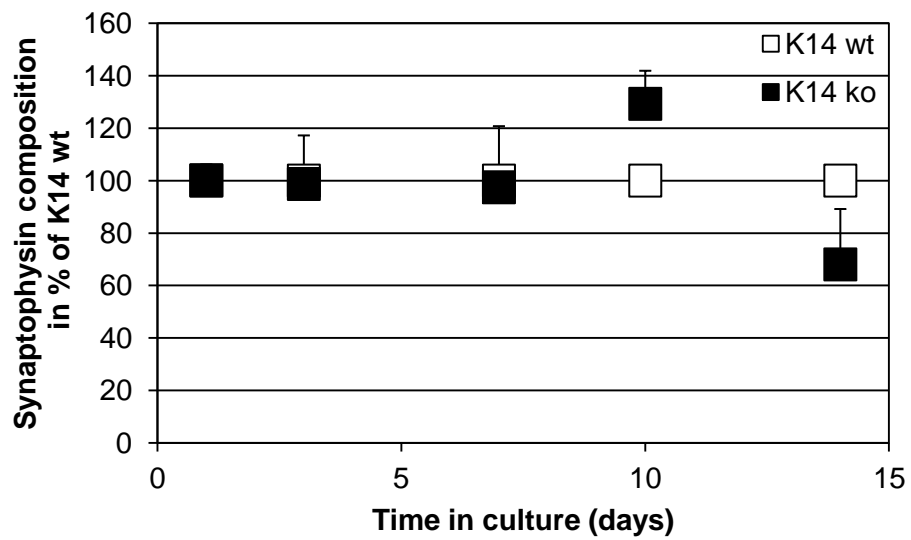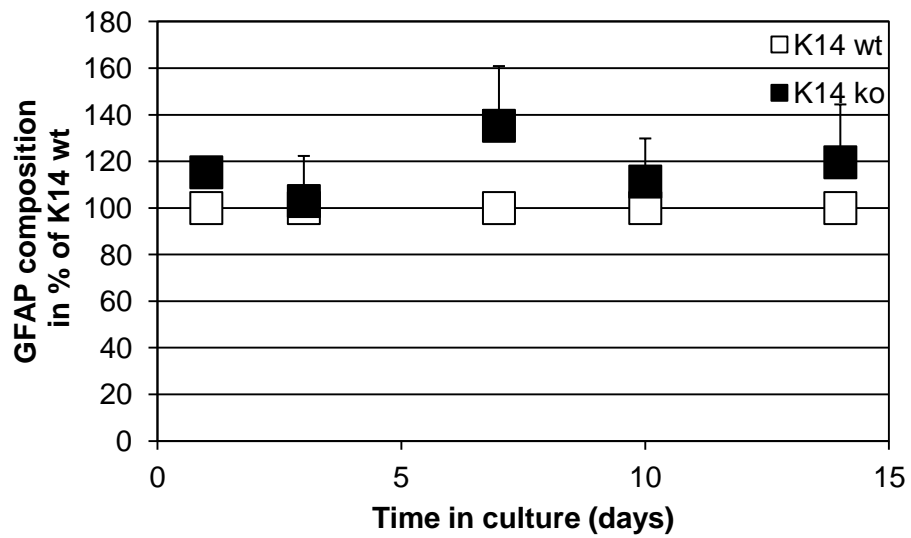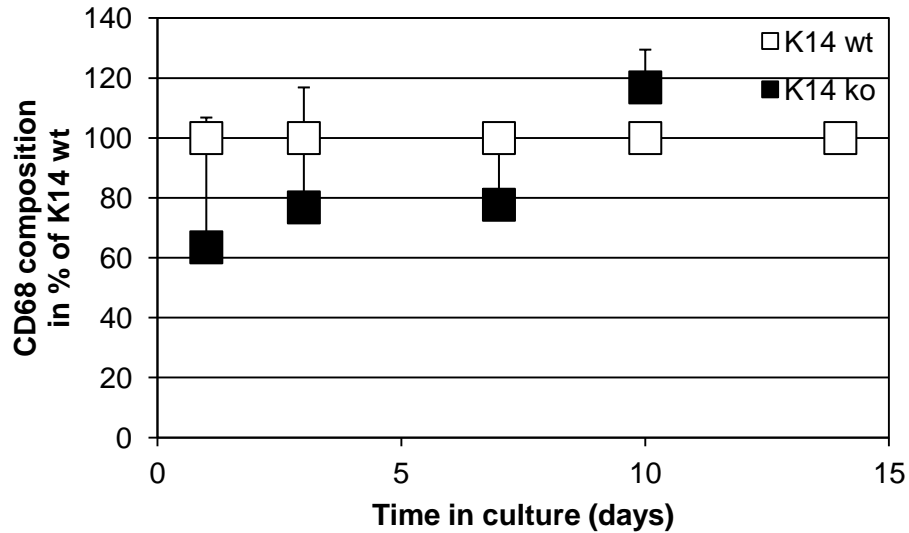
Figure 29: Statistical analysis of WB data of cortical organotypic brain-slices
Results from slice of K14 wt mice were set 100% for each incubation day. A: comparison of protein expression of GFAP expressing cells over time. B: Comparison of protein expression of synaptophysin expressing cells over time. C: comparison of protein expression of CD68 expressing cells over time. Data shown are means ± SD of 3 mice of each genotype per group.

3.2.4.2 Viability of cortical organotypic brain-slices

To verify the viability of the organotypic slice cultures, Calcein staining was performed. As shown in Figure 30, cortical organotypic brain-slices were successfully stained with Calcein, and predominant cells were stained green; even individual neurons can be distinguished. No obvious differences were seen between 2 days (Fig. 30A) and 4 days (Fig.30B) in culture.
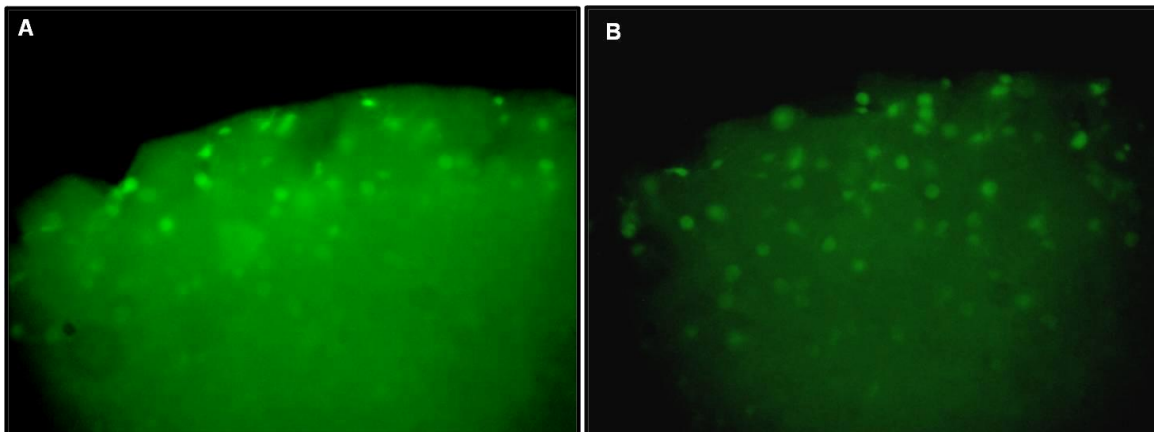

Figure 30: Calcein staining of cortical organotypic brain-slices
A: Calcein staining of cortical organotypic brain-slice after 2 days in culture. B: Calcein staining of cortical organotypic brain-slice after 4 days in culture.

3.2.4.3 Comparison of GCase activity between K14 wt and ko brain slices

The establishment of an *ex vivo* model which displays the disease Gaucher's disease type II depends on two factors: viability of K14 ko slices and reduced β-glucocerebrosidase activity. The viability was verified by the experiments described above and no obvious differences in culturing slices of K14 ko mice were observed when compared with slices from K14 mice. However, on the other hand, it was quite important to investigate whether the slices from K14 ko mice, which seem to be similar to slices from K14 wt mice show, reduced GCase activity.

Slices derived from K14 wt and K14 ko were harvested after different periods in culture and their Case activity was measured. For this purpose, each sample was adjusted to 2 µg/µl protein concentration, GCase activity was measured and the relative GCase activity was compared between the genotypes of K14 mice. Figure 31 shows that relative GCase activity was significantly decreased ($p < 0.01$) in organotypic slices from K14 ko mice compared with slices from K14 wt mice. The significant decrease of relative GCase activity in cortical organotypic brain-slices derived from K14 ko mice compared with K14 wt mice was observed for each culture period analysed. The same level of decrease was holding over the whole time of 18 days in culture.
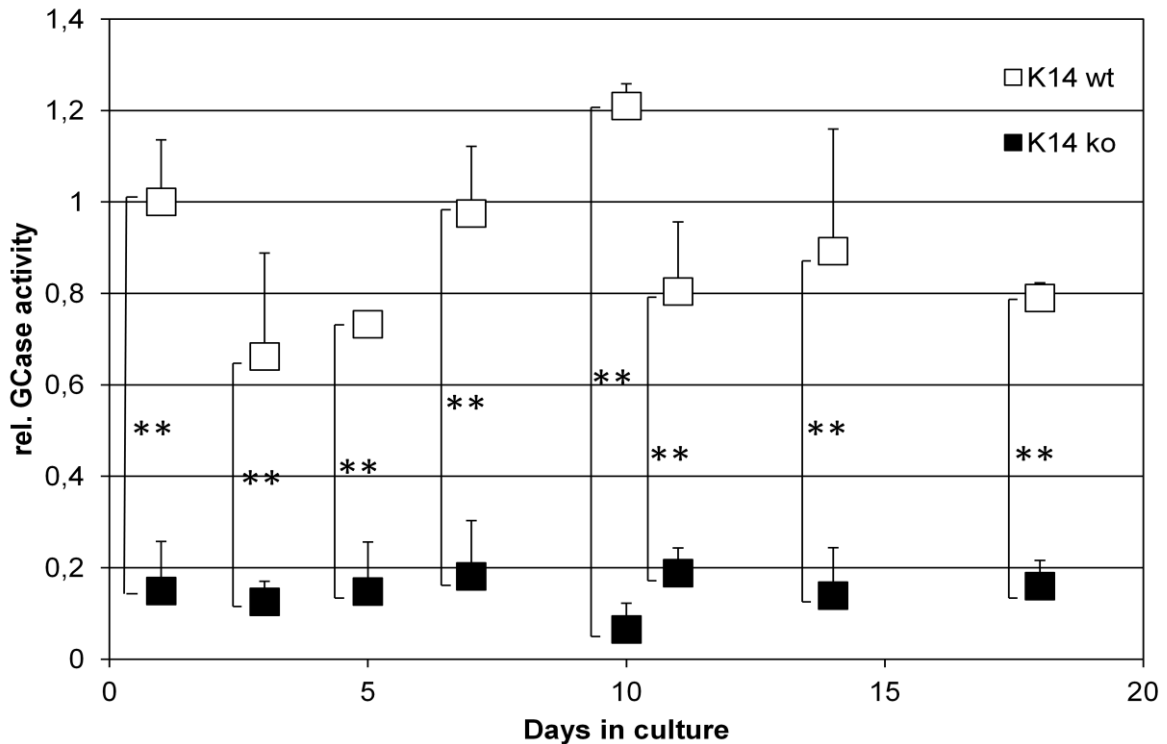
Figure 31: Relative GCase activity compared between slices from K14 wt and K14 ko mice

Slices were analysed after different culture periods. Relative GCase activity was compared between K14 wt and K14 ko slices for each time point as well as over the total time in culture. Measurements for wt DIV1 were set to 1 to allow relative GCase activity to be stated for all other samples. Data shown are means ± SD of 3–5 samples per group. All data were subjected to Student's *t* test; **$p < 0.01$.

3.3 Adeno-associated gene transfer of human β-glucocerebrosidase

The final experiments performed in the present study were aimed at investigating the transduction efficiency of the AAV2 particles previously produced and their ability to transfer the therapeutic enzyme, β-glucocerebrosidase, into cortical organotypic brain-slices derived from K14 ko mice.

3.3.1 Measurement of GCase activity in transduced slices of K14 ko mice

Cortical organotypic brai-slices derived from K14 ko mice were transduced in different ways. The same titre of AAV2 particles was added either to the culture medium or directly onto the slice itself. For clarity, a schematic drawing of an

organotypic slice in its culture well is provided in Section 2.7.7. For each experimental set-up, a control (non-transduced slice) was cultured in parallel. The slices transduced with AAV2 particles packed either with the plasmid pAAV.LacZ (mock; control) or pAAV.hGC were harvested after three different incubation time points (DIV 2, DIV 4 and DIV 7) whereas slices transduced with AAV2 particles packed with pFB.CAG were analysed after two time points (DIV 2 and DIV4). For clarity, the transduction protocol is shown schematically in Figure 32.
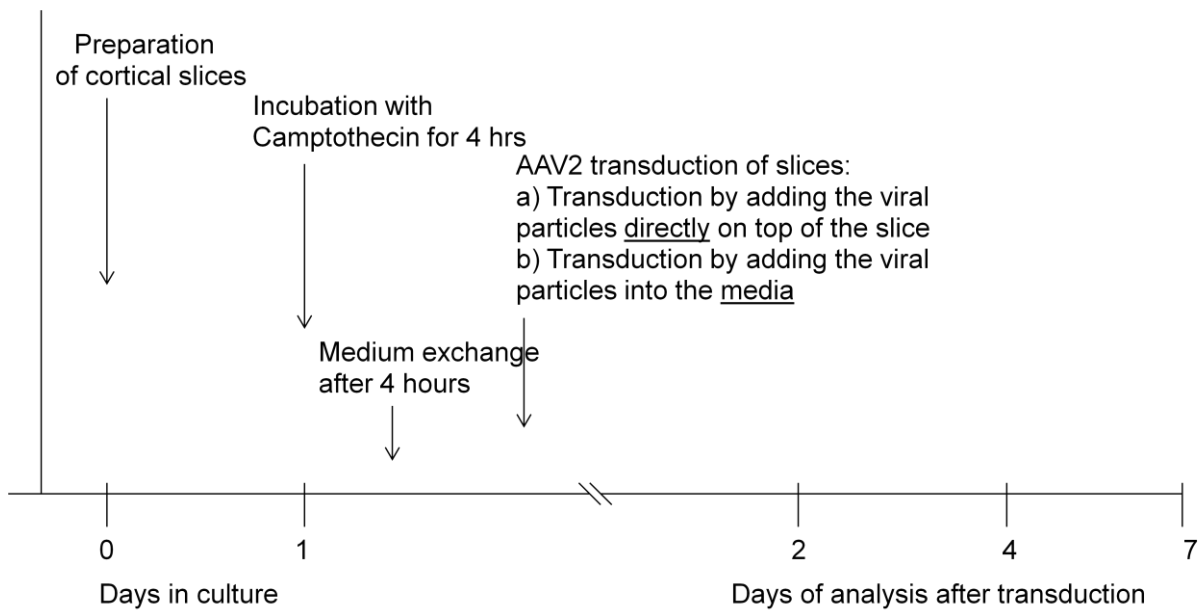

Figure 32: Protocol of transduction

As shown in Fig. 33A the transduction of slices with AAV2 particles packed with pAAV.LacZ (mock) showed no significant difference in relative GCase activity compared with the control slices.

Transducing K14 slices with pAAV.hGC-packed AAV2 particles led to a significant increase of relative GCase activity at each time point of measurement (see Fig. 33B). At DIV2 a significant increase (Student's t test: $p < 0.01$) was determined either by adding AAV2 particles to the culture medium (1.72 ± 0.15) or by direct (1.58 ± 0.39) transduction onto the slice, compared with the control slice (1 ± 0.17). A further significant (Student's t test: $p < 0.05$) increase was observed at DIV4 when the slice was transduced by adding AAV2 particles into the medium (1.55 ± 0.45) compared

with the control slice (1 ± 0.4). Increased relative GCase activity was also found for direct (1.56 ± 0.53) transduction, but this effect was not significant. Similar results were observed for DIV7. The transduction via the medium (2.27 ± 0.89) led to a significant (Student's *t* test: $p < 0.05$) increase in relative GCase activity compared with the control slice (1 ± 0.2), but the increased activity after direct transduction (1.46 ± 0.56) was not significant.

The transduction of slices from K14 ko mice with pFB.CAG-packed AAV2 particles (Fig. 33C) led to an increase in relative GCase activity, irrespective of whether the slice was transduced directly or the particles were added to the culture (compared with the control slice at each time point investigated). At DIV2 no significant increase (Student´s *t* test) was determined either by adding the particles to the medium (1.49 ± 0.02) or by direct transduction (1.46 ± 0.08) onto the slice compared with the control slice (1 ± 0.13). At DIV4, adding particles to the media (1.36 ± 0.14) or directly (1.04 ± 0.18) onto the slice led to no significant increase of GCase activity compared with the control slice (1 ± 0.22).

The transduction of K14 ko slices with AAV2 particles packed with pAAV.hGC, under the control of CMV promoter led to a significant increase in relative GCase activity. In contrast, the increased relative GCase activity found after transducing slices with AA2 particles packed with pFB.CAG was not significant.
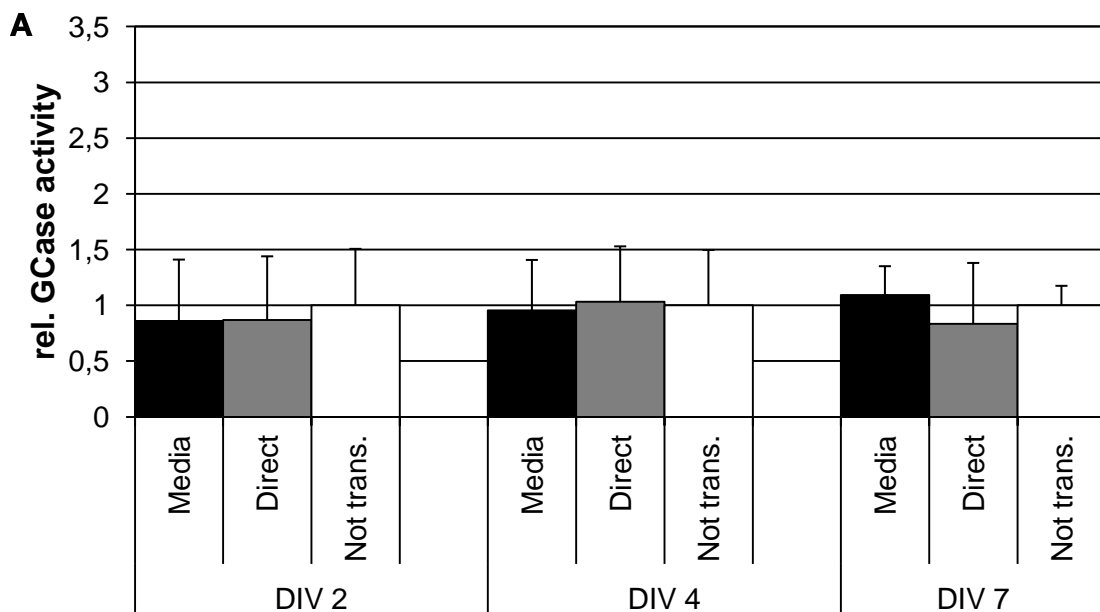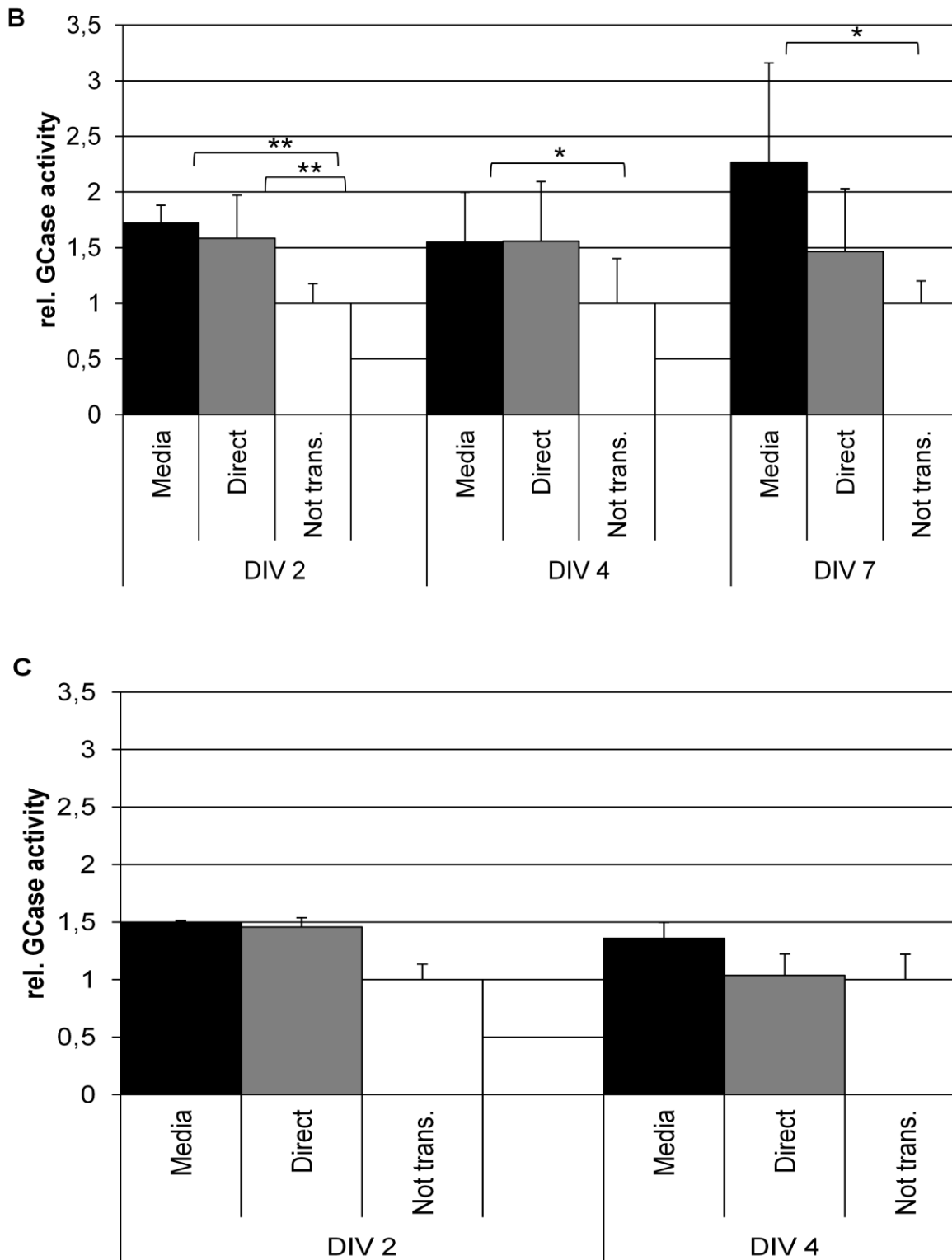
Figure 33: Relative GCase activity in transduced K14 ko brain slices
Relative GCase activity was determined by setting the control result (non- transduced slice) to 1 at each incubation time point. A: relative GCase activity after transducing the slice with the mock control. B: relative GCase activity after transducing slices with AAV2 particles packed with pAAV.hGC. C: relative GCase activity after transducing slices with AAV2 particles packed with pFB.CAG. Data shown are means ± SD of 8 slices (for A and B) and 3 slices (for C) of different mice per group. All data were subjected to Student's t test; ** $p < 0.01$, * $p < 0.05$.

3.3.2 Comparison of relative GCase activity in relation to mock-transduced K14 ko organotypic slices

In order to verify the results determined above and to be able to compare the efficiency of AAV2 particles packed either with pAAV.hGC or with pFB.CAG after transduction, results were compared with transduction results obtained on AAV2 particles packed with the mock vector. As the mock vector (pLacZ) does not encode human β-glucocerebrosidase, no increase in GCase activity was observed after transduction other than in the case of pAAV.hGC or pFB.CAG (Fig. 33). For this purpose, the GCase activity of transduced slices with the mock vector was set to 1 for each incubation time point. Only those results determined by transducing the organotypic slice cultures by adding AAV2 particles to the culture media were used for comparison.

As shown in Fig. 34, the transduction of K14 ko slices with pAAV.hGC-packed AAV2 particles resulted in a significant (Student's t test; $p < 0.01$) increase in relative GCase activity (2.14 ± 0.19) compared with slices transduced with AAV2 particles packed with the mock vector (1 ± 0.64) after 2 days in culture. The transduction of pFB.CAG-packed AAV2 particles also led to an increase in relative GCase activity (1.99 ± 0.03) compared with the slices transduced by AAV2 particles packed with the mock vector; however, this increase was not significant.

At DIV4, the transduction of K14 ko slices with pAAV.hGC-packed AAV2 particles (2.17 ± 0.62) also led to a significant (Student's t test; $p < 0.01$) increase in relative GCase activity compared with slices transduced with AAV2 particles packed with the mock vector (1 ± 0.47). The transduction with pFB.CAG-packed AAV2 particles (2.20 ± 0.22) also led to a significant (Student's t test; $p < 0.05$) increase in relative GCase activity compared with slices transduced by AAV2 particles packed with the mock vector.

The last incubation time point analysed after transducing K14 ko slices with AAV2 particles was 7 days in culture. An increase in relative GCase activity was observed after transducing K14 ko slices with pAAV.hGC packed AAV2 particles (1.71 ± 0.67) compared with slices transduced with AAV2 particles packed with the mock vector (1 ± 0.23); however, this increase was not significant (Student's t test).
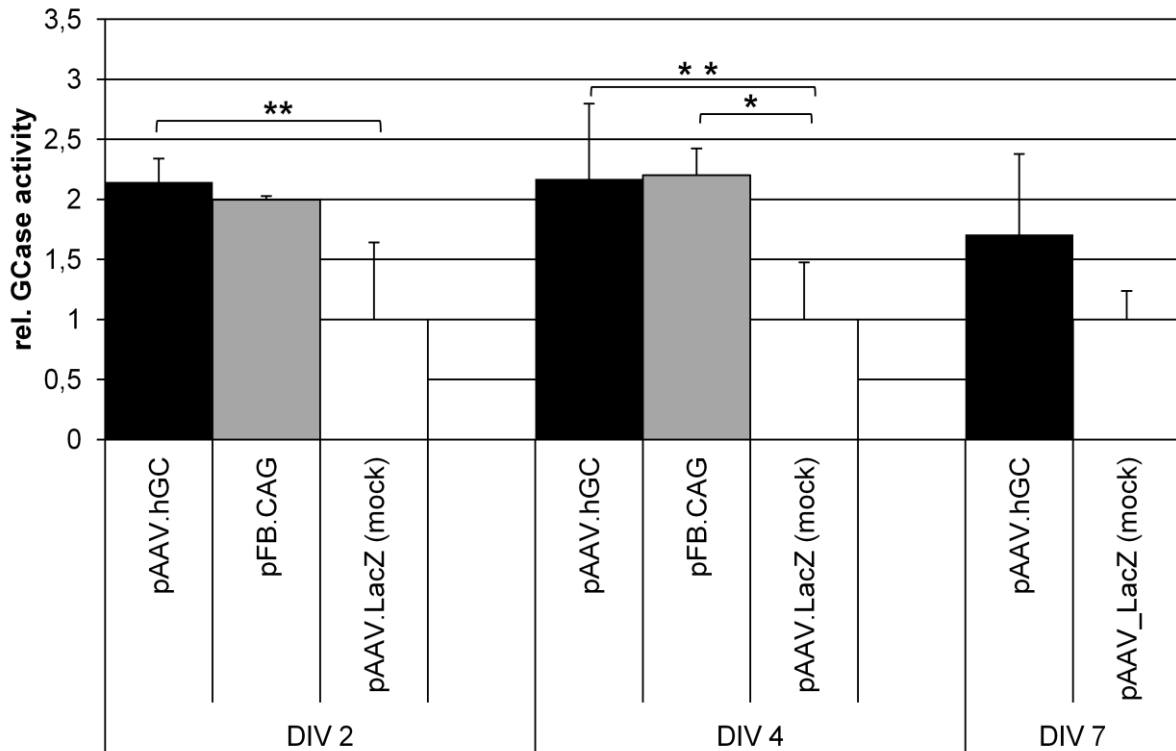
Figure 34: Comparison of relative GCase activity of transduced K14 ko slices with mock-vector-packed AAV2 particles
Relative GCase activity determined for mock-transduced K14 slices was set to 1. Results for pAAV.hGC or pFB.CAG packed AAV2 particles, transduction trough the culture media were compared with results obtained for AAV2 particles packed with mock vector. Data shown are means ± SD of 3 (DIV7) or 8 (DIV 2 and 4) slices of different mice per group. All data were subjected to Student's t test; ** $p < 0.01$, * $p < 0.05$.

These results verify the results obtained before (Section 3.3.1), i.e., that pAAV.hGC-packed AAV2 particles led to a significant increase in relative GCase activity 2 and 4 days after transduction. Even 7 days after transduction, relative GCase activity was highly increased compared with K14 ko slices transduced with mock-vector-packed AAV2 particles, even though this difference was not significant. Transductions of K14 ko slices with pFB.CAG-packed AAV2 particles led to a significant increase of relative GCase activity only at one time point, namely 4 days after transduction. Therefore, the analysis of transduction efficiency after 7 days was only done for pAAV.hGC and for the mock-vector-packed AAV2 particles.

Further western blot analysis of protein expression of the fusion protein tagged to HA also detected distinct bands only in those slices where the transfer of β-glucocerebrosidase was successful. Figure 35 shows, as an example, one western

blot of slices transduced with AAV2 particles packed with pAAV.hGC and analysed 2 and 7 days after transduction.
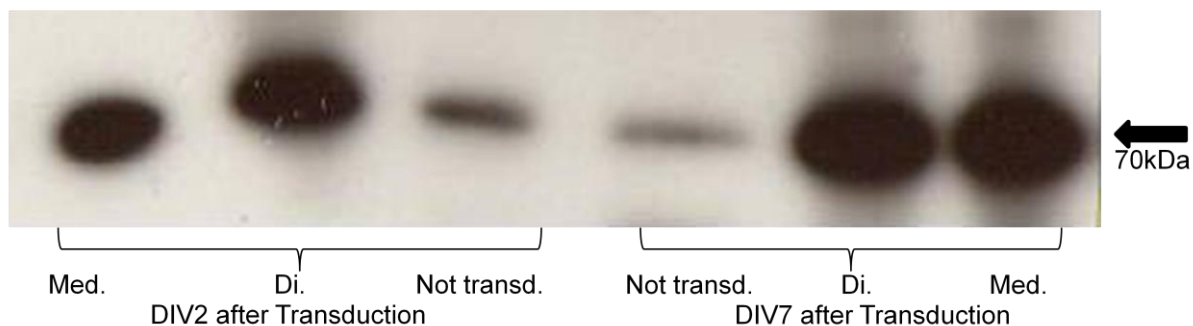

Figure 35: Protein expression of HA-tagged fusion protein in transduced slices
The western blot shows, as an example transduced slices with AAV2 particles packed with AAV_hGC analysed 2 and 7 days after transduction. The slices transduced by adding the AAV2 particles into the medium (Med.) or directly (Di.) onto the slice showed distinct bands at approximately 70 kDa, whereas no distinct band was shown for control (Not transd.) slices.

3.3.3 LDH Cytotoxicity measurement of transduced K14 ko slices

Investigation of possible cytotoxicity of transduction of K14 ko cortical organotypic brain-slices was performed with the LDH cytotoxicity kit. The lactate dehydrogenase assay is often used to quantify possible cell damage. Quantification is possible as LDH is a stable enzyme found in all cell types. Cell membrane damage results in the rapid release of LDH into the cell culture media.

Media were analysed from directly transduced K14 slices with differently packed AAV2 particles. Samples taken from slices transduced by adding AAV2 particles to media would have led to adulterated results (data not shown). As an example, Figure 36 shows the cytotoxicity determined for slices cultured for two days after transduction. LDH release from damaged organotypic slices was measured by incubating the slices with Triton X-100; the result was 100% ± 12.4. This result was used to compare the measurement determined from slices transduced directly with pAAV.LacZ (10.89% ± 2.74), with pAAV.hGC (14.15% ± 3.5) or with pFB.CAG (14.15 ± 0.2). These do not increase the release of LDH into the culture media, compared with non-transduced control slices, two days after incubation. The same

results were obtained for transduced slices after 4 and 7 days in culture (data not shown).
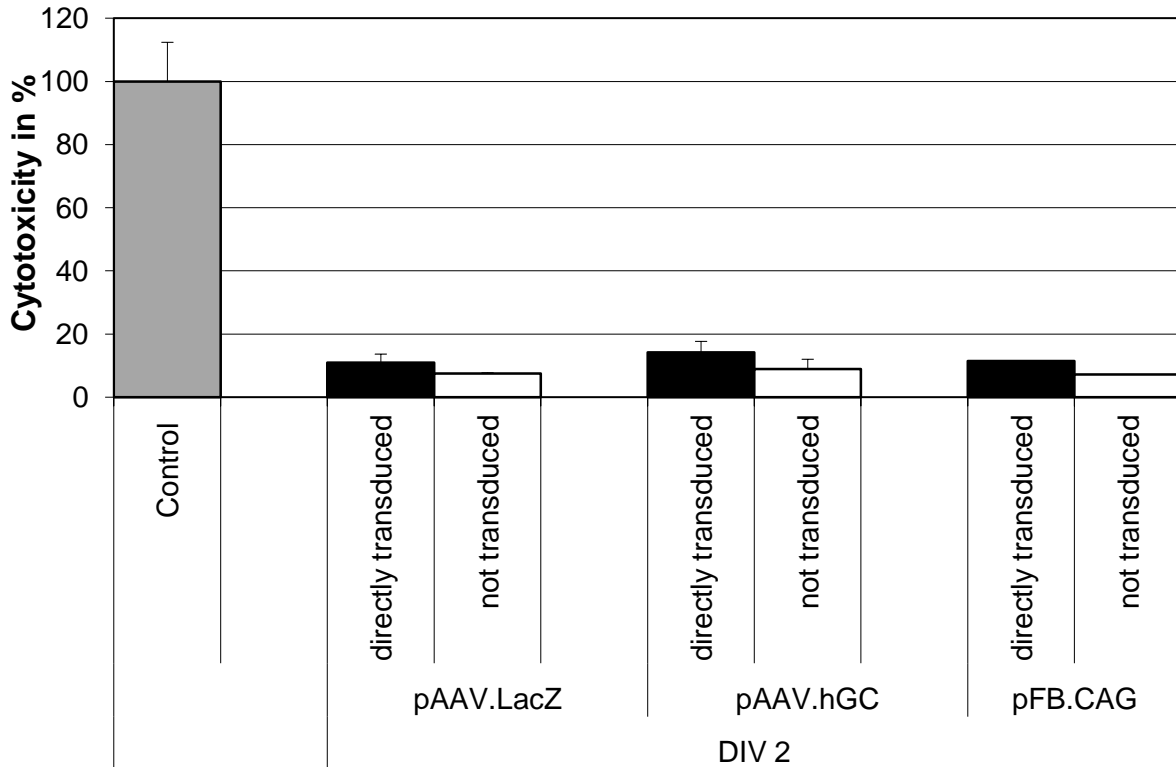
Figure 36: LDH Cytotoxicity of directly transduced K14 slices compared with damaged brain slices
Cytotoxicity measurement by LDH release into culture media. The grey bar indicates cell death due to Triton-X incubation. Black and white bars are examples of the cytotoxicity measured from transduced slices compared with non-transduced slices 2 days after transduction. The three differently packed AAV2 particles contained pAAV.LacZ, pAAV.hGC or pFB.CAG. Data shown are means ± SD of 3 samples per group.

4. Discussion

4.1 Characterisation of the K14 lnl mouse model

The development of a murine model for Gaucher's disease type II has become of greater and greater interest in recent years. The pathological mechanisms underlying the disease are only partially understood. The reduced activity of β-glucocerebrosidase in Gaucher's disease, which plays a key role in the disease, leads to the accumulation of glucosylceramide in the lysosomal compartment of cells throughout the body. However, the abnormal accumulation of the lipids does not seem to be the primary cause of the development of disease-specific symptoms such as organ enlargement or neuron death (Jmoudiak and Futerman, 2005; Brady, 2006). Various hypotheses have been made, describing a variety of pathological mechanisms that might explain the devastating development of Gaucher's disease, and especially of type II. The generation of a mouse model for Gaucher's disease type II was expected to afford deeper insight into the various pathological mechanisms that play a role in the disease. This was especially the case as it is not possible to correlate any genotype with a specific phenotype in Gaucher's disease (Brady, 2006). Furthermore, no efficient therapy has been developed for either type II or type III. Therefore, a mouse model for Gaucher's disease type II could also provide an *in vivo* model capable of use for attempts at gene therapy and their assessment. Another advantage of an *in* vivo model would be the possibility of overcoming the presence of the blood–brain barrier, which was the major obstacle leading to the failure of trials that attempted to transport a therapeutic enzyme, such as β-glucocerebrosidase, to cells of the CNS.

Only few attempts have been made to generate such an animal model. These have used different strategies. In the first strategy, conduritol-β-epoxide – the specific inhibitor of GCase – was used to induce chemically the reduction of GCase activity (Kanfer *et al.*, 1975). The mice developed a reduction in GCase activity of > 90% and they accumulated glucosylceramide after being injected intraperitoneally every day. Further models have been generated by chemical induction; this has not been widely used, even though it is a very quick and inexpensive strategy. Another strategy was to knock out the *Gba* gene completely (Tybulewicz *et al.*, 1992) by inserting a *Neo*

cassette into exons 9 and 10 of the *Gba* gene, leading to a mouse that carried a null mutation. These mice also showed a reduced GCase activity of < 4%, they developed a robust phenotype, and glucosylceramide accumulation was observed as well. However, these mice died as neonates because of elevated water loss through the epidermis. This was due to the fact that glycosylceramides are normally important for lipid closure in the epidermis. Further attempts to generate mouse models for Gaucher's disease type II with a longer lifespan were made by using point mutations. Using point mutations in mice that corresponded to those found in human patients was thought to promise success, as the genes in mice and humans have an identity of 82% (Farfel-Becker *et al.*, 2011). The first such attempt was made in 1998 (Liu *et al.*, 1998) by producing mice carrying the so-called "RecNcil" mutation (L444P/A456P). This mutation normally causes Gaucher's disease type II in humans. Mice displayed a reduced GCase activity (less than 4% to 9% of that in wild-type mice), but the mutant mice died soon after birth because of abnormal skin function. In mice bearing the point mutations D409V, D409H or V394L, no further phenotypic abnormalities or glucosylceramide storage was observed, even though the GCase activity was reduced to below 4%–10%. A major breakthrough in the development of Gaucher's disease type II mice was the generation of a conditional knockout mouse model for type I in 2006. To generate this mouse model the Mx1-Cre-loxP system was used, which also led to a strategy for generating a mouse model for type II (Enquist *et al.*, 2006). Finally, in 2007, the same group generated the first mouse model of Gaucher's disease type II (Enquist *et al*, 2007).

In the present study the Gaucher's disease type II mouse model K14 lnl of Enquist *et al.* (2007), was used. The loxP-Neo-loxP cassette was inserted into the *Gba* intron 8, leading to knockout mice. These *gba*$^{lnl/lnl}$ knockout mice were further crossbred with K (keratin) 14-Cre transgenic mice to generate K14 lnl/lnl mice. Crossbreeding was performed in order to restore epidermal function, to overcome the early death due to dehydration. This was possible because cre recombinase expression, driven by the K14 promoter, allows the expression of *gba*$^{lnl/lnl}$ in the skin. At the beginning of the present study, K14 ko mice were characterised and compared with K14 wt mice before they were used for the establishment of cortical organotypic brain-slice cultures.

In the present study K14 lnl pups were divided into three groups representing the different stages of disease on the basis of the clinical symptoms observed in K14 ko mice. In the first group, 7-day-old mice presenting the symptom-free stage of disease were investigated. The second group included 11-day-old mice with mild symptoms such as abnormal gait and hyperextension of the neck. In the last group, at the end-stage of disease, 13-day-old mice that developed spontaneous seizures were investigated. The symptoms such as hyperextension of the neck and seizures observed in the K14 mouse model are in general the same as those occurring in Gaucher's disease type II patients (Pelled *et al.*, 2005; Jmoudiak and Futerman, 2005; Pastores, 2010). The symptom-free stage observed in the present study differed from that described by Enquist and colleagues (Enquist *et al.*, 2007), who reported a symptom-free phase of approximately 10 days.

The architecture and cellular compartments of brain from K14 ko mice were compared histologically with those of K14 wt mice brains. This gave an insight into disease-related changes in the brains of K14 ko mice. Nissl staining was used especially, to investigate the presence of neurons in different parts of the brain. The Nissl staining revealed no difference in the gross architecture, at least as far as could be distinguished by comparing brains obtained from K14 ko mice with those from K14 wt mice of the same age which were stained by Nissl. Further, microscopic study revealed a reduced cellular density and a distinct neuronal loss in some parts of the brain, especially the cortex and the cerebellum, in K14 ko mice. Focusing on the cortex, it was obvious that the number of large pyramidal neurons was decreased in brains of K14 ko compared with brains of K14 wt mice. These results are in line with the observations made by Enquist *et al.* in 2007. The distinct neuronal loss has also been described in patients suffering from Gaucher's disease type II (Pelled *et al.*, 2005). Besides the neuronal death, astrogliosis has also been reported to occur in patients with Gaucher's disease type II; the progress of astrogliosis is associated with disease development in patients (Kaye *et al.*, 1986; Tybulewicz *et al.*, 1992). The results of the present study showed a developing astrogliosis at both developmental stages investigated in K14 ko mice, as compared with K14 wt mice. Furthermore, as described in patients as well, the astrogliosis was observed to be more extensive in older K14 ko mice than in younger ones, an observation that accords with the development of disease severity. These findings were also paralleled to the results of

Enquist and colleagues made in 2007. The expression, as well as the activity, of β-glucocerebrosidase was of great interest for characterising and comparing the brains of K14 ko mice with those of K14 wt mice In healthy individuals, β-glucocerebrosidase is found in every cell throughout the body and brain. Therefore, in the present study only two exemplary, distinct parts of the brain (hippocampus and cortex) were used to verify the expected reduced presence of β-glucocerebrosidase staining in K14 ko mice compared with K14 wt mice.

In the present study, the investigations of β-glucocerebrosidase activity were based on the established biochemical activity assay using the substrate 4-MUD. The specific activity of β-glucocerebrosidase towards 4-MUD was verified by using the inhibitor CBE. Significant reduction in GCase activity was found in those samples in which CBE was additionally used during incubation. The GCase activity measured was of almost the same level as that found in control samples in which the enzyme had been heat-inactivated. Thus, 4-MUD was confirmed to be a specific substrate for β-glucocerebrosidase. These results are in accordance with data published by Fink *et al.* in 1989.

The GCase activity of K14 mice was measured separately in the cerebrum and cerebellum of K14 ko mice and compared with the corresponding activity in K14 wt mice in each of the three groups, as described above. For a better comparison of mice within a given developmental group, the relative GCase activity was set to 1 for the K14 wt. The GCase activity was significantly reduced in both the cerebellum and the cerebrum of the K14 ko mice compared with the K14 wt mice. These results had been expected, as a correlation between reduced GCase activity is thought to be in accord with the increase of the severity of both pathological and clinical symptoms that takes place as the disease develops. The reduction in GCase activity observed further confirms the findings obtained from the histological staining, discussed above. These results are again in line with the findings by Enquist and colleagues (Enquist *et al.*, 2007).

Ho was the first to describe the presence of two different forms of β-glucocerebrosidase, a "neutral" and an "acidic" form (Ho, 1973), whereby the "acidic" form is the one playing the key role in Gaucher's disease. Further studies by Daniels and colleagues (Daniels *et al.*, 1982) discovered that the "neutral" form of

GCase seems to be resistant to CBE treatment in the biochemical assay. Therefore this membrane-bound "neutral" form of GCase might explain the residual activity of GCase that was found in homogenates from the K14 ko mice in all three groups. Residual activity was also found by Enquist *et al.* (2007). The GCase deficiency in K14 ko mice is in general caused by the aberrant splicing of the gba mRNA. Another possible reason, which would explain the residual activity of GCase found in K14 ko mice, could be the presence of correctly spliced *GBA* mRNA still present at low levels in K14 ko mice (Enquist *et al.*, 2007).

In summary, the characterisation findings in this study demonstrate that the K14 ko mice develop severe neurodegenerative pathology similar to that found in patients suffering from Gaucher's disease type II.

4.2 Cloning vectors expressing the transgene β-glucocerebrosidase, packaging into AAV2 particles and an e*x vivo* model of Gaucher's disease type II

Most approaches to optimise viral vectors such as AAV´s have traditionally been implemented at the nucleic acid level, involving promoter and other gene regulatory elements (Xu *et al.*, 2001). In the present study, two vectors expressing the transgene β-glucocerebrosidase fused to the ApoB binding domain under the control of either the CMV or the CAG promoter were examined and compared.

First, the initial vector pFB.CMV_sGBA had to be modified in order to obtain the sequence coding for β-glucocerebrosidase fused to the ApoB binding domain. Different approaches had to be tried as the easiest way, directional cloning by restriction digestion, was not possible. At the beginning, after designing specific primers containing additional restrictions sites at their respective 5´ end, PCR amplification of the required sequence was performed. Several attempts were made to clone the PCR fragments by using slightly differing primers, but all these attempts were unsuccessful. It is well known that PCR amplification can be very awkward, as successful amplification depends on the specificity of primers and the type of vector to be cloned in; even using the common Taq polymerase is a problem, and quite often intermediate cloning steps have to be performed as well. Therefore it was finally

decided to perform a subcloning step into the pQE TriSystem vector before cloning into pAAV.MCS. This strategy made it possible to perform restriction digestion of the gene of interest. Those clones that were found by restriction digestion to be positive for the vector encoding the sequence for β-glucocerebrosidase were tested further by sequence analysis. For this purpose sequencing of isolated plasmids from putatively positive clones was performed in order to align the sequence of pAAV.hGC with the sequence of human GCase itself, as well as with the AAV.MCS backbone, for verification. The alignment revealed 100% sequence identity between pAAV.hGC and the human GCase and 96% identity between pAAV.hGC and the pAAV.MCS backbone. Slight differences in identity between two sequences may be due to the length of the sequence as quite often unspecific binding of primers occurs at the end of sequencing. Therefore, the results obtained in the present study confirm the expected positive outcome of cloning and the presence of the gene of interest in pAAV.MCS.

The activity and expression of the enzyme β-glucocerebrosidase had to be verified. For this purpose, two different types of cells were used: fibroblasts derived from a Morbus Gaucher patient and from a healthy individual, and primary neurons derived from K14 ko embryos. It was not known whether the fibroblasts were derived from a patient suffering from type II or type III Gaucher's disease; however, this did not affect the measurement of possible GCase activity after transfection of the cells with either of the vectors. As expected, both vectors led to a significant increase in relative GCase activity (by a factor of almost 3) compared with the non-transfected fibroblasts. Patients with Morbus Gaucher still displayed a residual GCase activity, as had also been described by Daniels et al. (1982). Moreover, the level of GCase activity was even slightly elevated in fibroblasts transfected with either pAAV.hGC or pFB.CAG as compared with the GCase activity measured in fibroblasts from a healthy individual. The culture medium of transfected fibroblasts was also analysed, as the sequence used in the vectors supposedly encodes a secretable form of the enzyme. As expected, the GCase activity of the culture medium from transfected fibroblasts was significantly higher than that in culture media from non-transfected fibroblasts of the same patient. The GCase activity was also significantly higher in the medium of transfected fibroblasts compared with that of fibroblasts from the healthy individual. This was also expected, as normally GCase is not secreted by cells as it

was observed in the present study, in cells transfected by the secretable form. The GCase activity was further verified by transfecting primary neurons derived from K14 ko embryos with either one of the vectors. So far, quite a few methods have been used to deliver genes into cultured neurons: however, each method has one or more of the following drawbacks: very low efficiency, short-term gene expression, toxicity, inability to express common reporter genes, and the requirement to transfect immature neurons (Royo *et al.*, 2008). In the present study, nucleofection was used, which leads to stable gene expression in cultured neurons from two days to two weeks after nucleofection, representing quite a high efficiency (up to 60%) and no toxicity (Lonza Inc., instruction manual). One major drawback of this method is the fact that primary neurons have to be nucleofected before being cultured. As expected, the nucleofection of primary neurons derived from K14 ko mice with pAAV.hGC led to a significantly increased GCase activity compared with the GCase activity measured in non nucleofected primary neurons. The nucleofection of the neurons with pFB.CAG also led to an increase in GCase activity compared with that of non-nucleofected neurons, but this increase was not significant. The lack of significance in the case of pFB.CAG might be explained by the fact that fewer experiments were performed, owing to breeding problems as discussed above *(see 3.1).* Serotypes 1, 2, 7, 8 and 9 (single dose of 2.0–2.5 x 10^{11} genome copies of each viral vector) have also been reported to mediate highly efficient, non-toxic, stable, long-term gene expression in cultured cortical and hippocampal neurons (Royo *et al.*, 2008).

After both vectors had been successfully validated, they were packed separately into AAV2 particles. The *lacZ*-expressing vector (pAAV.LacZ) was also packed into AAV2 particles, to assess the transduction efficiency and to allow indirect measurement of the titre of AAV2 in the viral stocks produced in this study. In order to generate AAV2 viral particles, the helper-virus-free method was used. Earlier, helper viruses such as wild-type adenoviruses or herpes simplex viruses were used to produce AAV particles. However, this always required further purification steps to remove the helper viruses before the stocks could be used for further experiments. Matsushita and colleagues established that AAV vector preparations with adenovirus as helper virus were essentially indistinguishable from those obtained by the helper-virus-free method in respect of particle density, particle-to-infectivity ratio, capsid ratio and

efficiency of muscle transduction *in vivo* (Matsushita *et al.*, 1998). Furthermore, it was found that AAV is able to integrate into the cellular genome during infection in the absence of a helper virus such as herpes simplex or a wild-type adenovirus. This feature allows long-term gene expression with AAV vectors *in vivo* (Vincent *et al.*, 1996) which was important for the proof-of-principle experiments performed in cortical organotypic brain-slice cultures in the present study.

After AAV2 viral particle production, indirect titre measurement was performed by using the vector coding the *LacZ* gene in AAV-HT1080 cells. Transduction efficiency measurement and titre determination were performed by using the β-X-Gal staining system, which leads to blue staining of positively transduced cells. The mean transduction efficiency of AAV2 viral particles was found to be approximately 50% (out of four viral supernatants), produced at different days, at a mean of 10×10^6 IP/ml. The amount of infectious particles (8.9×10^6 IP/ml) produced in our laboratory sufficed for the final e*x vivo* proof-of-principle experiments in the present study.

These proof-of-principle experiments, discussed in section 4.3, were performed in cortical organotypic brain-slice cultures derived from K14 ko mice. These slices were used as an e*x vivo* model for Gaucher's disease type II. Cortical organotypic brain-slice cultures have already been used as models for stroke, epilepsy, neuronal injury and neuroprotection (Staal *et al.*, 2011). In the present study, slices were prepared from 8/9day-old mice which suited best for establishing slice cultures. These investigations are in accordance with data published by Staal and colleagues (Staal *et al.*, 2011). These workers found reduced cell death over 14 days in cultures of whole-brain slices from neonates (P0–P8), whereas slices taken from older mice (P25) showed increased cell death over the same period. A gradual and significant increase in metabolic activity over 14 days in culture was found in slices obtained from P6 mice. Therefore, neonates are ideally suited for culturing, as they appear to survive explantation more readily than slices taken from older mice (Staal *et al.*, 2011). For slices from K14 ko mice, it had to be confirmed whether they could be used as a Gaucher's disease type II model. For this purpose, the cell composition and the GCase activity of these slices were compared with those of slices derived from K14 wt mice. The cell composition in slices was compared by protein expression using three different cell markers representing astrocytes, neurons and microglia. To correct any loading discrepancies during the experiments, GAPDH was used, as an

internal standard for adjusting protein concentration. This excludes any possible mistakes leading to unrepresentative results due to the use of unrepresentative loading volumes. The comparison of the cell compositions in cortical organotypic brain-slices led to the conclusion that no differences were detected between slices from K14 ko and from K14 wt mice. These results differ from those obtained in the histological characterisation of brains derived from K14 lnl mouse pups. The histological analysis showed increased neuronal loss as well as an increased number of astrocytes in the brain from K14 ko mice compared with K14 wt mice. These differences could be explained, as quite a number of cells are already lost during the preparation of slices. This loss could explain the lack of differences in cell composition between slices from K14 ko mice compared with slices from K14 wt mice, i.e., a reduced number of cells from the beginning. No obvious differences were observed during the culturing of the slices, which suggests that the disease itself does not alter the conditions of slices in culture, at least during the observed time span. Furthermore, to verify the viability of slices from K14 ko and K14 wt mice, slices were stained with Calcein. Calcein staining showed viable slices after different periods in culture. While the validation of viable slices was one aspect of this work, the most important feature in the present study is the reduced GCase activity in slices from K14 ko mice, which defines them as a usable model to represent type II of Gaucher's disease. For this purpose, GCase activity from cortical organotypic brain-slices derived from K14 ko mice was compared with the GCase activity of K14 wt mice over time. As expected, GCase activity measured from slices of K14 ko mice was significantly reduced in comparison with slices from K14 wt mice over the whole time in culture. Therefore, slices from K14 ko mice could be used as an *ex vivo* model representing Gaucher's disease type II. The residual activity of β-glucocerebrosidase measured in slices from K14 ko mice was expected and it is in line with the results obtained in characterising the K14 lnl mouse strain (section 4.1).

After characterising the K14 mouse model, establishing and improving all methods, cloning vectors with active GCase, producing AAV2 viral particles and establishing an *ex vivo* model representing Gaucher's disease type II, the following proof-of-principle experiments were performed. These were designed to investigate the possible gene transfer of β-glucocerebrosidase into the slices by AAV2 transduction and to validate the possible use of these viral particles for gene therapeutic approaches.

4.3 Gene transfer of β-glucocerebrosidase

During the last few years, much progress has been made in treating lysosomal storage disorders. Several different therapeutic approaches have been evaluated for potential treatments of Gaucher's disease, such as bone-marrow transplantation, substrate inhibition therapy and enzyme replacement therapy. So far, most progress has been made for type I Gaucher's disease and only little for types II and III, which involve the CNS. The main aim of the present study was to find a useful therapeutic approach using AAV2 viral particles to transduce cortical organotypic brain-slices representing type II Gaucher's disease.

Clinical research has highlighted several major obstacles to gene therapy. These include gene silencing, insertional mutagenesis, phenotoxicity, immunotoxicity, risks of horizontal transmission (from one individual to another) and vertical transmission (transfer from one generation to the next, either genetically or congenitally) of the donated DNA. All of these need to be overcome. AAVs are of great interest as gene-therapeutic vehicles, as the drawbacks listed above have not been associated with AAVs, at least so far (Mingozzi and High, 2007). No human disease has been associated with AAV infections (Vincent et al., 1996). In general, the innate immune response to single-stranded AAV vectors is typically low (Zaiss et al., 2002). Especially AAV2 shows low immunogenicity, which is believed to be due to the inability of AAV2 to infect antigen-presenting cells (Gao et al., 2002). First attempts at gene therapies for patients with lysosomal storage disorders – such as Gaucher's, Hunter's and Hurler's disease – were performed with transplanted, retrovirally transduced, bone-marrow stem cells or mobilised peripheral blood monocytes. However, the efficiency of retroviral transduction of these cells was too low; the engraftment of such modified stem cells was transient and occurred at a low, ineffective level (Cheng and Smith, 2003). The trial in Leber´s congenital amaurosis (LCA) represents the first example of a successful AAV gene therapy in humans without immune consequences. Patients suffering from LCA received a subretinal injection of rAAV, tolerated the transgene well and showed improved visual capability, as measured by both psychophysical and functional tests (Rogers et al., 2011). Moreover, several studies have shown that direct infusions of AAV2 vectors into the brain parenchyma in humans were well tolerated (Bowers et al., 2011). A large number of studies have been performed with recombinant adenoviral vectors as

those result in efficient transduction of the liver cells and high-level expression and secretion of lysosomal enzymes (Cheng and Smith, 2003). One challenge facing gene transfer to the CNS has been the development of viral vectors with appropriate cell tropism, efficient transduction and stable levels of expression (Xu *et al.*, 2001). AAV2-mediated gene transfer confers extremely stable transgene expression upon tissues such as muscle, retina and the CNS (Gao *et al.*, 2002).

The tissue tropism, low immunogenicity and stable expression of the transgene described for AAV2 led to the decision to use this AAV serotype for the proof-of-principle experiments performed in the present study before going into the K14 lnl mouse model itself. The general idea of the BMBF-funded project "Gene therapy for Gaucher's disease type II" was to infect cells of a depot organ of the K14 lnl mouse with AAV2 viral particles. At the best, the fusion protein is able to bind through its ApoB binding domain to the LDLR found on the endothelial cells of the BBB and is transcytosed and transported across the BBB whereafter it is taken up by cells of the CNS such as neurons, leading to a correction of type II Gaucher's disease. Spencer and Verma fused the low-density lipoprotein receptor-binding domain of the apolipoprotein B to the secretable form of the lysosomal enzyme glucocerebrosidase, which was expressed by a lentiviral vector system. Intraperitoneal injection of the lentiviral vector into adult mice led to a sufficient delivery of the protein to the CNS across the BBB (Spencer and Verma, 2007).

Therefore in the present study, proof-of principle experiments were performed in order to investigate the therapeutic efficiency of AAV2-produced particles by transducing the cortical organotypic brain-slices representing type II Gaucher's disease before performing any animal experiments. The slices were used to investigate the transduction potential of the differently packed AAV2 particles towards different cell types. As a secretable form was cloned into the vectors used for AAV2 viral production, cells in the slice that are not transduced by the virus itself should be able to take up the GCase from their surroundings, this in turn leading to an increase of total GCase activity. This is expected to occur because the gene coding for the human GCase was fused to the ApoB binding domain. AAV2 particles were packed with one of three different vectors. Two of the vectors code the transgene β-glucocerebrosidase, which was verified to be active in advance (section 4.2), either under the control of the CMV (pAAV.hGC) or the CAG (pFB.CAG) promoter and a

third vector used as mock vector expressing LacZ. Before slices were transduced with any viral particles, they were incubated with camptothecin to increase the transduction efficiency. The transduction efficiencies of AAV vectors are increased by prior use of topoisomerase inhibitors such as camptothecin. The transduction efficiencies could be increased over 300-fold in stationary cultures at concentrations of camptothecin that affect neither the cell's availability nor its proliferative potential (Russel *et al.*, 1995). Topoisomerase inhibitors can also inhibit and reduce DNA repair functions which are required as host DNA polymerases; therefore, they accelerate the conversion of single-stranded vector genomes into double-stranded molecules (Russel *et al.*, 1995).

In order to obtain confirmation that whether the proof-of-principle experiments in the present study were successful; GCase activity of transduced slices was measured and compared with that of slices transduced with the mock vector. Two further different techniques of transduction were compared, (i) directly adding the viral particles on top of the slice and (ii) adding them to the culture medium. The effect of each vector towards GCase activity in brain-slice cultures was investigated separately. As expected, no differences in GCase activity was seen in slices transduced by the AAV2 particles packed with the mock vector compared with non-transduced slices, at any time point. In slices transduced with AVV2 particles packed with pAAV.hGC, GCase activity was significantly increased compared with that of non-transduced slices from the same animal on days 2, 4 and 7 in culture. The time window for the therapeutic approach in the K14 mouse model itself is very short, as mice die around day 14 (Enquist *et al.*, 2007). Therefore, a short time window of analysis after transduction was chosen for the slices as well. The route of transduction of cortical organotypic brain-slice cultures also seems to be relevant. The results showed the significant effect of measured GCase activity when AAV2 particles were given into the culture media directly. When slices were transduced by directly adding the AAV particles on top of the slice, a significant increase in GCase activity was only observed when the slice was analysed after 2 days in culture. This fact could be explained by the preparation procedure: After some time, scar tissue develops on top of the slice because of the cutting procedures. It is possible that this scar tissue is already too dense to be penetrated by the AAV particles after 4 days in culture. In contrast, the bottom of the slice lies flat on a penetrated membrane on top

of the culture media, through which all nutrients as well as viral particles can be taken up. Further slices were transduced with AAV2 particles packed with pFB.CAG; this led to a level of GCase activity that was increased, though not significantly so, compared with that of the non-transduced slices. AAV2 particles packed with pFB.CAG showed less efficiency in increasing GCase activity than did AAV2 particles packed with pAAV.hGC. Because of this, and also owing to the lack of animals, those experiments were only performed at two time points.

In order to obtain further confirmation that there had been no cross-reactivity due to the viral particles themselves (leading to false positive results), both vectors expressing the transgene were compared with results obtained with the mock vector. Therefore, only results obtained from transducing the slices by adding the viral particles to the media were compared. Again, as expected, the GCase activity was significantly increased (and even more than doubled) in slices transduced with AAV2 particles packed with pAAV.hGC compared with slices transduced with AAV2 particles packed with the mock vector; this was seen on days 2 and 4 after transduction. On day 7 an increase in GCase activity was still observed but this was no longer significant. In the case of the AAV2 particles packed with pFB.CAG, GCase activity was also increased on days 2 and 4 after transduction compared with slices transduced with the mock vector; here, only the result for day 4 was significant.

The CMV expression cassette is commonly used (Roy *et al.*, 2008) for gene-therapeutic approaches and also led to better results in the present study than did the CAG expression cassette. McEachern and colleagues investigated sustained hepatic secretion of human GCase after intravenous injection of AAV8 (3×10^{10} IP/ml) bearing human GCase driven by hepatocyte-restricted enhancer/promoter DC172 into pre-symptomatic Gaucher type I mice. Secretion was at such a level that it prevented glucosylceramide accumulation and the appearance of Gaucher cells in the liver, spleen and lungs. Furthermore, they observed normalisation of glucosylceramide level after AAV administration in mice at older stages (McEachern *et al.*, 2006). Duque and colleagues (Duque *et al.*, 2009) described the first successful transduction of motor neurons in adult animals after intravenous delivery of AAV9 vectors (1×10^{12} viral particles per mouse). Transduction was achieved without pharmacological disruption of the BBB, and transgene expression persisted for 5 months. Systemic delivery of recombinant AAV2 encoding α-galactosidase A

into Fabry mice, or encoding β-glucuronidase in neonatal MPS VII mice, resulted in the reconstitution of the respective enzymes in several tissues to 10–80% of normal levels. In Fabry mice, injection of an AAV vector encoding α-galactosidase A under the control of a chimeric human liver-restricted promoter resulted in undiminished expression for up to one year, in contrast to an expression cassette under the control of the CMV promoter (Ziegler *et al.*, 2002). Intracranial injections of recombinant AAV2 vectors encoding β-glucuronidase into MPS VII mice resulted not only in the correction of the characteristic cellular pathologies but also in improvements in cognitive function (Frisella *et al.*, 2001). It has been shown that AAV-mediated transgene expression in the primate brain continues for at least eight years with no evidence of neuroinflammation or reactive gliosis (Bowers *et al.*, 2011). Injection of recombinant AAV6 expressing enhanced green fluorescent protein into the gastrocnemius muscle of African green monkey led to a successful expression of GFP in cells of the spinal cord up to 4 weeks after intramuscular injection. In some cross-sections more than half of motor neurons were reached (Towne *et al.*, 2010). AAV9 produced global expression in the brain and spinal cord after peripheral, systemic administration in neonatal mice (Dayton *et al.*, 2012).

A visual verification of positively transduced cortical organotypic brain-slices with AAV2 particles was not possible. It would have been interesting to see which cell types are actually transduced by the viral particles. However, direct staining was not possible because the slices prepared for culturing and transduction were too thick for any colouring dye to reach the deeper layers of the slice. The attempt was made to re-slice the transduced organotypic slices at different time points in culture. However, during this process the slices invariably broke into small pieces; this may have been due to lack of myelination in slices of K14 ko mice. So far, our group has investigated the event of flattening of the slice after approximately 4 weeks in culture (N. Maschalek, personal communication). Staining after this period of time might also be possible, but would not contribute to the transduction time window of interest. Another possibility, for future studies, could be the use of CLARITY to visualise positively transduced cells. The method called CLARITY was recently published by Chung *et al.* (2013). This method makes it possible to transform intact tissue into a nanoporous hydrogel-hybridised form that is fully assembled but optically transparent and permeable toward macromolecules.

Finally, in order to exclude any possible toxicity caused by the viral particles themselves, which would exclude them from use in further studies in animals, lactate dehydrogenase in the medium was measured. LDH is often used to determine the amount of dead cells due to any cell membrane damage. LDH measurement is one of the first signs of non-intact cells, as LDH is rapidly released into the culture medium. Media from transduced slices were analysed and compared with media from non-transduced slices. As expected, the results showed no increased cytotoxicity in the media surrounding slices transduced with viral particles packed with the various vectors.

Our results are in parallel to the investigations conducted by Cabrera-Salazar and colleagues (Cabrera Salazar *et al.*, 2010). Cabrera-Salazar *et al.* compared the effect of intracerebroventricular administration either of a recombinant human glucocerebrosidase or of AAV1 encoding human glucocerebrosidase in K14 lnl mice. In both cases, the enzyme distribution was observed throughout the brain and resulted in a dose-dependent decrease of glucosylceramide and glucosylsphingosine. The treatment resulted in a further extension of survival of K14 mice. A single intracerebroventricular (ICV) injection of recombinant human glucocerebrosidase led to a survival of up to 19 days whereas a single ICV dose of the AAV1 encoding human GCase led to a median lifespan of 28.5 days (Cabrera Salazar *et al.*, 2010). Nevertheless repeated administration of an exogenous protein bears the risk of inducing an immune response that may interfere with therapeutic enzymes or even neutralise their activity. The successful results of the present study; the increase of GCase activity of transduced slices leads also to the possibility of ICV injections of the AAV2 packed particles as therapeutic approach. Another possibility would be to use the AAV2 packed particles for injection into the cerebrospinal fluid or into the nasal epithelia in order to prolong lifespan, thus engendering a therapeutic effect.

In summary, the present study has shown that the AAV2 particles produced were able to transduce the cortical organotypic brain-slices efficiently and led to a significant increase in GCase activity. Furthermore, the low immunogenicity of the AAV2 particles packed with pAAV.hGC means that they can be administered to K14 ko mice.

5. Outlook

In this study it was shown that cortical organotypic brain-slice cultures representing Gaucher's disease type II could be successfully transduced by the AAV2, particles packed with pAAV.hGC and pFB.CAG that were produced in the study. The successful transduction led to an increase in GCase activity level.

The successful outcome of the proof-of-principle experiments in the present study, and also the successful transduction of liver slices from K14 ko mice with the AAV2 particles (performed by B. Vorwerk), support the adoption of a therapeutic approach in K14 ko mice. Therefore, the transgene coding β-glucocerebrosidase was fused to the ApoB binding domain in vectors used for packing AAV2 particles, as it is believed that this might be successful way to overcome the blood–brain barrier. Spencer and Verma investigated the successful delivery of a fused β-glucocerebrosidase to the LDLR-binding domain of Apo B across the blood–brain barrier into the central nervous system after lentiviral injection into adult mice (Spencer and Verma, 2007).

The animal experiments planned by our group have already been approved by the LaGESO. In order to perform animal experiments a higher viral titre is required than is used to transduce organotypic slice cultures, as was done in the present study. Therefore, the vector pAAV.hGC was sent to an external group in Naples for higher titre production. The planned animal experiments involve intraperitoneal and intranasal injection of AAV2 particles into K14 ko mice, and also K 14 wt mice as controls. The various methods and assays developed in the present study will be used to investigate the brains of transduced mice. The expectation from these experiments is an increase in GCase activity in K14 ko mice compared with that in K 14 wt mice. In fact, enzyme activities of only 10–20% of the physiological level may be sufficient prevent disease-specific alterations such as lysosomal lipid accumulation in cells (Tomanin *et al.*, 2012). Such an increase would eventually lead to an increase of lifespan of K14 ko mice, which would represent a successful therapeutic approach to cure the type II Gaucher's disease.

6. Summary

Gaucher's disease belongs to the rare lysosomal storage disorders and occurs with a frequency of 1 in 40,000–60,000 in the general population. The disease is caused by a defect in the activity of the lysosomal enzyme β-glucocerebrosidase. Three distinct clinical types have been identified: Type I (non-neuronopathic), involving only the peripheral nervous system occur the most frequently. Patients show a variety of symptoms, but enlargement of the spleen or liver and anaemia are often manifested. Gaucher's disease type II (acute neuronopathic) and type III (chronic or subacute neuronopathic) involve the peripheral as well as the central nervous system. In type II, disease onset occurs already between 3–6 months after birth and patients die within the first 2–3 years of life. This type of disease is the most devastating one. Type III occurs later in life than type II, and patients survive to their third or fourth decade of life. Over 250 mutations have been described in the gene encoding β-glucocerebrosidase. Therefore, as in most lysosomal storage diseases, a direct genotype–phenotype correlation is impossible.

So far, therapeutic approaches for treating Gaucher's disease have not been fully satisfactory. The therapy in most frequent current use, and the most promising, is enzyme replacement therapy for type I. In types II and III this treatment fails to bring about any improvements, owing to the inability of the replacement enzymes to cross the blood–brain barrier. In the past, different approaches have been taken to find a way to overcome the blood–brain barrier in order to present therapeutic enzymes such as β-glucocerebrosidase to cells in the brain. Until today, such approaches have not been sufficient. Therefore, the aim of this study was the establishment and optimisation of the adeno-associated viral gene transfer of β-glucocerebrosidase into cortical organotypic brain-slice cultures representing Gaucher's disease type II.

The K14 lnl mouse strain, characterised in the present study, showed the typical signs of disease. The homozygous knockout mice showed distinctly reduced GCase activity in the brain compared with their healthy littermates, representing Gaucher's disease type II. Further neuronal loss and astrogliosis was detected in K14 knockout mice. Moreover, a vector coding for the therapeutic gene β-glucocerebrosidase under the control of the CMV promoter was cloned. Successful GCase activity of this vector

and of a vector under the control of the CAG promoter was determined after transfecting fibroblasts from a Gaucher patient and in primary neurons derived from K14 embryos. Thereafter, AAV2 viral particles were packed with vectors coding either the β-glucocerebrosidase fused to the ApoB binding domain or the *LacZ* gene. Characterised K14 knockout mice were used to establish an *ex vivo* model of cortical organotypic brain-slice cultures representing Gaucher's disease type II. These characterised cortical organotypic brain-slice cultures of K14 knockout mice were transduced with the differently packed AAV2 particles to investigate the transfer of the β-glucocerebrosidase gene. Significant increases of GCase activity were measured in slices transduced with AAV2 particles containing the therapeutic enzyme, compared with either mock transduced slices or non-transduced slices.

The overall results obtained in the present study lead to the conclusion that the packed AAV2 particles produced appear to be sufficient for further tests of their applicability in therapeutic approaches.

7. Zusammenfassung

Morbus Gaucher gehört zu den seltenen lysosomalen Speicherkrankheiten und tritt bei 1 von 40.000–60.000 der allgemeinen Bevölkerung auf. Die Krankheit wird durch einen Defekt in der Aktivität des lysosmalen Enzyms β-Glukozerebrosidase hervorgerufen. Drei unterschiedliche klinische Typen sind bekannt und beschrieben worden. Bei Typ I (nicht-neuronopathisch), der am Häufigsten auftritt, ist ausschließlich das periphere Nervensystem involviert. Die Patienten zeigen eine Vielfalt an Symptomen, jedoch äußern sich eine Organvergrößerung der Milz und Leber, sowie Anämie häufig. Bei den Morbus Gaucher Typen II (akut neuronopathisch) und III (chronisch oder subakut neuronopathisch) ist sowohl das periphere, als auch das zentrale Nervensystem involviert. In Typ II, dem verheerendsten der drei Typen, manifestiert sich die Krankheit bereits in den ersten 3-6 Monaten nach der Geburt und die Patienten sterben innerhalb ihrer ersten 2-3 Lebensjahre. Typ III tritt später als Typ II auf und die Patienten überleben bis in ihre 30er / 40er Jahre. Über 250 Mutationen wurden im Gen der β-Glukozerebrosidase beschrieben, daher ist eine direkte Genotyp-Phänotyp Korrelation, wie in den meisten lysosmalen Speicherkrankheiten, nicht möglich.

Bis dato, waren die therapeutischen Versuche Morbus Gaucher zu heilen nicht erfolgsversprechend. Die Therapie die mittlerweile am häufigsten zum Einsatz kommt, ist die Enzymersatztherapie für Typ I. Bei Typ II und III führt diese Therapie zu keinen Verbesserungen, da das rekombinante Enzym die Blut-Hirn-Schranke nicht passieren kann. In den letzten Jahren wurden einige Versuche unternommen um Enzyme, wie die β-Glukozerebrosidase über die Blut-Hirn-Schranke zu bringen und den Zellen im Gehirn zu präsentieren. Bis heute waren diese Versuche ohne Erfolg. Daher war das Ziel der vorliegenden These, die Etablierung und Optimierung eines Adeno-assoziierten viralen Gentransfers der β-Glukozerebrosidase in organotypische Hirnschnittkulturen, die den Typ II des Morbus Gaucher wiederspiegeln.

Die K14-lnl-Mäuse, die in dieser Studie charakterisiert wurden, zeigten die typischen Symptome der Krankheit des akut neuronopathischen Typen. Die homozygoten (knockout) Mäuse wiesen eine signifikant reduzierte Aktivität der Glukozerebrosidase

im Gehirn, verglichen mit der Aktivität im Gehirn ihrer gesunden Geschwistertiere auf. Des Weiteren konnte der Verlust von Nervenzellen und eine Astrogliose im Gehirn der K14-Knoukout-Mäuse histologisch nachgewiesen werden. Außerdem wurde ein Vektor kloniert, der die β-Glukozerebrosidase unter der Kontrolle des CMV-Promoters exprimieren soll. Die GCase-Aktivität und -Expression wurde erfolgreich durch die Transfektion primärer Neuronenkulturen von K14-ko-Mäusen und Fibroblasten von M.G. Patienten mit dem klonierten Vektor unter CMV Kontrolle und einem Vektor unter Kontrolle des CAG-Promoters nachgewiesen. Danach wurden AAV2 virale Partikel verpackt, entweder mit einem der Vektoren, die die β-Glukozerebrosidase epximieren oder LacZ. Für die Etablierung kortikaler organotypischer Hirnschnitte, die ein e*x-vivo*-Modell des Morbus Gaucher Typ II repräsentieren, wurden die zuvor charakterisierten K14 ko Mäuse verwendet. Die charakterisierten Hirnschnitte wurden mit unterschiedlich verpackten AAV2 Partikeln transduziert, um den Gentransfer der β-Glukozerebrosidase zu untersuchen. Die GCase-Aktivität war in Schnitten die mit den GCase verpackten AAV2 Partikeln transduziert wurden, verglichen mit Mock-transduzierten oder nicht transduzierten Schnitte signifikant erhöht.

Die Ergebnisse der vorliegenden Studie zeigen, dass die produzierten AAV2 Partikel für weitere Tests, bezüglich Ihrer therapeutischen Wirkung, anwendbar sind.

8. References

Aerts J.M.F.G., Kallemeijn W.W., Wegdam W., Ferraz M.J., van Breemen M.J., Dekker N., Kramer G., Poorthius B.J., Groener J.E.M., Cox-Brinkman J., Rombach S.M., Hollak C.E.M., Linthorst G.E., Witte M.D., Gold H., van der Marel G.A. Overkleeft H.S. and Boot R.G. (2011) "Biomarkers in the diagnosis of lysosomal storage disorders: protein, lipids and inhibodies." J Inherit Metab Di **34:** 605-619

Ballabio A. and Gieselmann V. (2009) "Lysosomal disorders: From storage to cellular damage." BBA **1793 (4):** 684-696

Beck M. (2010) "Therapy for Lysosomal Storage Disorders." Life **62 (1):** 33-40

Benbrook D.M. (2006) "Organotypic cultures represent tumor microenvironment for drug testing." Drug Discovery Today: Disease Models **3 (2):** 143-148

Beutler E. (1992) "Gaucher Disease: New Molecular Approaches to Diagnosis and Treatment." Science **256:** 794-799

Bickel U., Yoshikawa T., Landaw E.M., Faull K.F. and Pardridge W.M. (1993) "Pharmacologic effects *in vivo* in brain by vector-mediated peptide drug delivery." Proc Natl Acad Sci USA **90:** 2618-2622

Bodennec J, Pelled D., Riebelin C., Trajkovic S. and Futerman A.H. (2002) "Phosphatidylcholine synthesis is elevated in neuronal models of Gaucher disease due to direct activation of CTP:phosphocholine cytidylyltransferase by glucosylceramide. " FASEB J **16:** 1814-1816

Bowers W.J., Breakefield X.O. and Sena-Esteves M. (2011) "Genetic therapy for the nervous system." Hum Mol Genet **20 (1):** 28-41

Brady R.O. (2006) "Emerging Strategies for the Treatment of Hereditary Metabolic Storage Disorders." Rejuvenation Res. **9 (2):** 237-244

Brady R.O., Yang C. and Zhuang Z. (2012) "An innovative approach to the treatment of Gaucher disease and possibly other metabolic disorders of the brain." J Inherit Metab Dis **36 (3):** 451-454

References

Büning H., Perabo L., Coutelle O., Quadt-Humme S., Hallek M. (2008) "Recent developments in adeno-associated virus vector technology." J Gene Med. **10:** 717-733

Burmshtein B., Salinas P., Peterson B., Chan V., Silman I., Sussman J.L., Savickas P.J., Robinson G.S. and Futerman A.H. (2010) "Characterization of gene-activated human acid-β-glucosidase: Crystal structure, glycan composition, and internalization into macrophages." Glycobiology **20 (1):** 24-32

Butters T.D. (2007) "Gaucher disease." Curr Opin Chem Biol **11:**412-418

Cabrera-Salazar M.A., Bercury S.D., Ziegler R.J., Marshall J., Hodges B.L., Chuang W.-L., Pacheco J., Li L., Cheng S.H. and Scheule R.K. (2010) "Intracerebroventricular delivery of glucocerebrosidase reduces substrates and increases lifespan in a mouse model of neuronopathic Gaucher disease." Exp Neurol **225 (2):** 436-444

Carstea E.D., Murray G.J. and O'Neil R.R: (1992) "Molecular and Functional Characterization of the Murine Glucocerebrosidase Gene." Biochem Biophys Res Commun **184 (3):** 1477-1483

Cavaliere F. and Matute C. (XX) "Utility of Organotypic Slices in Parkinson´s Disease Research." Towards New Therapies for Parkinson's Disease, Prof. David Finkelstein (Ed.) ISBN: 978-953-307-463-4: **Chapter 6:** 101-112

Cheng S.H. and Smith A.E. (2003) "Gene therapy proress an prospects: gene therapy of lysosomal storage disorders." Gene Ther **10:** 1275-1281

Cho S., Wood A. and Bowlby M.R. (2007) "Brain Slices as Models for Neurodegenerative Disease and Screening Platforms to Identify Novel Therapeutics." Curr Neuropharmacol **5:** 19-33

Correll P.H., Fink J.K., Brady R.O., Perry L.K. and Karlsson S. (1989) "Production of human glucocerebrosidase in mice after retroviral gene transfer into multipotential hematopoietic progenitor cells." Proc Natl Acad Sci USA **86:** 8921-8916

Daniels L.B., Coyle P.J., Gelw R.H., Radin N.S. and Labow R.S. (1982) "Brain Glucocerebrosidase in Gaucher´s Disease." Arch Neurol **39:** 550-556

References

D'Azzo A. (2003) "Gene Transfer Strategies for Correction of Lysosomal Storage Disorders." Acta Haematol **11:** 71-85

Daya S. and Berns K.I. (2008) "Gene Therapy Using Adeno-Associated Virus Vectors." Clin Microbiol Rev **21 (4):** 583-593

Dayton R.D., Wang D.B. and Klein R.L. (2012) "The advent of AAV9 expands applications for brain and spinal cord gene delivery." Expert Opin Biol Ther **12 (6):** 757-766

De Simini A., Griesinger C.B. and Edwards F.A. (2003) "Development of rat CA_1 neurones in acute *versus* organotypic slices: role of experience in synaptic morphology and activity." J Physiol **550:** 135-147

Dunbar C., Kohn D., Schiffmann R., Barton N., Nolta J., Esplin J., Pensiero M., Long Z., Lockey C., Emmons R., Csik S., Leitman S., Krebs C., Carter C., Brady R. and Karlsson S. (1998) "Retroviral transfer of the glucocerebrosidase gene into CD34+ cells from patients with Gaucher disease: In vivo detection of transduced cells without myeloablation." Hum Gene Ther **9 (17):** 2629-2640

Duque S., Joussemet B., riviere C., Marais T., Dubreil L., Douar A.-M., Fyfe J., Moullier P., Colle M.-A. and Barkats M. (2009) "Intravenous Administration of Self-complementary AAV9 Enables Transgene Delivery to Adult Motor Neurons." Mol Ther **17 (7):** 1187-1196

Erickson A.H., Ginns E.I. and Barranger J.A. (1985) "Biosynthesis of the Lysosomal Enzyme Glucocerebrosidase." J Biol Chem **260 (26):** 14319-14324

Enquist I.B., Lo Bianco C., Ooka A., Nilsson E., Månsson J.E., Ehinger M., Richter J., Brady R.O., Kirik D. and Karlsson S. (2007) "Murine models of acute neuronopathic Gaucher disease." PNAS **104 (44):** 17483-17488

Enquist I.B., Nilsson e., Ooka A., Mansson J.E., Ehinger M., Richter J., Brady R.O., Kirik D. and Karlsson S. (2006) "Effective cell and gene therapy in a murine model of Gaucher disease." Proc Natl Acad Sci USA **103:** 13819-13824

Farfel-Becker T., Vitner E.B. and Futerman A.H. (2011) "Animal models for Gaucher disease research." DMM **4:** 746-752

References

Felgner P.L., Gadek T.R., Holm M., Roman R., Chan H.W., Northrop J.P., Ringold G.M. and Danielsen M. (1987) "Lipofection: a highly efficient, lipid-mediated DNA-transfection procedure." PNAS **84 (21):** 7413-7417

Fink J.K., Correll P.H., Perry L.K. Brady R.O. and Karlsson S. (1990) "Correction of glucocerebrosidase deficiency after retroviral-mediated gene transfer into hematopoietic progenitor cells from patients with Gaucher disease." Proc Natl Acad Sci USA **87:** 2334-2338

Frisella W.A., O´connor L.H., Vogler C.A., Roberts A., Walkley S., Levy B., Daly T.M. and Sands M.S. (2001) "Intracranial Injection of Recombinant Adeno-associated Virus Improves Cognitive Function in a Murine Model of Mucopolysaccharidosis Type VII." Mol Ther **3:**351-358

Futerman A.H. and van Meer G. (2004) "The cell biology of ysosomal storage disorders." Nat Rev **5:** 554-565.

Gao G.-P., Alvira M.R., Wang L., Calcedo R., Johnston J. and Wilson J.M. (2002) "Novel adeno-associated viruses from rhesus monkeys as vectors for human gene therapy." PNAS **99 (18):** 11854-11859

Godyna S., Liau G., Popa I., Stefansson S. and Argraves W.C. (1995) "Identification of the Low Denisity Lipoprotein Receptor-related Protein (LRP) as an Endocytic Receptor for Thrombospondin-1." J Cell Biol **129 (5):** 1403-1410

Gonçalves M.A.F.V. (2005) "Adeno-associatd virus: from defective virus to effective vector." Virol J **2 (43):** 1-17

Grimm, D. and Kleinschmidt J.A. (1999) "Progress in Adeno-Associated Virus Type 2 Vector Production: Promises and Prospects for Clinical Use." Hum Gen Ther **10:**2445-2450

Gupta N., Oppenheim I.M., Kauvar E.F., Tayebi N. and Sidransky E. (2011) "Type 2 Gaucher disease: phenotypic variation and genotypic heterogeneity." Blood Cells Mol Dis **46 (1):** 75-84

Ho M.W. (1973) "Identity of 'Acid' β-Glucosidase and Glucocerebrosidase in Human Spleen." Biochem J **136:** 721-729

References

Hughes D.A. and Pastores G.M. (2010) "The pathophysiology of GD – current understanding and rationale for existing and emerging therapeutic approaches." <u>Wien Med Wochenschr</u> **160 (23-24):** 594-599

Hussain M.M., Strickland D.K. and Bakillah A. (1999) "The Mammalian Low-Density Lipoprotein Receptor Family." <u>Annu Rev Nutr</u> **19:** 141-172

Hruska K.S., LaMarca M.E., Scott C.R. and Sidransky E. (2008) "Gaucher Disease: Mutation and Polymorphyism Spectrum in the Glucocerebrosidase Gene (GBA)." <u>Hum Mutat</u> **29 (5):** 567-583

Jmoudiak M. and Futerman A.H. (2005) "Gaucher disease:pathological mechanisms and modern management." <u>BJH Review</u> **129:** 178-188

Jung S.C., Han I.P., Limaye A., Xu R., Gelderman M.P., Zerfas P., Tirumalai K., Murray G.J., During M.J., Brady R.O. and Qasba P. (2001) "Adeno-associated viral vector-mediated gene transfer results in long-term enzymatic and functional correction in multiple organs of Fabry mice." <u>Proc Natl Acad Sci USA</u> **98:** 2676–2681

Kacher Y., Brumshtein B., Boldin-Adamsky S., Toker L., Schainskya A., Silman I., Sussman J.L. and Futerman A.H. (2008) "Acid β-glucosidase: insights from structural analysis and relevance to Gaucher disease therapy." <u>Biol Chem</u> **389:** 1361-1369

Kanfer J.N., Legler G., Sullivan J., raghavan S.S. and Mumford R.A. (1975) "The Gaucher mouse." <u>Biochem Biophys Res Commun</u> **67:** 85-90

Kaye E.M., Ullman, M.D., Wilson E.R. and Barranger J.A. (1986) "Type 2 and type 3 Gaucher disease: a morphological and biochemical study." <u>Ann Neurol</u> **20:** 223-230

Kremer E.J. (2005) "Gene Transfer to the Central Nervous System: Current State of the Art of Viral Vectors." <u>Curr Genomics</u> **6:** 13-37

Korkotian E., Schwarz A., Pelled D., Schwarzmann G. Segal M. and Futerman A.H. (1999) "Enhanced calcium release in the acute neuronopathic form of Gaucher disease." <u>Neurobiol Dis</u> **18:** 83-88

Kwanghun C., Wallace J., Kim S.-Y., Kalayanasundaram S., Andalman A.S., Davidson R.J., Mirzabekov J.J., Zalocusky K.A., Mattis J., Denisin A.K., Pak S.,

Bernstein H., Ramakrishnan C., Grosenick L., Gradinaru V. and Deisseroth K. (2013) "Structural and molecular interrogation of intact biological systems" <u>Nature</u> **497:** 332-337

Lai C.M., Lai Y.K.Y. and Rakoczy E.P. (2002) "Adenovirus and Adeno-Associated Virus Vectors." <u>DNA Cell Biol</u> **21 (12):** 895-913

Leimig T., Mann L., Martin Md.P., Bonten E., Persons D., Knowles J., Allay J.A., Cunningham J., Nienhuis A.W., Smeyne R. and d'Azzo A. (2002) "Functional amelioration of murine galactosialidosis by genetically modified bone marrow hematopoietic progenitor cells." <u>Blood</u> **99:** 3169–3178

Liu Y., Suzuki K., Reed J.D., Grinberg A., Westphal H., Hoffmann A., Doring T., Sandhoff K. and Proia R.L. (1998) "Mice with type 2 and 3 Gaucher disease point mutations generated by a single insertion mutagenesis procedure." <u>Proc Natl Acad Sci USA</u> **95:** 2503-2508

Lossi L., Alasia S., Salio C. and Merighi A. (2009) "Cell death and proliferation in acute slices and organotypic cultures of mammalian CNS." <u>Prog Neurobiol</u> **88:** 221-245

Marshall J., McEacher K.A., Cavanagh Kyros J.A., Nietupski J.B., Budzinksi T.L., Ziegler R.J., Yew N.S., Sullivan J., Scaria A., van Rooijen N., Barranger J.A. and Cheng S.H. (2002) "Demonstration of Feasibility of *In vivo* Gene Therapy fpr Gaucher Disease Using a Chemically Induced Mouse Model." <u>Mol Ther</u> **6 (2):** 179-189

Matsushita T., Elliger S., Elliger C., Podsakoff G., Villarreal L., Kurtzman G.J. and Iwaki Y. (1998) „Adeno-associated virus vectors can be efficiently produced without helper virus." <u>Gene Ther</u> **5:** 938-945

Matzner U., Harzer K., Learish R.D., Barranger J.A. and Gieselmann V. (2000) "Long-term expression and transfer of arylsulfatase A into brain of arylsulfatase A-deficient mice transplanted with bone marrow expressing the arylsulfatase A cDNA from a retroviral vector." <u>Gene Ther</u> **7:** 1250–1257

McCarty D.M. (2008) "Self-complementary AAV Vectors; Advances and Applications" <u>Mol Ther</u> **16 (10):** 1648-1656

McEachern K.A., Nietupski J.B., Chuang W.-L., Armentano D., Johnson J., Hutto e., Grabowski G.A., Cheng S.H. and Marshall J. (2006) "AAV8-mediated expression of glucocerebrosidase ameliorates the storage pathology in the visceral organs of a mouse model of Gaucher disease." J Gene Med **8:** 719-729

Mingozzi F. and high K.A. (2007) "Immune Responses to AAV in clinical Trials." Curr Gene Ther **7:** 316-324

Mueller C. and Flotte T.R. (2008) "Clinical gene therapy using recombinant adeno-associated virus vectors." Gene Ther **15:** 858-863

Murphy R.C. and Messer A. (2000) "Gene Transfer Methods for CNS Organptypic Cultures: A Comparison of Three Nonviral Methods." Mol Ther **3 (1):** 113-121

Niidome T. and Huang L. (2002) "Gene Therapy Progress and Prospects: Nonviral vectors." Gene Ther **9:** 1647-1652

Pardridge W.M. (2005) "The Blood-Brain Barrier and Neurotherapeutics." NeuroRx **2:** 1-2

Pastores G.M. (2010) "Neuropathic Gaucher Disease." WMW **160 (23-24):** 605-608

Pelled D., Trajkovic-Bodenec S., Lloyd-Evans E., Sidransky E., Schiffmann R. and Futerman A.H. (2005) "Enhanced calcium release in the acute neuronopathic form of Gaucher disease." Neurobiol Dis **18:** 83-88

Persidsky Y., Ramirez S.H., Haorah J. and Kanmogne G.D. (2006) "Blood-brain barrier: structural components and function under physiologic and pathologic conditions." J Neuroimmune Pharmacol **1:** 223-236

Ponce E., Witte D.P., Hung A. and Grabowski G.A. (2001) "Temporal and Spatial Expression of Murine Acid β-Glucosidase mRNA." Mol Genet Metab **74:** 426-434

Rahin A.A., Wong A.M.S., Hoefer K., Buckley S.M.K., Mattar C.N., Cheng S.H., Chan J.K.Y., Cooper J.D. and Waddington S.N. (2011) "Intravenous administration of AAV2/9 to the fetal and neonatal mouse leads to differential targeting of CNS cell types and extensive transduction of the nervous system." FASEB **25:** 1-14

Rapoport S.I. (1996) "Modulation of Blood-Brain Barrier Permeability." J Drug Target **3:** 417-425

Rjinboutt S., Aerts H.M.F.G., Geuze H.J., Tager J.M. and Strous G.J. (1991) "Mannose 6-Phosphate-independent Membrane Association of Cathepsin D, Glucocerebrosidase, and Sphingolipid-Activating Protein in HepG2 Cells." J Biol Chem **266(8):** 4862-4868

Rogers G.L., Martino A.T., Aslanidi G.V., Jayandharan G.R., Srivastava A and Herzog R.W. (2011) "Innate immune responses to AAV vectors." Front Microbiol **2:** 1-8

Rosenberg S.A., Blaese R.M., Brenner M.K., Deisseroth A.B., Ledley F.D., Lotze M.T., Wilson J.M., Nabel G.J., Cornetta K., Economou J.S., Freeman S.M., Riddell S.R., Brenner M., Oldfield E., Gansbacher B., Dunbar C., Walker R.E., Schuening F.G., Roth J.A., Crystal R.G., Welsh M.J., Culver K., Heslop H.E., Simons J., Wilmott R.W., Boucher R.C., Siegler H.F., Barranger J.A., Karlsson S., Kohn D., Galpin J.E., Raffel C., Hesdorffer C., Ilan J., Cassileth P., O'Shaughnessy J., Kun L.E., Das T.K., Wong-Staal F., Sobol R.E., Haubrich R., Sznol M., Rubin J., Sorcher E.J., Rosenblatt J., Walker R., Brigham K., Vogelzang N., Hersh E. and Eck S.L. (2000) "Human gene marker/therapy clinical protocols." Hum Gene Ther **11:** 919–979

Royo N.C., Vandenberghe L.H., Ma J.-Y., Hauspurg A., Yu L., Maronski M., Johnston J., dichter M.A., Wilson J.M. and Watson D.J. (2008) "Specific AAV Serotypes Stably Transduce Primary Hippocampal and Cortical Cultures with High Efficiency and Low Toxicity." Brain Res **1190:** 15-22

Russel D.W., Alexander I.E. and Miller A.D. (1995) "DNA synthesis and topoisomerase inhibitors increase transduction by adeno-associated virus vectors." Proc Natl Acad Sci **92:** 5719-5723

Sands M.S. and Haskins M.E. (2008) "CNS-directed gene therapy for lysosomal storage diseases." Acta Paediatr Suppl. **97 (457):** 22-27

References

Schuening F., Longo W., Atkinson M., Zaboikin M., Kiem H., Sanders J., Scott C., Storb R., Miller A., Reynolds T., Bensinger W., Rowley S., Gooley T., Darovsky B. and Appelbaum F. (1997) "Retrovirus-mediated transfer of the cDNA for human glucocerebrosidase into peripheral blood repopulation cells of patients with Gaucher's disease." Hum Gene Ther **8:** 2143–2160

Schueler U.H., Kolter T., Kaneski C.R., Blusztajn J.K., Herkenham M., Sandhoff K. and Brady R.O. (2003) "Toxicity of glucosylsphingosine (glucopsychosine) to cultured neuronal cells: a model system for assessing neuronal damage in Gaucher disease type 2 and 3." Neurobiol Dis **14:** 595-601

Sidransky E. (2004) "Gaucher Disease: complexity in a 'simple' disorder." Mol Genet Metab **83:** 6-15

Spencer B.J. and Verma I.M. (2007) "Targeted delivery of proteins across the blood-brain barrier." PNAS **104 (18):** 7594-7599

Staal J.A., Alexander S.R., Liu Y., Dickson T.D. and Vickers J.C. (2011) "Characterization of Cortical Neuronal and Glial Alterations during Culture of Organotypic Whole Brain Slices from Neonatal and Mature Mice." PLOS **6 (7):**1-10

Su T., Paradiso B., Long Y.S., Liao W.P. and Simonato M. (2011) "Evaluation of cell damage in organotypic hippocampal slice culture from adult mouse: A potential model system to study neuroprotection." Brain Res **1385:** 68-76

Sund Y., Liou B., Xu Y.H., Quinn B., Zhang W., Hamler R., Scetchell K.D.R. and Grabowski G.A. (2012) "*Ex Vivo* and *in Vivo* Effects of Isofagomine on Acid β-Glucosidase Variants and Substrate Levels in Gaucher Disease." J Biol Chem **287 (6):** 4275-4287

Takenaka T., Murray G.J., Qin G., Quirk J.M., Ohshima T., Qasba P., Clark K., Kulkarni A.B., Brady R.O. and Medin J.A. (2000) "Long-term enzyme correction and lipid reduction in multiple organs of primary and secondary transplanted Fabry mice receiving transduced bone marrow cells." Proc Natl Acad Sci USA **97:** 7515–7520

Tomanin R., Zanetti A., Zaccariotto E., D'Avanzo F., Bellettato C.M. and Scarpa M. (2012) "Gene therapy approaches for lysosomal storage diorders, a good model for the treatment of mendelian diseases." Acta Pædiatrica **101:** 692-701

Towne C., Schneider B.L., Kieran D., Redmond D.E. and Aebischer P. (2010) "Efficient transduction of non-human primate motor neurons after intramuscular delivery of recombinant AAV serotype 6." Gene Ther **17:** 141-146

Twisk J., Gillian-Daniel D.L., Tebon A., Wang L., Barrett P.H.R. and Attie A.D. (2000) "The role of the LDL receptor in apolipoprotein B secretion." J Clin Invest **105:** 521-532

Tybulewicz V.L., Tremblay M.L., LaMarca M.E., Willemsen R., Stubblefield B.K., Winfield S., Zablocka B., Sidransky e., Martin B.M. and Huang S.P. (1992) "Animal model of Gaucher´s disease from targeted disruption of the mouse glucocerebrosidase gene." Nature **357:** 407-410

Van Vliet K.M., Blouin V., Brument N., Agbandje-McKenna M. and Snyder R.O. (2008) "The Role of the Adeno-Associated Virus Capsid in Gene Transfer." Methods in Molecular Biology **437:** 51-91

Vasileva A. and Jessberger R. (2005) "Precise hit: Adeno-associated virus in gene targeting." Nature **3:** 837-847

Vitner E.B., Farfel-Becker T., Eilam R., Biton I. and Futerman A.H. (2012) "Contribution of brain inflammation to neuronal cell death in neuronopathic forms og Gaucher´s disease." Brain 1-12

Wang D., El-Amouri S.S., Dai M., Kuan C.-Y., Hui D.Y., Brady R.O. and Pan D. (2013) "Engineering a lysosomal enzyme with a derivative of receptor-binding domain of apoE enables delivery across the blood-brain barrier." PNAS **110 (8):** 2999-3004

Wang J., Faust S.M. and Rabinowitz J.E. (2011) "The next step in gene delivery: - molecular engineering of adeno-associated virus serotypes." J Mol Cell Cardiol **50:** 793-802

Weitzman M.D. and Linden R.M. (2011) "Adeno-Associated Virus Biology." Methods Mol Biol **807:** 1-23

Xu R., Janson C.G., Mastakov M., Lawlor P., Young D., Mouravlev A., Fitzsimons H., Choi K.L., Ma H., Dragunow M., Leone P., Chen Q., Dicker B. and During M.J. (2001) "Quantitative comparison of expression with adeno-associated virus (AAV-2) brain-specific gene cassettes." Gene Ther **8:** 1323-1332

Yamamoto N., Kurotani T. and Toyama K. (1989) "Neural connections between the lateral geniculate nucleus and visual cortex in vitro." Science **245:** 192-194

Yamamoto N., Yamada K., Kurotani T. and Toyama K. (1992) "Laminar specificity of extrinsic cortical connections studied in coculture preparations." Neuron **9:** 217-228

Zaiss A.-K., Liu Q., Bowen G.P., Wong N.C.W., Bartlett J.S. and Muruve D.A. (2002) "Differential Activation of Innate Immune Responses by Adenovirus and Adeno-Associated Virus Vectors" J Virol **76(9):** 4580–4590.

Ziegler R *et al.* (2002) "Improved adeno-associated viral vectors for gene therapy of Fabry disease." Mol Ther **5:** 91.

9. List of Figures

10. List of Tables

11. Appendix

11.1 Abbreviations

%	Percent
°C	Degree Celsius
4-MUD	4-Methylumbelliferyl-β-D-glucopyranoside
AAV	Adeno-associated virus
Ab	Antibody
Amp	Ampicillin
AP	Thermosensitive alkaline phosphatase
ApoB	Apolipoprotein B
ApoE	Apolipoprotein E
Approx.	Approximately
BCA	Bicinchoninic acid
BSA	Bovine serum albumine
bp	Base pairs
CBE	Conduritol B epoxide
CMV	Cytomegalovirus
CNS	Central nervous system
Co	Control
$CuSO_4$	Copper sulfate
Da	Dalton
DAB	3,3'-diaminobenzidine
dH_2O	Distilled water
Di.	Direct
DMSO	Dimethylsulfoxide
DNA	Deoxyriobnucleic acid

dNTP-mix	Deoxyribonucleotide triphosphates
E.coli	*Escherichia coli*
FBS	Fetal bovine serum
Fig.	Figure
HE staining	Hematoxylin and eosin staining
HSPG	Receptor heparin sulfate proteoglycan
g	Gram
GC, GCase or GBA	Glucocerebrosidase
Hank´s w Ca^{2+}/Mg^{2+}	Hank´s salt solution with Ca^{2+}, Mg^{2+}
Hank´s w/o Ca^{2+}/Mg^{2+}	Hank´s salt solution without Ca^{2+}, Mg^{2+}
IP/ml	Infectious particles per milliliter
ITRs	Inverted terminal repeats
Kan	Kanamycin
kbp	Kilo basepairs
kDa	Kilodalton
ko or -/-	Knockout
l	Liter
LB	Luria Bertani
LDH	Lactate dehydragenase
LDLR	Low-density lipoprotein receptor
M	Mole per liter
Med.	Medium
µg	Microgram
mg	Milligram
M.G.	Morbus Gaucher
min	Minute
µl	Micro liter

µM	Micro molar
ml	Milliliter
mM	Millie molar
N_2	Nitrogen
NHS	Normal horse serum
Nm	Nanometer
Not transd.	Not transduced
ON	Overnight culture
ORF	Open reading frame
pAAV.hGC	pAAV.CMV_sGBA_HA_ApoB
PBS	Phosphate buffered saline
PCR	Polymerase chain reaction
Pen/Strep	Penecillin/Streptomycin
PFA	Paraformaldhyde
pFB_CAG	pFB.CAG_sGBA_HA_ApoB_1249
RNA	Ribonucleic acid
rpm	Rounds per minute
RT	Room temperature
sec	Seconds
SDS	Sodium dodecyl sulfate
Slices	Organotypical cortical brain slice culrures
Tet	Tetracycline
U	Units
V	Volt
Vol.	Volume
VP	Viral protein
v/v	Volume per volume

WB   Western blot

Wt or wt   Wild-type

w/v   Weight per volume

11.2 Maps of plasmids

Figure 37 shows graphic maps of the plasmids, with their most important features and prominent restriction enzymes, used for cloning in the present study.
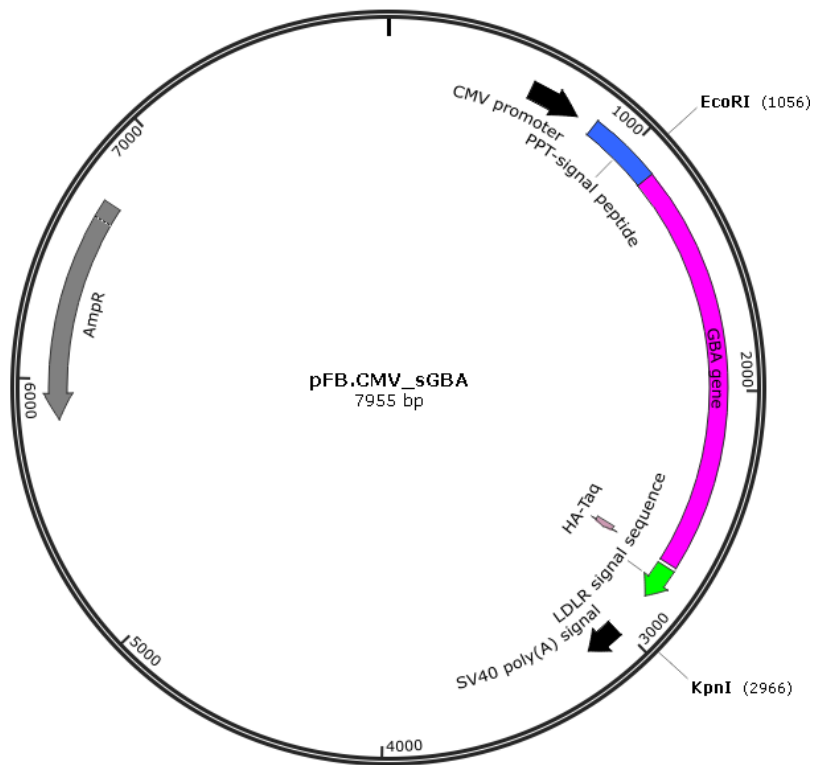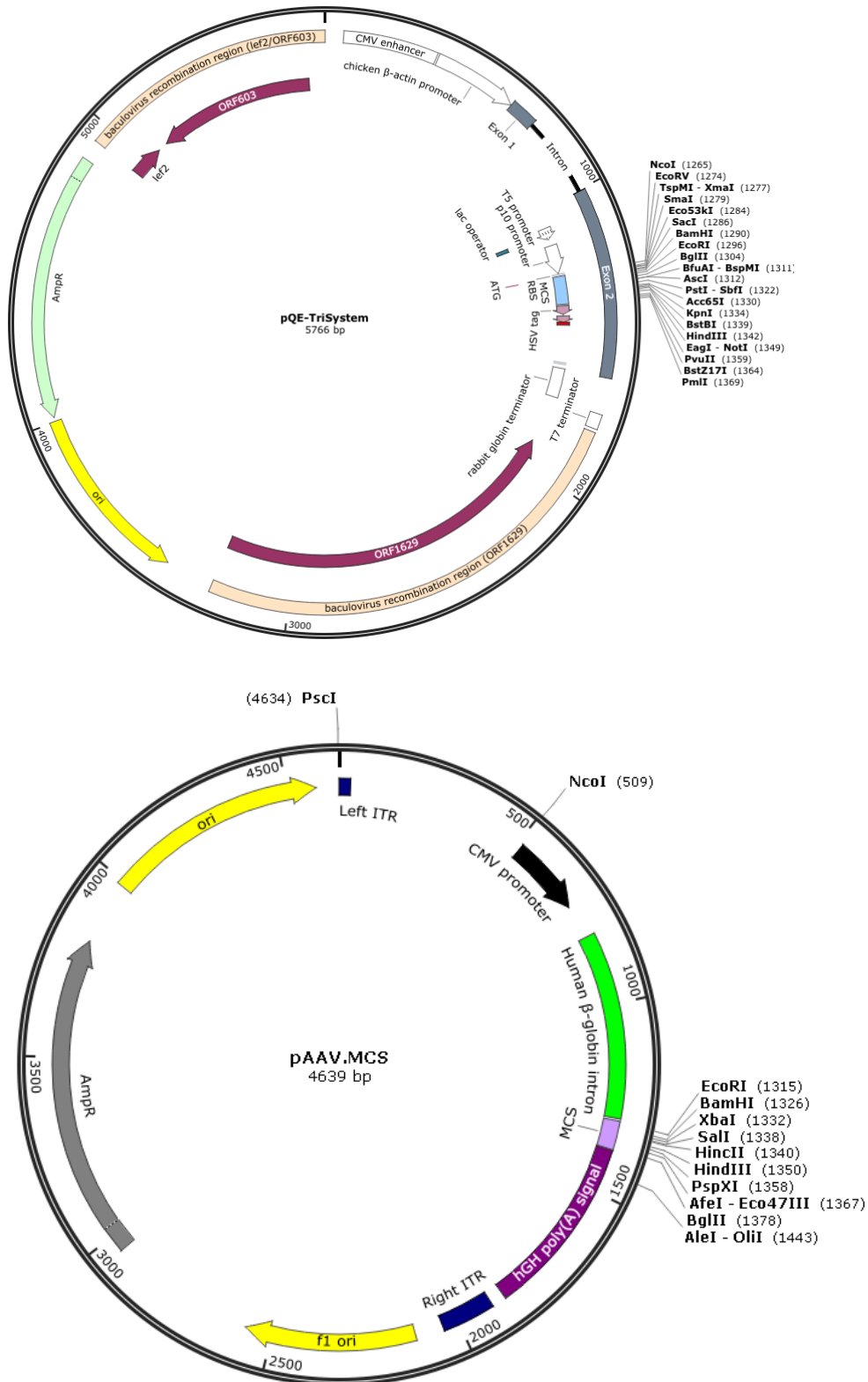
Figure 37: Schematic overview of plasmids used in the present study
GBA gene: *β-glucocerebrosidase gene*; LDLR: *low-density-lipoprotein receptor signal sequence*; hGH pplyA: *human growth hormone poly A signal*; AmpR: *ampicillin resistance gene*; CMV promoter: *cytomegalovirus;* CAG: *a combination of CMV early enhancer element and chicken beta-actin promoter*; ITR: *internal repeats*; ori: *origin of replication*; f1 ori: *F1 origin of replication*; EcoRI, BamHI, XbaI, SalI, HincII, HindIII, PspXI, AfeI, BglII, AleI, KpnI: *restriction sites of restriction enzymes*

11.3 Sequencing results and alignments

```
Query 123-182  GGATCCGCCATGTCTGCCCTGCTGATCCTGGCTCTGGTCGGAGCTGCTGTGGCTCTCGAG

               ||||||||||||||||||||||||||||||||||||||||||||||||||||||||||||

Sbjct  9-68    GGATCCGCCATGTCTGCCCTGCTGATCCTGGCTCTGGTCGGAGCTGCTGTGGCTCTCGAG


Query 183-242  ATGGCTGGCAGCCTGACAGGACTGCTGCTGCTGCAGGCCGTGTCTTGGGCCAGCGGCGCC

               ||||||||||||||||||||||||||||||||||||||||||||||||||||||||||||

Sbjct  69-128  ATGGCTGGCAGCCTGACAGGACTGCTGCTGCTGCAGGCCGTGTCTTGGGCCAGCGGCGCC


Query 243-302  AGACCTTGCATCCCCAAGAGCTTCGGCTACAGCAGCGTGGTCTGCGTGTGCAACGCCACC

               ||||||||||||||||||||||||||||||||||||||||||||||||||||||||||||

Sbjct 129-188  AGACCTTGCATCCCCAAGAGCTTCGGCTACAGCAGCGTGGTCTGCGTGTGCAACGCCACC


Query 303-362  TACTGCGACAGCTTCGACCCCCCCTACCTTCCCTGCTCTGGGCACCTTCAGCAGATACGAG

               ||||||||||||||||||||||||||||||||||||||||||||||||||||||||||||

Sbjct 189-248  TACTGCGACAGCTTCGACCCCCCCTACCTTCCCTGCTCTGGGCACCTTCAGCAGATACGAG


Query 363-422  AGCACCCGCAGCGGCAGACGGATGGAACTGAGCATGGGCCCCATCCAGGCCAATCACACC

               ||||||||||||||||||||||||||||||||||||||||||||||||||||||||||||

Sbjct 249-308  AGCACCCGCAGCGGCAGACGGATGGAACTGAGCATGGGCCCCATCCAGGCCAATCACACC


Query 423-482  GGAACCGGCCTGCTGCTGACCCTGCAGCCCGAGCAGAAATTCCAGAAAGTGAAGGGCTTC

               ||||||||||||||||||||||||||||||||||||||||||||||||||||||||||||

Sbjct 309-368  GGAACCGGCCTGCTGCTGACCCTGCAGCCCGAGCAGAAATTCCAGAAAGTGAAGGGCTTC


Query 483-542  GGCGGAGCCATGACAGACGCCGCAGCCCTGAACATCCTGGCCCTGAGCCCCCCTGCTCAG

               ||||||||||||||||||||||||||||||||||||||||||||||||||||||||||||

Sbjct 369-428  GGCGGAGCCATGACAGACGCCGCAGCCCTGAACATCCTGGCCCTGAGCCCCCCTGCTCAG


Query 543-602  AATCTGCTGCTGAAGTCCTACTTCAGCGAGGAAGGCATCGGCTACAACATCATCCGGGTG

               ||||||||||||||||||||||||||||||||||||||||||||||||||||||||||||

Sbjct 429-488  AATCTGCTGCTGAAGTCCTACTTCAGCGAGGAAGGCATCGGCTACAACATCATCCGGGTG
```

```
Query 603-662  CCCATGGCCAGCTGCGACTTCAGCATCAGAACCTACACCTACGCTGACACCCCCGACGAC

               ||||||||||||||||||||||||||||||||||||||||||||||||||||||||||||

Sbjct 489-548  CCCATGGCCAGCTGCGACTTCAGCATCAGAACCTACACCTACGCTGACACCCCCGACGAC


Query 663-722  TTCCAGCTGCACAACTTCAGCCTGCCCGAAGAGGACACCAAGCTGAAGATCCCCCTGATC

               ||||||||||||||||||||||||||||||||||||||||||||||||||||||||||||

Sbjct 549-608  TTCCAGCTGCACAACTTCAGCCTGCCCGAAGAGGACACCAAGCTGAAGATCCCCCTGATC


Query 723-782  CACAGAGCCCTGCAGCTGGCCCAGAGGCCTGTGTCTCTGCTGGCCAGCCCTTGGACCAGC

               ||||||||||||||||||||||||||||||||||||||||||||||||||||||||||||

Sbjct 609-668  CACAGAGCCCTGCAGCTGGCCCAGAGGCCTGTGTCTCTGCTGGCCAGCCCTTGGACCAGC


Query 783- CCCACCTGGCTGAAAACAAA  802

           ||||||||||||||||||||

Sbjct 669- CCCACCTGGCTGAAAACAAA  688
```

Figure 38: Sequence alignment after cloning pAAV.hGC (Clone 2) with human GCase data base sequence
'Query' represents the sequence of pAAV.hGC and 'Sbjct' the sequence of the human GCase. Sequence identity was 100% (680 of 680 bases). Strands compared were Plus/Plus.

```
Query1215-1274  TTTGCTAATCATGTTCATACCTCTTATCTTCCTCCCACAGCTCCTGGGCAACGTGCTGGT

                ||||||| ||  |||| |||||||||||||||||||||||||||||||||||||||||||
Sbjct  2-60    TTTGCT-ATACTGTTACTACCTCTTATCTTCCTCCCACAGCTCCTGGGCAACGTGCTGGT


Query1275-1334  CTGTGTGCTGGCCCATCACTTTGGCAAAGAATTGGGATTCGAACATCGATTGAATTCCCC

                ||||||||||||||||||||||||||||||||||||||||||||||||||||||||||||
Sbjct  61-120   CTGTGTGCTGGCCCATCACTTTGGCAAAGAATTGGGATTCGAACATCGATTGAATTCCCC


Query 1335    GGGGATCC  1342

              ||||||||
Sbjct 121     GGGGATCC  128
```

Figure 39: Sequence alignment sequence after cloning pAAV.hGC (Clone 2) with the pAAV.MCS data base sequence
'Query' represents the sequence of pAAV.hGC sequence and 'Sbjct' the sequence of the backbone vector pAAV.MCS. Sequence identity was 96% (123 of 126 bases, Gaps = 1 of 126). Strands compared were Plus/Plus.